Technological Advances in Molecular Pathology

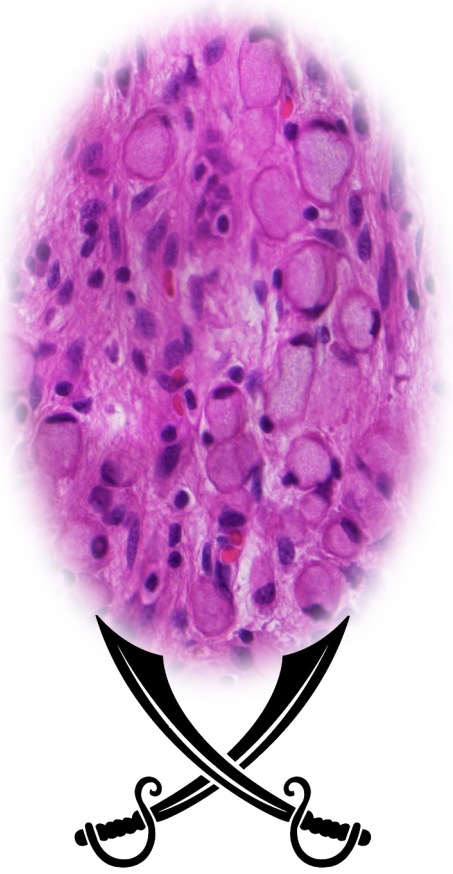

A Journey into the Archives

Ronald van Eijk

Technological Advances in Molecular Pathology:

A Journey into the Archives

Ronald van Eijk

Technological Advances in Molecular Pathology: A Journey into the Archives

ISBN: 978-94-90858-19-3

Printing: drukkerij Mostert, Leiden

Cover design: Based on an HE colored slide with “signet ring cells” in a stomach carcinoma. Ronald van Eijk & Frans Prins

Text editing: Parts of this thesis have been edited by: American Journal Experts

Technological Advances in Molecular Pathology: A Journey into the Archives

Proefschrift

ter verkrijging van
de graad van Doctor aan de Universiteit Leiden,
op gezag van Rector Magnificus prof.mr. C.J.J.M. Stolker,
volgens besluit van het College voor Promoties
te verdedigen op woensdag 8 mei 2013
klokke 11.15 uur

door

Ronald van Eijk
geboren te Leiden
in 1964

Promotiecommissie

Promotor:	Prof. Dr. J. Morreau
Copromotor:	Dr. T. van Wezel
Overige leden:	Prof. Dr. C. Cornelisse
	Prof. Dr. P. Devilee
	Prof. Dr. P. H.C. Eilers (Erasmus University Rotterdam)
	Dr. M. Ligtenberg (Radboud University Medical Center)

The printing of this thesis has been financially supported by: MRC-Holland, Amsterdam and Life Technologies Europe BV, Bleiswijk

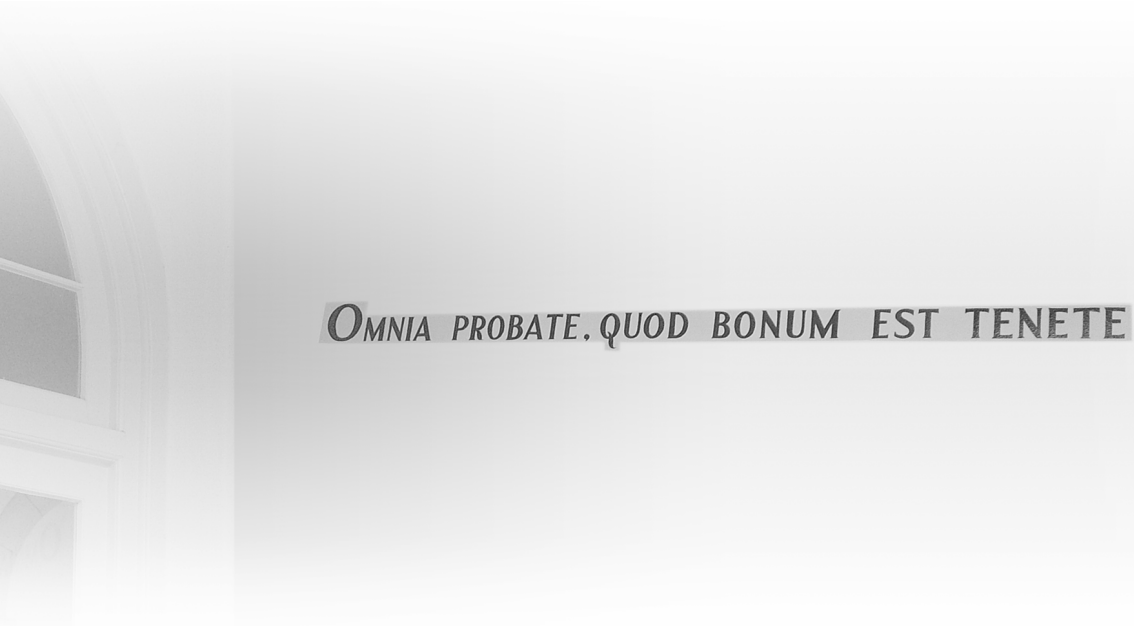

Entrance of the “old” Pathology building. Wassenaarseweg, Leiden

Aan Marianne

Contents

Chapter 1	General introduction	11
Chapter 2	Assessment of a fully automated high-throughput DNA extraction method from formalin-fixed, paraffin-embedded tissue for KRAS, and BRAF somatic mutation analysis Exp. Mol. Pathol. 2013 Feb;94(1): 121	51
Chapter 3	Multiplex ligation-dependent probe amplification for the detection of 1p and 19q chromosomal loss in oligodendroglial tumors Brain Pathol. 2005 Jul;15(3):192	63
Chapter 4	MLPAINTER: An integrated approach to analysis, visualization and data management of Multiplex Ligation-dependent Probe Amplification BMC Bioinformatics. 2010 Jan;11:67	77
Chapter 5	Sensitive and specific KRAS somatic mutation analysis on whole-genome amplified DNA from archival tissues J Mol Diagn. 2010 Jan;12(1):27	91
Chapter 6	Rapid KRAS, EGFR, BRAF and PIK3CA mutation analysis of fine needle aspirates from non-small-cell lung cancer using allele-specific qPCR PLoS One. 2011 Mar;6(3):e17791	109
Chapter 7	Concluding remarks and future directions	125
Chapter 8	Summary and “Nederlandse samenvatting”	133
	List of publications	139
	Acknowledgements	147
	Curriculum vitae	149

Aims and outline

Pathology laboratories throughout the world have compiled large archives of unique collections of tissue specimens. These tissue samples are used for patient diagnostics and research. Novel molecular insights into alterations in normal cellular function have led to the identification of targets for innovative therapies. Testing for biomarkers combined with molecular pathology has created the potential for “personalized medicine” and improved diagnosis, treatment and prognosis. New technologies for molecular analysis in molecular tumor diagnostics and research must be developed and implemented to keep pace with the latest insights, resulting in a constant cycle of change. Such translational research can only progress if patient material can be accessed from the archives for further study. The resulting new insights and strategies will eventually be implemented in patient care.

This thesis describes three important issues in this cycle of change with a focus on molecular pathology.
First, due to advances in the treatment of cancer, the amount of patient material that is available for diagnostics and research is decreasing, while the number of requests for diagnostics is rapidly increasing. Early diagnosis and the increasing application of neoadjuvant therapies are primarily responsible for this trend. The latter is, without a doubt, beneficial to the patient but makes the (molecular) diagnostics of the material increasingly challenging.
Before molecular techniques can be applied for diagnostics or research, nucleic acids must be extracted from the archived tissue. Because the tissue is fixed in formalin and embedded in paraffin, the nucleic acids are crosslinked and fragmented and, consequently, of poor quality. Therefore, DNA isolation procedures must be improved, and if the amount of DNA remains too low for biomarker testing, analysis methods such as whole genome amplification should be considered.
Second, new state-of-the-art technologies must be developed constantly. Methods should be validated and implemented and be applicable for use with the small amounts of DNA isolated from tissue that is heavily degraded in the embedding process.
The third focus of this thesis is the use of bio-informatics approaches. For the genomic data analysis of tumors in some applications, only limited analysis software is available. In a research environment, new tools must be developed, applied, or adapted for the analysis of the acquired data. After validation, these tools can be implemented in the daily routine of molecular tumor diagnostics.

In **chapter 1**, developments in pathology over the centuries and molecular technology and pathology in recent decades are summarized in a historical perspective. Some important genes and interesting genomic phenomena are highlighted in the context of their clinical implications. Guided by the description of a DNA analysis pipeline, the three different foci of this thesis, pre-analysis

technologies, technological advances and analysis strategies, are further introduced. **Chapter 2** demonstrates how DNA can be isolated from formalin-fixed, paraffin-embedded (FFPE) material and compares two different techniques: a manual method and a fully automated DNA isolation method. **Chapters 3 and 4** describe multiplex ligation-dependent probe amplification (MLPA) as an assay for the detection of multiple chromosomal deletions in tumor tissue in a single experiment. We developed and validated a MLPA-based assay to identify chromosomal losses in formalin-fixed and paraffin-embedded oligodendroglial tumors. To assure a reliable workflow for this technology, a data management system, MLPAInter, was developed to interpret the MLPA data stream. **Chapter 5** reveals how limited amounts of DNA can be amplified in a whole-genome amplification (WGA) process in which a two-step mutation screening protocol is applied. First, a high-resolution melting analysis (HRM) is used as a prescreening method for samples harboring mutations, and direct Sanger sequencing is then employed for the final diagnosis of the mutations. The *KRAS* gene was used as a model system because the accurate detection of *KRAS* mutations is critical for the molecular diagnosis of cancer and may guide proper treatment selection. In **chapter 6**, the reliability with which allele-specific quantitative real-time PCR with hydrolysis probes could be performed on fine-needle aspirates from non-small-cell lung cancer (NSCLC) patients was studied by comparing the results with histological material from the same patients. Finally, future directions and concluding remarks are presented in **chapter 7**.

Chapter 1

General Introduction

Parts of this chapter have been published previously and have been adapted in a modified form.

High-Resolution Analysis of Genomic Copy Number Changes.
Hermsen M, Coffa J, Ylstra B, Meijer G, Morreau H, van Eijk R, Oosting J and van Wezel T. (2010) High-Resolution Analysis of Genomic Copy Number Changes, in Genomics: Essential Methods (eds M. Starkey and R. Elaswarapu), John Wiley & Sons, Ltd, Chichester, UK. doi: 10.1002/9780470711675.ch1

Genotyping and LOH Analysis on Archival Tissue using SNP Arrays.
van Eijk R, Middeldorp A, Lips EH, van Puijenbroek M, Morreau H, Oosting J and van Wezel T. (2010) Genotyping and LOH Analysis on Archival Tissue using SNP Arrays, in Genomics: Essential Methods (eds M. Starkey and R. Elaswarapu), John Wiley & Sons, Ltd, Chichester, UK. doi: 10.1002/9780470711675.ch3

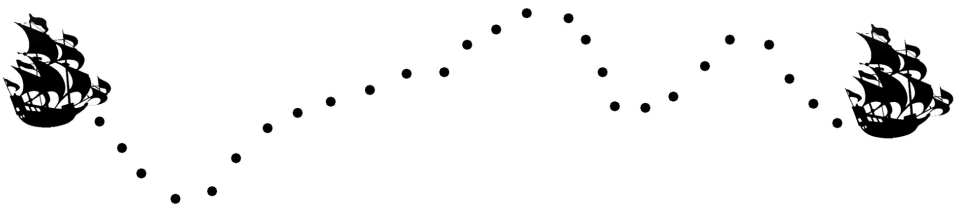

Pathology: a historical perspective

The history of pathology began 3500 years ago with the documentation of disease by the Egyptians. Throughout the centuries, individuals in the Greek (Hippocrates and Aristotle, 4th century BC), Roman (Celsus, 1st century AD, and Galen, 2nd century AD), medieval Byzantine (Aetius, 6th century AD) and Arab (Avicenna and Avenzovar, 11th century AD) empires contributed to the medical field. [1] It can be claimed that anatomical pathology, or pathology as a separate medical specialty, began with the work of the Florentine physician Antonio Benivieni (1443-1502) [1,2]. Benivieni described autopsies and case histories and his work was published titled *De Abditis Morborum Causis* (The Hidden Causes of Disease). Some of his autopsy protocols are similar to those currently in use [2]. The first modern book of anatomy is mostly attributed to Andreas Vesalius (1514-1564). He published his *De humani corporis fabrica* (The Fabric of the Human Body) in 1543 (Nutton 2012). In 1554 Jean Francois Fernel (1497-1558) introduced the term "Pathology" in his *Medicina [3].*

The work of these pioneers was continued by others, including Giovanni Batista Morgagni (1682-1771) who started correlating signs and symptoms with findings at dissection, John Hunter (1728-1793) considered founder of scientific surgery, Mathew Baillie (1761-1823) by introducing the systematic study of pathology and Marie Francois Xavier Bichat (1771-1802), who contributed to the founding of histology [1,4–7]. Unfortunately, all this work did not contribute much to the health of the individual patient. Many pathological observations were made post-mortem, and patient treatment did not significantly improve for centuries [8]. Pathology was inseparable from other medical specialties, and individuals often had both pathological and clinical skills [1].

New spectacular developments in pathology arose in the mid-nineteenth century, largely because of the introduction and implementation of novel medical technologies; for the first time, it became common practice to apply pathological findings in patient care. Together with these changes, pathology developed as an independent medical profession. Thomas Hodgkin (1798-1866), later known for the eponymous disease, was one of the first to recognize that the "*microscope might lead to useful discoveries in the future*" [1]. Indeed, the microscope changed pathology by making it possible to histologically examine tissue on the cellular level. Since Rudolf Virchow published his text entitled *Cellular Pathology* in 1858, the basic understanding of cancer has greatly changed from an organ-based disease to a cell-based disease [9,10]. During this time period, along with anatomical pathology, "surgical pathology" was introduced in 1819 [10]. Other technological advances further enhanced the ability to pathologically examine tissue. In 1863, the introduction of the natural dye hematoxylin, derived from the logwood tree (*Haematoxylum campechianum*), led to the first successful description of the hematoxylin staining technique that is utilized today [11]. Beginning in 1826 synthetic aniline dyes were developed and contributed to the development of numerous histochemical stains [12]. The introduction of

the freezing microtome in the 1870s, paraffin wax embedding (1869, Edward Klebs) and tissue fixation with formaldehyde (1893, Ferdinand Blum) began a new area for the “modern” pathologist. It became possible to pre- or intra-operatively contribute to the diagnosis and treatment of a patient [10]. In the 1870s, Carl Ruge, a German gynecologist, microscopically diagnosed cervical and uterine cancer and may have been one of the first international consultants to interpret material from other countries [13]. In the 1890s, frozen sections were examined during breast cancer surgery. In this early period of surgical pathology, misdiagnosis and technological issues contributed to debate on the usefulness of these technologies, which lasted until additional technological advances were introduced in the pre-World War II era [10]. In 1941, Albert Coons and colleagues labeled an antibody with a fluorescent dye and used it to identify an antigen in tissue sections: Immunohistochemistry (IHC) was born. Since that time, tumor diagnosis has relied primarily on histopathological and immunohistological features [14,15].

The dawn of another era that significantly influenced pathology was at the horizon, “Molecular Pathology”. Although the cellular nature of tumors was described in the early nineteenth century, it was not until 1890 that David Paul von Hansemann (1858-1920), a German pathologist and a coworker of Rudolf Virchow, introduced the term “*anaplasia*” and proposed that normal cells are converted to tumor cells when they acquire chromosomal abnormalities[16]. At the same time, Theodor Boveri (1862-1915), who did not focus his studies on cancer, applied his observations of dividing sea urchin eggs and their abnormalities to what he perceived to be the genetic basis of malignancy. In 1914, he formulated 20 specific hypotheses regarding cancer biology in his book *zur Frage der Entstehung maligner Tumoren*; almost all of these hypotheses have been verified by studying cancer chromosomes in the 100 years after his publication [16,17]. These discoveries would not have been possible without yet another breakthrough that revolutionized pathology.

This was the description of the DNA double helix in 1953 by Watson and Crick [18]. This was the starting point of many new developments in molecular technologies which yielded many new insights into the molecular pathogenesis of cancer. These insights have had a large impact on cancer diagnosis, prognosis and therapeutics [19]. Fluorescence in situ hybridization (FISH) was first described in 1969 [20] and was applied in clinical diagnostics to detect HER2 amplification in breast cancer in 1992 [21]. The application of Southern blotting [22] and comparable techniques, such as pulsed-field gel electrophoresis [23], allowed researchers to identify molecular variations more rapidly. The construction of molecular probe collections and the discovery of restriction fragment length polymorphisms (RFLPs) enabled the mapping of the human genome [24] and the positioning of many genes [25–27] (figure 1). The study of the molecular basis of disease was further facilitated by the development of the polymerase chain reaction in the early 1980s at Cetus Corporation in California. Kary Mullis

was awarded the Nobel Prize for chemistry in 1993 for his contributions [28]. The introduction of fluorescent PCR, in which the increase in fluorescence per cycle can be monitored, made PCR the method of choice for gene expression studies and direct mutation analysis (Deepak et al., 2007).
Sanger sequencing was described in 1977 [29], and the combination of this method with PCR led to the detection of point mutations, polymorphisms and other small DNA rearrangements [30]. Sanger sequencing was most likely the first molecular methodology suitable for high-throughput, fully automated data acquisition and commercialization [31] and led to the first complete sequencing of the human genome [32,33]. With the introduction of massive parallel sequencing or "next-generation" sequencing strategies, DNA sequencing costs were dramatically reduced. The 1000 Genomes Project was consequently launched in 2008 [34–36], and reliable sequencing and analysis of complete cancer genomes became possible [37].

3110 *Nucleic Acids Research, Vol. 18, No. 10*

An additional MspI RFLP at the human hepatic lipase (HL) gene locus

R.van Eyk, L.Chan[1], B.Top, A.F.H.Stalenhoef[2], L.M.Havekes[3] and R.R.Frants
Department of Human Genetics, State University Leiden, PO Box 9503, 2300 RA Leiden, The Netherlands, [1]Departments of Cell Biology and Medicine, Baylor College of Medicine, Houston, TX 77030, USA, [2]Department of Medicine, University Hospital Nijmegen, PO Box 9101, 6500 HB Nijmegen and [3]Gaubius Institute TNO, PO Box 612, 2300 AP Leiden, The Netherlands

Source/Description: λHL2 contains a cDNA corresponding to the human hepatic lipase mRNA from position −8 to the poly A tail (1).

Polymorphism: In addition to the previously reported 1.0/1.2 kb MspI RFLP (1) MspI detects an additional RFLP with two allelic fragments of 4.8 and 5.8 kb.

Frequency: Studied in 61 Caucasians: 5.8 kb allele = 0.95
4.8 kb allele = 0.05

Not Polymorphic For: See (1).

Chromosomal Localisation: Human hepatic lipase is assigned to chromosome 15q15-q22 (1).

Mendelian Inheritance: Co-dominant inheritance demonstrated in four 2-generation families with 30 members.

Probe Availability: Request for probe to LC at the above address.

Acknowledgements: This work was supported partly by the Dutch Heart Foundation (88.100 to AFHS and RRF) and by the U.S. National Institutes of Health (HL-16512 to LC).

Reference: 1) S. Datta *et al.* (1988) *J. Biol. Chem.* **263**, 1107−1110.

Figure 1. An additional MspI RFLP at the human hepatic lipase (HL) gene locus.

These technological advances over the years have and will continue to have a large impact on cancer research. Molecular pathology in combination with molecular tumor diagnostics has become standard hospital practice for genetic and genomic testing for clinically relevant discoveries in cancer [38,39].
The discovery of activating mutations in *BRAF* in several cancer sub-types in 2002 and the report of activating mutations in *EGFR* in lung cancer [19] in 2004 led to the development of high-throughput molecular screening methodologies. Personalized medicine has become an important strategy for oncologists, with the consequent need to test small or limited amounts of material and deliver the test results to the clinic as quickly as possible [40,41]. This all contributed to unprecedented beneficial outcomes for oncology patients. One of the most imaginative examples is the “Lazarus” effect, the concept that patients almost literally rise from the dead, on lung cancer patients with a specific EGFR mutation, and therefore a poor prognosis, that are subsequently treated with tyrosine kinase inhibitors [42].

Pathology: a local perspective
Leiden University, founded in 1575, and the Leiden University Hospital have a long history of developing and implementing novel ideas and technologies in anatomical and clinical pathology. In 1593, one of the first anatomical theaters in Europe was established [43]. A reconstruction of this theater can be visited in the Boerhaave museum in Leiden. Nicolaes Tulp (1593-1674), later portrayed by Rembrandt in “The Anatomy Lesson of Dr Nicolaes Tulp”, studied medicine in Leiden and, after moving to Amsterdam, contributed to medicine with his work *Observationes Medicae*. In it, he described in detail more than 200 cases of disease and death [44].

In the same period, Franciscus de le Boë Sylvius (1614-1672) came to Leiden as a physician and anatomist. At his instigation, the first University Chemical laboratory in Europe was founded in 1669 [45]. One of his students was Theodor Kerckring (1638-1693), who published the *Spicilegium anatomicum*, an anatomical atlas of clinical observations, medical curiosities, autopsy discoveries and general anatomical information. He used a microscope to investigate the folds in the small intestine [46].

Herman Boerhaave (1668-1738) made an important contribution to pathology by publishing autopsy reports of patients with a documented recent medical history [1]. Bernhard Siegfried Albinus (1697-1770), one of Boerhaave’s students, became one of the most famous anatomy teachers in Europe. In his work, *Tabulae sceleti et musculorum corporis human*, Albinus and his coworker, the artist and engraver Jan Wandelaar (1690-1759), employed a novel technique to increase the scientific accuracy of the anatomical illustrations. It was based on the artists’ traditional drawing-frame, which contained a grid to achieve systematic control over the rendering from a precisely established viewpoint [47].

Figure 2. Leiden Professors of Pathology in the 19th and 20th century.

A
S.S. Rosenstein (1832-1906)
Special Collections, Leiden University library

B
T.H. MacGillavry (1835-1921)
From the LUMC Department of Pathology Collection

C
D.E. Siegenbeek van Heukelom (1850-1900)

D
N. P. Tendeloo (1864-1945)

E
G.O.E. Lignac (1891-1954)

F
Th. G. van Rijssel (1917-1994)

G
A. Schaberg (1918-1999)

H
Ph.J. Hoedemaeker (1937-2007)

Gerard Conrad Bernard Suringar (1802-1874) contributed to this early part of the "Leiden history of medicine" by publishing 18 articles on it in the Nederlandsch Tijdschrift voor Geneeskunde between 1860 and 1870. Allard Calcoen, in his thesis *Onder Studenten* [48] describes the role of Leiden pathologists contributing to new directions in pathology in the second half of the 19th century.

Samuel Siegmund Rosenstein (1832-1906, figure 2), a prominent student of Rudolf Virchow became, after a period in Groningen, a professor at Leiden in 1873. He was one of the first clinicians in the Netherlands to recognize the importance of micro-organisms as a cause of infectious disease, and he was the first to describe and demonstrate the presence of tuberculosis cells in patients with kidney tuberculosis [48]. In 1899, he reminisced about the significant progress in the clinical treatment of patients, especially in the second half of the 19th century. Medicine moved from a time when theoretical and practical medicine were distinct to a period of close collaboration between physiological and pathological anatomy and the clinic, which he described as a "threefold alliance". As examples of the technical advances that contributed to this alliance, he described the application of the ophthalmoscope, the laryngeal mirror and the thermometer and laboratory developments in electric equipment, microscopy, the microtome and staining methods. Significant breakthroughs in surgery, bacteriology and pharmacology also contributed to improved patient care [49].

Other pioneers in this "new directions in medicine" included Theodorus Henricus MacGillavry (1835-1921, figure 2) and Daniel Eliza Siegenbeek van Heukelom (1850-1900, figure 2). Macgillavry, once characterized as "a man who can think microscopic", employed light microscopy techniques to study human leukemia [50]. When he arrived at Leiden, he remarked that the University was flourishing; however, he was unable to find a space that, in his opinion, could rightly be named a "Pathological Laboratory" unless "pathologically would be translated as inadequate and laboratory by booth." He sometimes performed pathological experiments in his house. His efforts contributed to the construction of a new laboratory that opened in 1885: The Boerhaave Pathologic Anatomic Laboratory located at Steenstraat 1A in Leiden (Figure 3). Siegenbeek van Heukelom, another skilled microscopist, garnered the most fame in the area of medicina forensis. In his capacity as 'police doctor', he observed organic changes in individuals who died post-operatively or collapsed after receiving chloroform anesthesia and consequentially contributed to the reduced use of chloroform as an anesthetic [48].
Nicolaas Philip Tendeloo (1864-1945) elevated the level of study in general pathology and pathological anatomy in the Netherlands, and a new laboratory for general pathology, anatomy and forensic medicine was designed and built based on his ideas and opened in 1925 at Wassenaarseweg 62/70 (Figure 3) [51,52]. This laboratory was used until 1994, when the department of pathology moved to its current location in the LUMC building at the Albinusdreef (Cicero 1994, vol 9, p16).

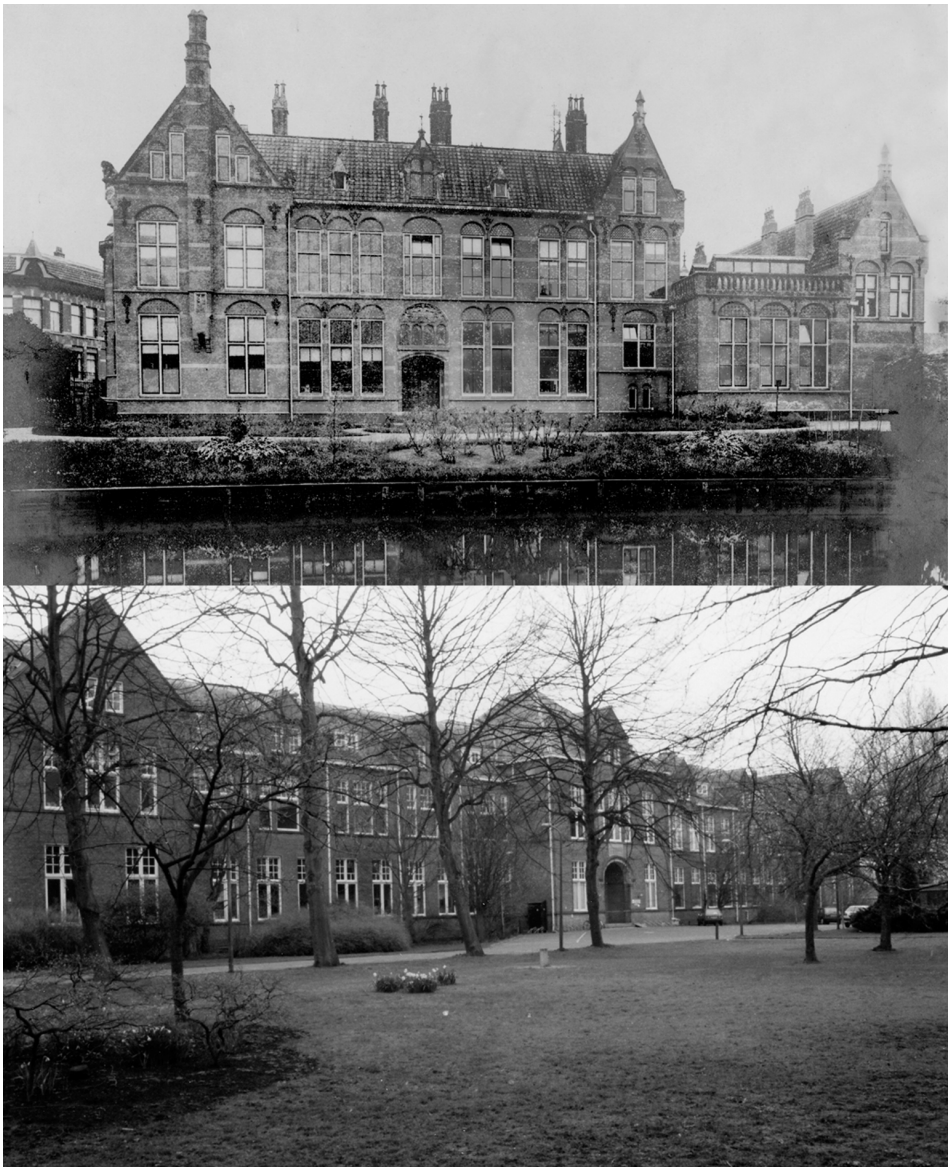

Figure 3.
Upper: The Boerhaave Pathologic Anatomic Laboratory at Steenstraat 1A, Leiden. In use from 1885-1925. Photo by amanuensis A. Mulder 1915.
Lower: Pathology Laboratory at Wassenaarseweg 62, Leiden. In use from 1925-1994. Photo by K.G. van der Ham, ca. 1993.

"*Quo vadis?*" was the intriguing title of an article published in 1952 in the "Nederlandse tijdschrift voor Geneeskunde" by George Otto Emile Lignac (1891-1954, figure 2) [53]. After reviewing the history of pathology, he predicted the biological importance of ribonucleotides and deoxyribonucleotides and concluded by stating: "Van de cellulaire tot de moleculairer pathologie, zal men zeggen. Inderdaad, deze weg moet onvermijdelijk worden begaan", which means:
"From cellular to molecular pathology, man will say: Indeed, this road must inevitably be chosen". And indeed, that road was taken.
An early reference to the use of molecular technology in the department is found in the 1958-1959 Pathology Annual Report. It states that Aart Schaberg (1918-1999, figure 2) initiated research to image chromosomes in malignant tumors (Verslag over de cursus 1958-1959, p4-§G3
As early as 1954, the year that Prof. Lignac tragically died in an airplane crash, Piet van Duijn (1921-2007) published a "new method" for the "combined staining of DNA and a number of polysaccharides" [54]. Theo van Rijssel (1917-1994, figure 2) succeeded Lignac in 1956, and he united diagnostics, educational and research. Several new technologies were introduced [55]. In the early 1960s Piet van Duijn expanded his interest to quantitative cytochemistry of DNA in the nucleus of different cell types and at different stages of cell division. He and his coworkers contributed much to the automation of cytochemical and cytogenetic analysis and the introduction of FISH (fluorescent in situ hybridization) in cytogenetic diagnosis. (van Duyn, 1960) (http://www.knaw.nl, accessed January, 2013).
In the same period and in collaboration with the Department of Histo and Cytochemistry, Sebastiaan Ploem developed an epi-illuminator known as the Ploem-opak, which has become an indispensable element in fluorescence microscopy (Cicero 2005, vol 12, p9).
The creation in 1971 of the "Foundation Pathological Anatomical National Automated Archive" (PALGA) was important for pathology in the Netherlands. Philippus Jacobus Hoedemaeker (1937-2007, figure 2) was one of the founders. Because of this system, the national cervical cancer screening study successfully began. Since then, the PALGA database has become a valuable resource for PA departments in the Netherlands to quickly and efficiently diagnose and determine the best treatment for cancer (http://www.knaw.nl, accessed January, 2013).
In the 1970s and 1980s, Cees Cornelisse, Dirk Ruiter, Philip Kluin and Gert-Jan Fleuren (head of the department 1993-2012), supported by their coworkers, further developed the molecular research in the department. DNA imaging technology and flow cytometry were used for the analysis of cervical and ovarian cancer [56–58]. From the early 1990s, in situ hybridization and chromosome and cosmic libraries were made available and used for the interpretation of chromosomal rearrangements [59–62]. PCR was introduced [63] and used to detect the loss of heterozygosity in fresh and archival tissue [64,65]. Polymorphic microsatellite markers were used to type flow cytometric sorted cells [66,67] and to identify potentially mixed-up samples [67].

Because of its clinical relevance, molecular diagnostic testing was first used in 1992 when clonality testing was performed using Southern blotting on 32 T-cell lymphomas (Jaarverslag Laboratorium voor Pathologie 1992, p28§F). Under the supervision of Hans Morreau, a preliminary list for molecular pathological indications was prepared in 1997, and in 1998 a quality control system for molecular testing was implemented in the laboratory (Jaarverslag Laboratorium voor Pathologie 1997, p32§E). In 1996, the first automated DNA sequencer, a gel-based ABI Prism® 377, was implemented in the laboratory, enabling new molecular testing techniques that focused on loss of heterozygosity (LOH) detection and microsatellite instability testing in colorectal cancer.
Since 1992, the number of molecular diagnostic consultations has increased to over 3000 in 2010. Over the years, there has been a constant demand for the development, validation and implementation of new and often high-throughput molecular technologies. In addition, new technological developments have been applied in the laboratory for molecular research. In 2003, the tissue microarray technique, which was developed by Sauter and Kallionemi [68], was introduced in Leiden [69], followed by microarray-based gene expression technologies [70]. Microarrays based on single nucleotide polymorphisms (SNPs) were used to detect the genome-wide loss of heterozygosity and other chromosomal aberrations [71,72], and since 2009, the first steps toward high-throughput sequencing have been made.

Pathological workflow
Tumor tissue becomes available for pathological examination at various disease stages through pre-operative testing by fine needle aspiration, tissue biopsy and the surgical treatment of patients with cancer. After delivering the crude material to the Department of Pathology, representative tissue samples are taken for further processing, including formalin-fixation and paraffin-embedding. In Dutch academic centers such as the LUMC, pathology departments maintain a systematic archive with millions of FFPE tissue blocks that have been collected and stored over the years. The oldest series of accessible paraffin blocks in the LUMC Department of Pathology dates back to 1946, and we estimate that a total of over 2.2 million blocks have been archived over the last 65 years.
To examine the material, pathological tissue sections are cut from the FFPE blocks with a microtome, stained with hematoxylin and eosin and delivered to the pathologist for initial examination and diagnosis.
The pathologist can further refine his diagnosis by making use of a selection of immunostaining, microscopy and molecular analysis techniques. After a molecular request is made, nucleic acids are extracted, the requested molecular analysis is performed and the results are reported and integrated in the pathological reports, which are communicated to the clinic. The remaining material is stored in the archives. Patient material can be subsequently used for scientific research and analysis according to medical ethical guidelines described in the Code for Proper Secondary Use of Human Tissue established by the Dutch Federation of Medical Sciences (http://www.federa.org, accessed January, 2013) as well as

local medical ethical guidelines. According to these guidelines, all human material used in research studies should be anonymized.
All clinical pathology processes are defined in protocols and standard operating procedures. The process of molecular analysis can be defined in a four-part workflow:

1: *Molecular pathological consultation*
2: *Pre-analysis technology*
3: *Molecular testing*
4: *Data acquisition, analysis and storage*

These four parts are schematically illustrated in figure 4. The majority of molecular pathological consultations can be handled using high-throughput processes, while customized solutions are available for less frequent tests. The workflow is not static but is influenced by technological and biological demands, developments and improvements. New developments should be validated and implemented to maintain high standards in patient care.

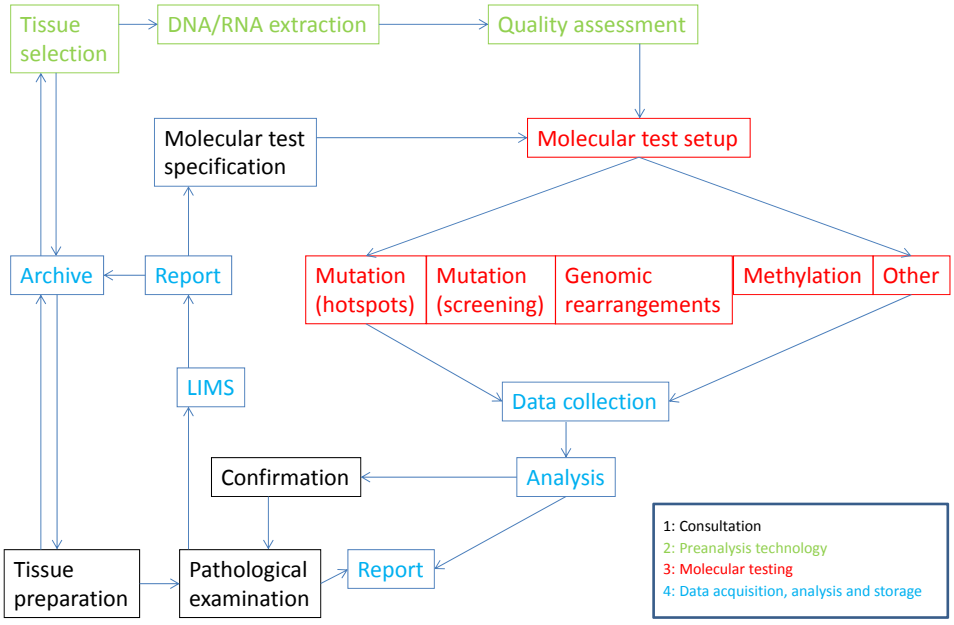

Figure 4. Diagram of the molecular analysis workflow.

Molecular analysis workflow

1: Molecular pathological consultation

The pathologist first decides which molecular pathological test to perform. Consultations for mutation hotspot analysis or extended mutation screening are frequent. Other consultations can be requested to detect genomic rearrangements and multi-gene or methylation-specific events. After a brief introduction to tumor genesis and general molecular principles, the different types of consultations for the detection of somatic mutations, multiple gene events, genomic rearrangements and methylation-specific events will be discussed.

Tumorigenesis

In essence, cancer is a genetic disease. Although certain cancers have specific unique characteristics, the development of human tumors is characterized by hallmarks that have been postulated and refined over recent decades. Mutations that affect oncogenes, tumor suppressor genes and tumor stability genes have been discovered, and these genes play an important role in tumor formation and progression [73–75].

Oncogenes and activated proto-oncogenes are characterized by a dominant gain of function and can have different origins. The first confirmed oncogene, Src, was discovered in 1976 by Bishop and Varmus, who received a Nobel Prize in 1989 for their work. Src encodes a tyrosine kinase, and mutations in Src lead to the malignant progression of cancer [76,77]. Src inhibitors have been developed and are utilized to treat cancer patients [78]. The Philadelphia Chromosome is another early example of an oncogene and became an early example of the use of chromosome analysis for cancer diagnostics. This chromosomal abnormality was first described in 1960 when Hungerford and Nowell detected a tiny aberration in the chromosomes of cultured blood cells taken from two patients with chronic myelogenous leukemia [79]. The Philadelphia Chromosome is created by the translocation of the sections of chromosomes 9 and 22 that include the Abl and Bcr genes, respectively. The Bcr-Abl fusion gene formed by this translocation codes for a constitutively active receptor tyrosine kinase that causes uncontrolled cell proliferation. Research efforts led to the development of imatinib mesylate (Gleevec), which was the first in a new class of genetically targeted agents, a major advance in cancer treatment [80]. *MYC* is another proto-oncogene and has been implicated in Burkitt's Lymphoma, named after Denis Parsons Burkitt, the surgeon who first described the disease in 1958 [81]. The MYC gene encodes a common transcription factor. In Burkitt's lymphoma, patients have a chromosomal translocation that moves an enhancer sequence near the *MYC* gene, resulting in increased expression of this transcription factor [82]

Tumor suppressor genes are divided in gatekeeper genes and caretaker genes, based on their function and generally follow the hypothesis that both alleles of the gene must be affected for cancer to develop. This two-hit hypothesis was

formulated by A.G. Knudson while studying retinoblastoma [83,84]. There are exceptions to the "Knudson" model for tumor suppressors; for example, "dominant-negative" mutations in the *TP53* gene produce a mutated p53 protein that inhibits the function of p53 produced by the wild-type allele [85]. Other exceptions to the Knudson model include tumor-suppressor genes that exhibit haploinsufficiency. In these cases, the level of one or multiple gene products is not sufficient for the cell to function normally. Haploinsufficiency of many genes, including *APC, ATM, BRCA1, BRCA2, TP53,* and *RB,* has been shown to contribute to tumorigenesis [86]. Gatekeeper genes such as *APC*, *RB* and *TP53* inhibit tumor growth or promote tumor death. Inactivation of a gatekeeper gene often leads to tissue specific types of cancer such a Retinoblastoma or Adenomatous polyposis coli [87,88]. Caretaker or stability genes are another class of tumor suppressor genes, that promotes tumorigenesis in a different, more indirect way, when mutated [75,88]. This class includes the mismatch repair (MMR), nucleotide-excision repair (NER) and base-excision repair (BER) genes responsible for repairing mistakes that occur during DNA replication or that are induced by mutagen exposure. Consequently, mutations in this class of genes increase the mutation rate of other genes. Similarly to tumor-suppressor genes, both alleles of stability genes typically must be inactivated to produce an effect [75]. Examples of genes in this class include *BRCA1, BRCA2,* which have been implicated in breast cancer and *MLH1, MSH2, PMS2, MSH6* and *MUTYH* in colon cancer. Many of these genes are currently being tested as molecular diagnostic markers.

Cancer cells can develop as a consequence of aberrations in these classes of genes. Eight different hallmarks of cancer cells have been postulated, and collectively they dictate malignant growth: self-sufficiency in growth signals, insensitivity to growth-inhibitory (antigrowth) signals, evasion of programmed cell death (apoptosis), limitless replicative potential, sustained angiogenesis, tissue invasion and metastasis, reprogramming of energy metabolism and evading immune destruction. Cancer cells do not act in isolation; rather, they subsist in a rich and heterogeneous microenvironment where the tumor stroma contributes to cancer initiation, growth and progression. All this should be considered in the molecular diagnosis and treatment of cancer [73,74,89].

Somatic mutations

Many examples are available to illustrate the need for somatic mutation analysis in patient care. For instance, mutations in the *KRAS* oncogene, codons 12, 13 and 61 are frequently found in many cancers. Activating mutations in *KRAS* codons 12 and 13 are associated with resistance to TKIs in non-small-cell lung carcinoma (NSCLC) [90,91] and are used to predict resistance to monoclonal antibody therapy in colorectal cancer (CRC) [92,93]. A specific *KRAS* c.34G>T transversion may indicate a failure in the base excision repair mechanism in colon cancer due to germline mutations in the *MUTYH* gene [94].

For *BRAF*, the V600E variant and the more rare V600K variant are found in the majority of cutaneous melanomas, and mutation-positive tumors can be treated with vemurafenib (PLX4032), which targets these molecules [95,96]. In papillary thyroid carcinoma (PTC), the V600E mutation appears to be refractory to radioactive iodine treatment, which consequently leads to a poor clinical prognosis [97,98]. However, initial studies have demonstrated that these thyroid cancers do not clinically react upon vemurafenib (PLX4032) treatment. Although reports indicate that the V600E alteration predicts resistance to monoclonal antibody therapy in colorectal cancer and NSCLC [90–93] , this knowledge has not been used clinically to date.
Mutations in the PIK3CA gene may play an important role in CRC but have not been associated with specific therapies and are still under study [99]. The *PIK3CA* hotspot mutations E542K, E545K, H1047R are also reported in NSCLC [90,91].
Hotspot mutations in *NRAS* and *HRAS* are present in specific types of benign and malignant thyroid cancers. *NRAS* mutations in codon 61 are reported to be involved in tumor progression and a more aggressive clinical behavior of the tumor [97,98,100].
Specific mutations in *GNA11* and *GNAQ* are found in uveal melanoma, which can be treated with MEK inhibitors [101].
Specific somatic heterozygous mutations in the isocitrate dehydrogenase genes *IDH1* and *IDH2* have been detected in the non-hereditary skeletal disorders Ollier disease and Maffucci syndrome and aid in the subclassification of these tumors [102]. Mutations in the *IDH1* gene are also found in malignant gliomas and have been used to further evaluate the disease [103]
A subset of NSCLC cancers may harbor an activating mutation in the *EGFR* kinase domain [104]. Deletions in exon 19 and the L858R variant in exon 21 are the most frequently found mutations, and tumors with these mutations are, in many cases, sensitive to tyrosine kinase inhibitors (TKIs). If the exon 19 and 21 hotspot mutations in NSCLC are not present, Sanger sequencing can be performed on exons 18-21 to identify rare variants that may predict a favorable response to TKI inhibitors [90,91].
The majority of gastrointestinal stromal tumors exhibit oncogenic activating mutations in the v-kit Hardy-Zuckerman 4 feline sarcoma viral oncogene homolog (*KIT* tyrosine kinase) and platelet-derived factor receptor α (*PDGFRA*) [105–107]. In different types of melanomas, mutations in *KIT* exons 11, 13 and 17 are observed, and designer compounds, such as Imatinib, may offer an immediate therapeutic benefit for these patients [108].
Sanger sequencing of exons 5-8 in *TP53* can predict if the tumor is metastatic or if a secondary primary tumor has emerged [107,109]. Beta-catenin (*CTNNB1*) analysis is performed in desmoid fibromatosis to establish differential diagnosis and prognosis. The most frequently found mutations are in exon 3 and serve as potential molecular tools for disease management [110].

Multiple gene events and genomic rearrangements
Two major genetic mechanisms are frequently involved in CRC formation: the

chromosome instability (CIN) and microsatellite instability (MSI) pathways. Testing for CIN and MSI status can provide insight into the prognosis of the patient. In general, CIN+ and MSI+ cancers have worse and better prognoses, respectively [111–113].
The detection of 1p/19q chromosomal deletions has become essential for treatment decisions for cancer of the central nervous system. Oligodendrogliomas presenting with 1p/19q chromosomal deletions have favorable responses to chemotherapy and a substantially longer survival [103,114].
Other markers used in the evaluation of malignant gliomas are alterations in the epidermal growth factor receptor (EGFR) pathway and chromosomal deletions and amplifications in *CDKN2A* (p16), *EGFR*, *ERBB2* (HER2), *PTEN* and *TP53* [114,115].
Chromosomal rearrangements also play an important role in the formation of the thyroid cancer variant PTC. The rearranged during transfection (RET) gene is a tyrosine kinase receptor located on chromosome 10 and is often found to be mutated in PTC. Thus far, 13 different types of *RET*/PTC rearrangements have been identified [116]. *RET*/PTC chimeric proteins lead to constitutive activation of the tyrosine kinase domain and other downstream pathways. Compounds that have an inhibitory effect on the kinase activity of RET have been identified and tested in multiple clinical trials [97,98,100].
Gene fusions, which occur due to specific chromosomal translocations, are observed in many soft tissue tumors, such as Ewing sarcomas. These rearrangements help to improve the diagnosis of a wide variety of sarcomas in children and young adults [117]. The fusion of anaplastic lymphoma kinase (*ALK*) with echinoderm microtubule-associated protein-like 4 (*EML4*) is present in approximately 5% of all NSCLC cases and has become a clinical target for ALK inhibitors [118].
Recently, more and different *RET*, *ALK* and *ROS* fusions have been identified in lung adenocarcinomas through whole-genome and transcriptome sequencing [119], targeted next-generation sequencing [120] and integrated molecular- and histopathology-based screening [121] and will most likely be identified as relevant clinical targets.

Methylation specific events
The inactivation of tumor-suppressor genes by DNA methylation in the promoter region of the gene is associated with a loss of expression and plays an important role in gene silencing. These effects are well recognized in carcinogenesis and can have diagnostic, prognostic and predictive value [122].
Hypermethylation of the *MLH1* promoter can be used to subclassify sporadic colon cancer patients with a microsatellite instable (MSI) pattern from those with Lynch syndrome MSI tumors [111,123].
The methylation status of the O-6 methylguanine-DNA methyltransferase (*MGMT*) promoter is used to evaluate malignant gliomas [124]. Epigenetic silencing of *MGMT* augments sensitivity to temozolomide, which damages DNA by methylating the O-6 position of guanine, leading to cell death [114,115]

2: Pre-analysis technology

The application of DNA methodology in tumor genetics and genomics has been hampered by two major factors. First, because the patient material is mainly used for microscopic examination and has to be prepared for long-term storage, almost all available patient material is formalin-fixed and paraffin-embedded . The fixation and embedding procedures leave cellular structures mainly intact but damage nucleic acids. Consequently, nucleic acid isolation is a challenging task and often yields heavily degraded DNA for use in further analyses. Second, due to early diagnosis and the use of novel neo-adjuvant patient treatments, the number of cases for which only very small amounts of material are available is increasing [15].

In this part of the workflow, the type of available material and how it must be processed must be defined before DNA can be isolated. In a minority of cases, high-quality DNA can be isolated from freshly frozen tumor samples, but generally, FFPE or cytological tissue is the primary source available for processing. The pathologist decides if tissue cores can be taken or if the isolation should be performed on tissue slices. If tissue slices are available, whether the whole slice can be used or if micro-dissection is necessary, should be determined. After isolation, the quality and quantity of the isolated DNA should be assessed to determine if it is sufficient to perform the next steps in the process. In some cases, the DNA has to be diluted, concentrated or treated with a whole genome amplification step. Material preservation, micro-dissection, DNA isolation, whole genome amplification and DNA quantification will be discussed further.

Tissue preservation

Fresh or freshly frozen materials are the best sources for the extraction of nucleic acids and protein. However, for the microscopic analysis of tissue slices, FFPE material has been used for over a century in daily pathological practices [125]. Storage of FFPE tissues is inexpensive, and the embedded tissue can be kept almost indefinitely at room temperature. Therefore, laboratories with pathological archives have endless amounts of FFPE tissue samples [125,126].

Tissue fixation is commonly achieved by the addition of a 4% aqueous solution of buffered formaldehyde [127]. However, in some tissue types, additional or pretreatment steps must be performed [128,129]. Unfortunately, in this process of fixation and embedding, chemical crosslinking between RNA, DNA and protein occurs. Together with the addition of monomethylol groups to nucleotide base pairs, the quality of the nucleotides in the tissue is diminished. Only degraded and short fragments of the DNA and RNA remain for use in molecular analyses [130].

Microdissection versus macrodissection

For pathological examination of FFPE material, tissue sections are cut from tissue blocks. The sections are stained with hematoxylin, which stains the cell nuclei blue, and eosin, which stains the cytoplasm and other extracellular substances red or pink. There are different methods for further processing the material to make it suitable for molecular testing. For solid tumors, it is likely that

tumor cells are present in high concentrations, making it possible to use whole tissue sections or tissue cores for DNA extraction. However, in the presence of abundant stroma and other normal cells, the tumor cells may be obscured, making these samples more difficult for specific DNA or RNA analysis. To circumvent this complication, tumor cell enrichment strategies, such as cell sorting, laser capture microdissection or manual microdissection, can be performed. With these methods, the tumor epithelium is separated from the surrounding stroma and healthy tissue [131,132].
In laser capture microdissection (LCM), a transparent thermoplastic film or other coating is applied to the surface of a tissue section on a glass slide. A laser pulse then specifically activates the film above the cells of interest, and consequently, a strong focal adhesion permits the selective procurement of the targeted cells [133,134]. LCM can process very tiny amounts of pure tumor cells, but unfortunately, this method is time consuming and labor intensive. Therefore, in many routine settings, manual microdissection is performed with a scalpel blade. In this method, guided by an H&E-stained slide, tumor fields are scratched from deparaffinized, hematoxylin-stained copies of the original tissue slice. If very little material is present, which is often the case in cytological smears of the lung, microdissection is initiated by marking the tumor foci with a diamond needle on the back of a H&E- or Giemsa-stained slide. The cover slips are removed by soaking the slides in xylene. Finally, the tumor foci are collected with a scalpel blade [135] [136].

DNA isolation
The isolation procedure begins with the deparaffinization of the tissue, which is a time-consuming step in most protocols and is often performed by xylene incubation followed by ethanol washing steps [137,138]. Several methods have been described to isolate DNA after deparaffinization. The majority of the methods require manual isolation steps, although some (semi-) automated methods have been described. Column- or bead-based methods are most commonly used [139–141]. The quality and quantity of the DNA obtained with these different techniques is variable, and the final DNA yield can be low and of reduced quality. The type, quality or quantity of the input material contributes to the DNA yield, but the isolation method can also play an important role [142,143].

Whole genome amplification
To obtain sufficient DNA for further molecular testing, additional steps, such as whole genome amplification (WGA) or other pre-amplification steps, may be necessary [144,145]. WGA ideally generates a new whole genome sample of amplified DNA (wgaDNA) that is indistinguishable from the original sample but contains a higher DNA concentration [142]. There are two types of WGA: WGA based on PCR and WGA with non-PCR-based linear amplification [146]. The major disadvantage of all WGA methods is that ideal conditions do not exist. De novo mutations can be introduced, and parts of the genome can be preferentially under- or over-represented in the wgaDNA due to GC content or repetitive

sequences. The introduction of de novo point mutations should be considered, particularly when performing further DNA tests, and wgaDNA should not be used in single nucleotide hotspot mutation analysis [147]. Some WGA methods require high molecular weight DNA. An example is the strand displacement amplification method (SDA), which is based on rolling circle amplification [148]. Primer extension pre-amplification methods have been more successfully applied to FFPE tissue because these methods can better accommodate fragmented DNA [149,150].

DNA quantification

Different methods are available to measure the quality and quantity of the isolated or amplified DNA. One method is to perform a spectrophotometric measurement using a NanoDrop® instrument. In this approach, the ratio of the absorbances at 260 nm and 280 nm is used to assess the purity of the DNA. A ratio of ~1.8 is generally accepted as “pure” for DNA. Little material is needed, and the method can be performed rapidly. However, the measured DNA concentration may be an overestimate because all DNA fragments, even if partly degraded, give a fluorescent signal. Additionally, ionic strength and pH can influence the estimated DNA concentration [151]. Nanodrop analysis is mainly used to measure the concentration of amplified DNA. If heavily degraded DNA isolated from FFPE material is measured, the DNA concentration can be overestimated, leading to the failure of downstream applications. In this situation, more accurate approaches should be used. This can be achieved by making use of an intercalating dye such as PicoGreen®. This dye is essentially non-fluorescent and will only exhibit fluorescence after binding to double-stranded DNA. A high linearity is achieved, and dsDNA concentrations can be deducted by making use of a standard curve [152]. Therefore, PicoGreen-based assays are preferred for quantitative measurements of DNA extracted from FFPE material over spectrophotometric approaches in which no, or limited, information is gained on the quality of the DNA. An apparently highly concentrated sample may be composed of heavily degraded DNA and short DNA fragments, while a sample with an apparently low DNA concentration may be composed of longer and better quality DNA. Consequently, the best way to gain insight into the quantity and quality of the DNA may be to perform “quality” PCR. In this approach, amplicons located on different loci in the genome and of different lengths (for instance, 100, 200 and 400 base pairs) are generated and further analyzed on an agarose gel or by real-time PCR, making use of threshold cycles (Cq) and melting curve profiles. The longer the fragments generated, the higher the quality of the DNA, and this can be taken into account when making DNA dilutions for genetic testing [153,154]. Alternatively, capillary electrophoresis using LabChip instruments, such as the low-throughput Agilent 2100 Bioanalyzer and the high-throughput Caliper LabChip GX can be used to give both qualitative and quantitative information about the samples. The Life technologies Qubit® 2.0 Fluorometer, used in combination with Molecular Probes® dyes or methods, is another alternative; it makes use of fluorescent dyes specific for non-degraded nucleic acids.

3 and 4: Molecular testing, data collection, analysis and storage

In the third part of the workflow, molecular testing is performed. Mutations can be detected with closed-tube (real-time) PCR technology and different types of low-throughput sequencing. Copy number and chromosomal rearrangements can be detected with more complex technologies such as multiplex ligation-dependent probe amplification (MLPA), CGH and SNP arrays. High-throughput sequencing technology can be used to combine mutation screening with chromosomal rearrangement analysis. In the fourth and last part of the workflow, all of the acquired data are processed and analyzed using dedicated software or specialized analysis tools. The analyzed data are linked to the clinical and pathological information of the patient. After a careful process of analysis and quality evaluation in a diagnostic setting, the final results are reported to the clinic. In a research setting, the data can be further processed and analyzed to answer biological hypotheses. In this section, different methods for somatic mutation detection and prescreening, including hydrolysis probe assays and high resolution melting and sequencing, will be presented. Copy number variation assays with MLPA and SNP arrays will be discussed, and high-throughput next-generation sequencing will be introduced.

Somatic mutation detection and analysis

Over the years, many different techniques have been developed and used in research and diagnostics to detect somatic mutations. Most of these techniques are based on PCR. Hotspot mutation analysis can be performed with hydrolysis probe assays [136], Matrix-assisted laser desorption ionization Time of Flight (MaldiToF) [155], SNPshot [156] and pyrosequencing [157]. For mutation scanning, Sanger sequencing, although it's sensitivity is limited to 10-20% for somatic mutations, remained for long the gold standard [158]. To accelerate the process and reduce costs, many types of prescreening methods can be applied. An example of prescreening methodology is high-resolution melting analysis (HRM or HRMA) [142], which can be used in combination with COLD-PCR [159]. Other examples include denaturing high-performance liquid chromatography (DHPLC) [160], conformation-sensitive gel electrophoresis (CSGE) [161] and single-strand conformational polymorphism detection (SSCP) [162]. High-throughput next-generation sequencing (HT-NGS), massive parallel sequencing and third-generation sequencing are all different terms for the methodologies developed over the last decade. These techniques have greatly increased sequence throughput while decreasing costs [163,164]. The first generation of HT-NGS platforms delivered 100 Mb (Roche 454 Genome Sequencer) to 3 Gb (Illumina Solid Genome Analyzer) of sequence data per run [165]. Since the introduction of HT-NGS, sequencing chemistry and hardware has rapidly improved. New small bench-top sequencers have been developed with simple sample preparation protocols and the potential for faster data generation and analysis, making them suitable for implementation in molecular diagnostics [164].

Hydrolysis probe assays

Real-time quantitative PCR permits the sensitive, specific and reproducible quantitation of nucleic acids [166] and can be used in high-throughput, automated technologies with lower turnaround times [167]. Some of the various real-time PCR chemistries use the double-stranded DNA-intercalating agent SYBR® Green 1, while others use hydrolysis probes, dual hybridization probes, molecular beacons or scorpion probes [168]. To detect hotspot mutations, the hydrolysis probe method is frequently used. This method is often referred to as the "TaqMan" assay, but this is a brand name. Concerning the chemistry of this method, the Expert Review of Molecular Diagnostics states, "*In the real-time quantitative TaqMan® assay, a fluorogenic nonextendable 'TaqMan' probe is used. The probe has a fluorescent reporter dye attached to its 5´ end and a quencher dye at its 3´ terminus. If the target sequence is present, the fluorogenic probe anneals downstream from one of the primer sites and is cleaved by the 5´ nuclease activity of the Taq polymerase enzyme during the extension phase of the PCR. While the probe is intact, FRET occurs, and the fluorescence emission of the reporter dye is absorbed by the quenching dye. Cleavage of the probe by Taq polymerase during PCR separates the reporter and quencher dyes, thereby increasing the fluorescence from the former. Additionally, cleavage removes the probe from the target strand, allowing primer extension to continue to the end of template strand, thereby not interfering with the exponential accumulation of PCR product. Additional reporter dye molecules are cleaved from their respective probes with each cycle, leading to an increase in fluorescence intensity proportional to the amount of amplicon produced*." [168]

Real-time PCR data acquisition is performed using the software provided with the real-time PCR equipment. These analysis platforms are often too basic for further data analysis, and additional dedicated software is required. For instance, to analyze expression data, Vandesompele developed the widely used tool "Genorm" [169]. The analysis of real-time SNP-type data is easier to perform. However, dedicated approaches must be used if multiple variations on the same locus are interrogated (this thesis). A very important development in real-time PCR analysis is the effort to come to a worldwide consensus on how best to perform and interpret quantitative real-time PCR (qPCR) experiments. This developments led to the drafting of a list of guidelines, the Minimum Information for Publication of Quantitative Real-Time PCR Experiments (MIQE) [170].

High Resolution Melting

HRM is a fast and simple alternative method for hydrolysis probe assays and mutation scanning in general [171]. This method is based on the principle that heating DNA results in the transition of the double-stranded DNA molecule into its two single strands. This process can be accurately monitored by measuring the fluorescence after the addition of a saturating DNA dye to the PCR reaction and after increasing time points and decreasing temperature units in an instrument with improved temperature precision [172]. A review by Erali et al. describes the main advantages of this method: *"Simultaneous genotyping with one or more*

unlabeled probes and mutation scanning of the entire amplicon can be performed at the same time in the same tube, vastly decreasing or eliminating the need for re-sequencing in genetic analysis." [173]
The analysis of HRM data depends on the instrument used and consists of one or two normalization steps. First, the fluorescence (Y) axes of HRM plots are normalized on a 0 to 100% scale. In the next, optional step, normalization to the temperature (X) axis can be applied to compensate for well-to-well temperature measurement variations between samples. Finally, the different genotypes can be identified by plotting the difference in fluorescence between the normalized melting curves. One melting curve is chosen as a reference, and the difference between each curve and the reference is plotted against temperature to yield a "fluorescence difference" plot. The original reference curve is a horizontal line at zero, and the different genotypes are clustered along different paths [171].

Sanger DNA sequencing
Sanger DNA sequencing has been one of the most widely used molecular techniques because it provides direct insight into the molecular composition of the material under investigation and can be easily automated. Sanger sequencing is based on the synthesis of a complementary copy of a single-stranded DNA template. To perform a sequencing reaction, a buffered mixture of DNA polymerase, a template-specific oligonucleotide, deoxynucleotides and fluorescently labeled dideoxynucleotides is added to the single-stranded DNA template. After cycling, DNA copies of various lengths are formed from the original template. The length of the products is determined by the position at which a fluorescent dideoxynucleotide is incorporated in the strand [31]. After capillary electrophoresis, the different length products are visualized and further analyzed with dedicated sequence analysis software. Mutation Surveyor, PolyPhred Sequencher and Sequence Pilot are commercial packages, but freeware for basic (Chromas, FinchTV) or more advanced sequence analysis (InSNP) can also be used [174]. It is important that the software can detect somatic mutations in cancer, which are often obscured as a consequence of tumor heterogeneity or the presence of excess normal DNA in the isolates. In addition, it is essential that information on mutations and variations in the human genome is communicated in a uniform way. In an effort to clarify the nomenclature, the Human Genome Variation Society (HGVS) has formulated guidelines and recommendations for gene variation nomenclature and variation databases [175–177]. Sequence variants in multiple genes per patient can be stored in a patient information system or database dedicated to the storage of gene variants, such as the Leiden Open-Source Variation Database (LOVD) [178,179].

Copy number variation detection and analysis
A number of methods can be used to detect copy number variation. A distinction can be made between methods that interrogate only one or a few loci and methods that can be applied for copy number variation analysis of the whole genome. Fluorescence in situ hybridization (FISH) and loss of heterozygosity (LOH) typing

with microsatellite markers are used to detect chromosomal imbalances in a single locus. To interrogate up to 50 different loci, multiplex ligation-dependent probe amplification (MLPA) can be performed. Genome-wide high-throughput methods, such as array-based comparative genome hybridization (array CGH) and single nucleotide polymorphism arrays (SNP arrays), have been applied in cancer research and diagnostics [72,180,181]. New developments in this field include the introduction of digital PCR for a single locus and high-throughput sequencing for whole genome-based copy number variation testing [182,183]. The use of MLPA and SNP array genomics will be discussed in more detail.

Multiplex ligation-dependent probe amplification

The MLPA technique was first described in 2002 [184] and has become a multiplex technique for determining the copy numbers of genomic DNA sequences and promoter methylation status, as well as for mRNA profiling [185]. MLPA is a PCR-based approach that is sufficiently sensitive, reproducible and sequence-specific and allows the relative quantification of up to 50 different targets simultaneously. MLPA is relatively easy to perform with standard laboratory equipment, a PCR instrument and a capillary sequencer. In MLPA, probes, not sample nucleic acids, are subject to amplification and quantification. Each locus is interrogated with two MLPA probes, which hybridize to adjacent sites of the target sequence. One probe is a short synthetic oligonucleotide, and the other is an M13-derived, long oligonucleotide. The short probe contains a target-specific sequence (21–30 nucleotides) and a 19-nucleotide sequence at the 5' end that is identical to the sequence of a labeled PCR primer. The long MLPA probe contains 24–43 nucleotides of target-specific sequence at the 5' phosphorylated end, a 36 nucleotide sequence that contains the complement of an unlabeled PCR primer at the 3' end, and a stuffer sequence of variable length in between. This variable-length fragment gives each complete probe the necessary size difference for detection and quantification using capillary gel electrophoresis [184]. When both probes are stably hybridized to adjacent sites of the target sequence, they are ligated by a specific ligase enzyme, permitting subsequent amplification. MLPA probes are identified after capillary separation by size using a selected size standard for the size calling procedure. The relative MLPA probe signals (fluorescent units) reflect the relative copy number of the target sequence. An indication of the DNA input in the MLPA reaction may be obtained by examining the dosage quotient (DQ) control fragments, fragments whose lengths always co-vary and are present in all MLPA kits. The signals of these fragments will be prominent if the amount of sample DNA is very low. By contrast, the fifth control band of 92 nucleotides is ligation-dependent and should have a signal similar to most of the other MLPA amplification products. Visual inspection of the peak pattern of a patient sample superimposed over a peak pattern of a reference run can be used to analyze a few samples [185].

The analysis of a larger series of samples, more complex diseases and MLPA runs performed with miscellaneous sample types and quality requires exportation of the peak signals and reliable normalization methods. Statistical methods

must be applied to identify probes that show aberrant copy numbers. Analysis overviews must be made available before the method can be applied in molecular diagnostics [186–188].

SNP arrays

Different methodologies of SNP typing and types of commercially available SNP arrays have been developed. Basically, two types of arrays exist: arrays with universal capture oligonucleotides or locus-specific arrays of oligonucleotides.

The SNP typing assays include methodologies such as allele-specific primer extension and whole genome sampling. Two different genotyping methods, molecular-inversion probe (MIP) genotyping and GoldenGate genotyping, are based on high-level multiplex PCR with universal primers in combination with universal arrays.

Molecular-inversion probe (MIP) genotyping arrays are commercially offered as Affymetrix OncoScan™ arrays. MIP genotyping utilizes a pool of locus-specific probes. The 5' and 3' ends of each circularizable probe anneal upstream and downstream of the SNP, respectively. The 1 bp gap is filled in a different reaction for each nucleotide. The probes are subsequently circularized using ligase to seal the remaining nick, and non-annealed and noncircular probes are removed by exonuclease treatment. Restriction digestion then releases the circularized probe, and the resulting template is PCR-amplified using common primers [189]. The reactions for each of the four nucleotides are labeled in different colors and pooled. Subsequently, the pool is hybridized to an array of universal-capture probes, and the four colors are read. With MIP arrays, the entire genome can be interrogated with more than 335,000 markers using 75 ng DNA isolated from FFPE tissue [190,191].

GoldenGate genotyping makes use of a multiplex mixture of probes for 96, 384, 768 or 1536 SNPs per array [192]. For each SNP, a combination of allele-specific and locus-specific primers are annealed to the SNP locus. These primers are tailed with common forward and reverse primers and a universal capture probe that is complementary to the locus-specific primer. The small gap between the allele and locus-specific probes is filled by allele-specific primer-extension and sealed with a ligase, resulting in an artificial allele-specific PCR template. This template is then PCR amplified using fluorescently labeled universal PCR primers. The resulting probe is hybridized to an array of universal-capture probes, and the array is scanned in a special reader, generating two fluorescent signals that represent the two different alleles of a SNP.

Locus-specific arrays of oligonucleotides, such as Affymetrix GeneChips, can detect over one million SNPs on a single chip. For instance, the Genome-Wide Human SNP Array 6.0 features 1.8 million genetic markers, including more than 906,600 single nucleotide polymorphisms (SNPs) and more than 946,000 probes to detect copy number variation. For each SNP, a set of locus-specific 25-mer oligonucleotides is present on the array. The sample is prepared according to the whole-genome sampling assay [193], a method in which the genomic complexity is reduced through restriction enzyme (RE) treatment of high-quality genomic

DNA and ligation of a common adaptor to the digested DNA. The subsequent single-primer PCR step reduces the genomic complexity through efficient size-selection in the PCR reaction. The product is then hybridized to a locus-specific array. The SNPs on the array are selected from the DNA that is represented after the complexity reduction PCR step [194].
Illumina Infinium arrays are locus-specific arrays with allele-specific capture probes. In this assay, whole-genome DNA is amplified and subsequently fragmented. The resulting probes are then denatured and hybridized to the array. An 'on the array'-allele-specific primer extension assay is followed by staining and read using standard immunohistochemical detection methods [195]. This type of array is available for genotyping, copy number variation (CNV) and cytogenetic analysis and consists of 300,000 to nearly 1.2 million markers.
After scanning the SNP arrays, the signal intensities must be converted into genotype calls. SNP calling software is available for each platform: BeadStudio for GoldenGate and Infinium, GTYPE and Genotyping Console for GeneChips, and GTGS for the MIP assay. All programs are essentially similar with three clusters automatically computed for each SNP: heterozygous AB and homozygous AA or BB. The clusters are based upon the allele-specific signal intensities. Genotyping errors and no-calls will hamper linkage and association studies, and reliable SNP calls are essential for these applications. Therefore, additional genotyping algorithms have been developed to improve the quality of the genotypes from SNP arrays. Examples of these methods are SNIPer [196] AccuTyping [197], SNPchip [198] and RLMM [199]. GTC software is available for the simultaneous analysis of SNPs, copy number polymorphisms (CNPs), rare copy number variations (CNVs) and cytogenetic aberrations (http://www.affymetrix.com/, accessed January, 2013). For sensitive analysis of copy number variation in tumors, BeadarraySNP, a Bioconductor package was introduced for the analysis of Illumina SNP array data. An algorithm, the lesser allele intensity ratio (LAIR), was developed to accurately determine allelic (im)balances. Further incorporation of the ploidy status of the tumor permits the identification of the allelic state of all chromosomal aberrations, including LOH, copy-neutral LOH, balanced amplifications and allelic imbalances. For the validation series, 300 k CytoSNP-12 (Illumina, USA) high-density SNP arrays were used [72].

High Throughput Next Generation Sequencing (HT-NGS)
With the current technological advances in next-generation sequencing, the simultaneous sequencing of hundreds of candidate genes up to the whole exome [34], the transcriptome [37,200], the epigenome [201] and the whole genome [202] has recently become feasible. HT-NGS technology provides the opportunity to identify previously unknown cancer-predisposing genes or somatic mutations in individual patients, families and tumors [203,204]. For instance, the identification of novel genes that predispose patients to colorectal cancer could be directly implemented in clinical practice. In clinical genetics centers, the knowledge of disease-related genetic mutations could be used for counseling and to advise the surveillance of these mutations in families. The identification of at-risk individuals

will result in timely and efficient customized surveillance through colonoscopy. Furthermore, these gene mutations may provide therapeutic leads to improve the treatment of cancer.

Commonly used second-generation HT-NGS platforms include the Roche 454 Genome sequencer, the Illumina Genome Analyzer and the Applied Biosystems SOLiD system [34]. These instruments are based on the massive parallel sequencing of spatially separated clonal amplicons [163]. They are mainly used to target thousands of genes in one or a few samples from which as much sequence as possible is retrieved, with the disadvantage of long runtimes of up to two weeks. In molecular tumor diagnostics, the demand will most likely be focused on the rapid sequencing of smaller subsets of genes in multiple samples with sufficient sequence depth to identify rare somatic variants in heterogeneous tumors. This demand can be met by using a combination of smaller, faster, benchtop sequencers in combination with the targeted sequencing of "DNA barcoded" samples. Instruments such as the 454 GS Junior (Roche), MiSeq (Illumina) and Ion Torrent PGM™ or Proton™ (Life Technologies) are currently available for this purpose and will likely have a decisive impact on diagnostics in the near future [205]. DNA barcoding can be achieved by adding unique tags to the ends of DNA fragments. These tags can be linked to the DNA during PCR or after the isolation of targeted sequences [34,206,207]. Targeted sequencing can be performed with customized panels, such as the Ion AmpliSeq™ Target Selection Technology, or dedicated "cancer panels", such as the Ion AmpliSeq™ Cancer Panel, which promises to assess hundreds of mutations in 10 ng of FFPE-DNA in a single day (http://www.lifetechnologies.com, accessed January, 2013). Another method that is likely suitable for this strategy was developed in Uppsala, Sweden and was first described in 2005 [208]. This method, the HaloPlex™ target enrichment system, was adapted by Agilent and is based on the digestion of DNA with different sets of restriction enzymes (http://www.agilent.com, accessed January, 2013). The targeted nucleic acid sequences are hybridized with oligonucleotide constructs called selectors. The selectors contain target-complementary end-sequences that are joined by a general linking sequence and that act as ligation templates to direct the circularization of target DNA fragments. Circularization only takes place if a ligation reaction has occurred, which makes the method theoretically very sensitive and specific. Only these circularized targets are then amplified in multiplex using one universal PCR primer pair that is specific for the general linking sequence in the selectors. By combining selector technology with high-throughput parallel sequencers, rapid resequencing can be accomplished from multiple genes and multiple specimens if DNA barcoding is applied [34,208]. A collaboration between Agilent Technologies and the LUMC Department of Pathology was initiated in 2011 to investigate the possibility of using this method for FFPE material; the performance of the method was determined by comparing DNA isolated from freshly frozen tumors with DNA from formalin-fixed and paraffin-embedded material isolated from the same tumor. The initial results are promising, even for heavily degraded DNA (Crobach and van Eijk et al., 2013 article in preparation).

Considerations in Molecular Pathology.
The role of the pathologist and his laboratory team has changed dramatically over time. After centuries of organ-based pathology that provided little benefit to patients, the field moved in the mid-nineteenth century to cellular-based clinical pathology with the potential to improve diagnosis and tumor classification, and, currently, the molecular pathologist plays an important role in 'personalized medicine'.

A pathologist has been described as the following: "a physician, concerned with human suffering and willing to make a considerable effort to decrease this suffering; a scientist with an inquiring mind, using advanced tools to study disease; an educator, sharing his knowledge, scientific inquiry methods and spirit with his students and other medical colleagues; and a leader in both pathology and medicine because he believes in quality assurance and the role of pathology in the overall advancement of medicine". Because of their multiple roles, pathologists continually build bridges between clinical medicine, surgery and basic science [209]. Microscopic tissue anatomy guides the initial classification of disease. Immunohistochemistry enables proteins to be visualized in tissue and facilitates the determination of the origin and nature of normal and aberrant cells. Developments in molecular biology improve the ability to examine the functional and genetic qualities of tissues, leading to better classification, diagnosis and treatment of disease [9].
Important aspects of molecular pathology must be further developed because the criteria and processes for implementing a molecular diagnostic test as the "standard-of-care" in a clinical setting have not been fully established. The following must be considered: resourcing appropriate patient material, assay development and supply, quality control, reporting and auditing, ethical and regulatory elements such as reimbursement and the role of the pharmaceutical industry [210]. With these considerations, it should be possible to develop a system that works locally to balance the increasing demands for higher quality specialist services [211].

Reference List

1. van den Tweel JG, Taylor CR (2010) A brief history of pathology: Preface to a forthcoming series that highlights milestones in the evolution of pathology as a discipline. Virchows Archiv : an international journal of pathology 457: 3-10.
2. Hajdu SI (2010) A note from history: the first printed case reports of cancer. Cancer 116: 2493-2498.
3. Cordier JF (2011) [Jean Fernel and the humanist spirit]. Bulletin de l'Academie nationale de medecine 195: 1399-1407.
4. Tubbs RS, Steck DT, Mortazavi MM, Shoja MM, Loukas M et al. (2012) Giovanni Battista Morgagni (1682-1771): his anatomic majesty's contributions to the neurosciences. Child's nervous system : ChNS : official journal of the International Society for Pediatric Neurosurgery 28: 1099-1102.
5. Androutsos G, Vladimiros L, Diamantis A (2007) John Hunter (1728-1793): founder of scientific surgery and precursor of oncology. Journal of B U ON : official journal of the Balkan Union of Oncology 12: 421-427.
6. Prichard R (1979) Selected items from the history of pathology: Matthew Baillie (1761-1823). The American journal of pathology 96: 278.
7. Shoja MM, Tubbs RS, Loukas M, Shokouhi G, Ardalan MR (2008) Marie-Francois Xavier Bichat (1771-1802) and his contributions to the foundations of pathological anatomy and modern medicine. Annals of anatomy = Anatomischer Anzeiger : official organ of the Anatomische Gesellschaft 190: 413-420.
8. Valentinuzzi ME, Leder RS (2012) The modern hospital in historical context: a modern health bonanza [retrospectroscope]. IEEE pulse 3: 66-72.
9. van Noesel CJM (2011) [The clinical molecular pathologist: beyond the image]. Nederlands tijdschrift voor geneeskunde 155: A2971.
10. Gal AA (2001) In search of the origins of modern surgical pathology. Advances in anatomic pathology 8: 1-13.
11. Titford M (2005) The long history of hematoxylin. Biotechnic & histochemistry : official publication of the Biological Stain Commission 80: 73-78.
12. Johnston WT (2008) The discovery of aniline and the origin of the term "aniline dye". Biotechnic & histochemistry : official publication of the Biological Stain Commission 83: 83-87.
13. Dallenbach-Hellweg G, Schmidt D (2004) History of gynecological pathology. XV. Dr. Carl Arnold Ruge. International journal of gynecological pathology : official journal of the International Society of Gynecological Pathologists 23: 83-90.
14. Grade M, Becker H, Ghadimi BM (2004) The impact of molecular pathology in oncology: The clinician's perspective. Analytical Cellular Pathology 26: 275-278.
15. Dietel M, Sers C (2006) Personalized medicine and development of targeted therapies: the upcoming challenge for diagnostic molecular pathology. A review. Virchows Archiv 448: 744-755.

16. Bignold LP, Coghlan BLD, Jersmann HPA (2006) Hansemann, Boveri, chromosomes and the gametogenesis-related theories of tumours. Cell biology international 30: 640-644.
17. Ried T (2009) Homage to Theodor Boveri (1862-1915): Boveri's theory of cancer as a disease of the chromosomes, and the landscape of genomic imbalances in human carcinomas. Environmental and molecular mutagenesis 50: 593-601.
18. Watson JD, Crick FHC (1953) Molecular structure of nucleic acids: A structure for deoxyribose nucleic acid. Nature 171: 737-738.
19. Sobel ME, Bagg A, Caliendo AM, Ladanyi M, Zehnbauer B (2008) The evolution of molecular genetic pathology: advancing 20th-century diagnostic methods into potent tools for the new millennium. The Journal of molecular diagnostics : JMD 10: 480-483.
20. Gall JG, Pardue ML (1969) Formation and detection of RNA-DNA hybrid molecules in cytological preparations. Proceedings of the National Academy of Sciences 63: 378-383.
21. Kallioniemi OP, Kallioniemi A, Kurisu W, Thor A, Chen LC et al. (1992) ERBB2 amplification in breast cancer analyzed by fluorescence in situ hybridization. Proceedings of the National Academy of Sciences 89: 5321-5325.
22. Southern EM (1975) Detection of specific sequences among DNA fragments separated by gel electrophoresis. Journal of molecular biology 98: 503-517.
23. Schwartz DC, Cantor CR (1984) Separation of yeast chromosome-sized DNAs by pulsed field gradient gel electrophoresis. Cell 37: 67-75.
24. Botstein D, White RL, Skolnick M, Davis RW (1980) Construction of a genetic linkage map in man using restriction fragment length polymorphisms. American Journal of Human Genetics 32: 314-331.
25. Cooper DN, Schmidtke J (1987) Diagnosis of genetic disease using recombinant DNA. Supplement. Human genetics 77: 66-75.
26. Weatherall DJ (1987) Molecular pathology of single gene disorders. Journal of clinical pathology 40: 959-970.
27. Van Eyk R, Chan L, Top B, Stalenhoef AF, Havekes LM et al. (1990) An additional MspI RFLP at the human hepatic lipase (HL) gene locus. Nucleic Acids Res 18: 3110.
28. Bartlett JMS, Stirling D (2003) A short history of the polymerase chain reaction. Methods in molecular biology (Clifton, N J) 226: 3-6.
29. Sanger F, Nicklen S, Coulson AR (1977) DNA sequencing with chain-terminating inhibitors. Proceedings of the National Academy of Sciences of the United States of America 74: 5463-5467.
30. Orita M, Suzuki Y, Sekiya T, Hayashi K (1989) Rapid and sensitive detection of point mutations and DNA polymorphisms using the polymerase chain reaction. Genomics 5: 874-879.
31. Hunkapiller T, Kaiser RJ, Koop BF, Hood L (1991) Large-scale and automated DNA sequence determination. Science (New York, N Y) 254: 59-67.
32. Venter JC, Adams MD, Myers EW, Li PW, Mural RJ et al. (2001) The sequence of the human genome. Science 291: 1304-1351.

33. Lander ES, Linton LM, Birren B, Nusbaum C, Zody MC et al. (2001) Initial sequencing and analysis of the human genome. Nature 409: 860-921.
34. ten Bosch JR, Grody WW (2008) Keeping up with the next generation: massively parallel sequencing in clinical diagnostics. The Journal of molecular diagnostics : JMD 10: 484-492.
35. The 1000 Genomes Project Consortium (2010) A map of human genome variation from population-scale sequencing. Nature 467: 1061-1073.
36. Pettersson E, Lundeberg J, Ahmadian A (2009) Generations of sequencing technologies. Genomics 93: 105-111.
37. Stratton MR (2011) Exploring the Genomes of Cancer Cells: Progress and Promise. Science 331: 1553-1558.
38. Tsongalis GJ, Silverman LM (2006) Molecular diagnostics: a historical perspective. Clinica chimica acta; international journal of clinical chemistry 369: 188-192.
39. Demidov VV (2003) DNA diagnostics in the fifty-year retrospect. Expert Rev Mol Diagn 3: 121-124.
40. Richman SD, Hutchins GGA, Seymour MT, Quirke P (2010) What can the molecular pathologist offer for optimal decision making? Annals of Oncology 21: vii123-vii129.
41. Tran B, Dancey JE, Kamel-Reid S, McPherson JD, Bedard PL et al. (2012) Cancer Genomics: Technology, Discovery, and Translation. J Clin Oncol 30: 647-660.
42. Gupta A, Raina V (2010) Geftinib. Journal of cancer research and therapeutics 6: 249-254.
43. Kidd M, Modlin IM (1999) The luminati of Leiden: from Bontius to Boerhaave. World journal of surgery 23: 1307-1314.
44. van Alphen HA (2001) Elective trepanation for acute epidural hematoma by Dr. Nicolaes Tulp (1593-1674). Neurosurgery 48: 401-404.
45. Williams TI (1948) Some medical contributors to chemistry. British medical bulletin 5: 369-372.
46. Somford MP, Marres GM, van der Schelling GP (2009) Excellent enteric explorers. Journal of gastrointestinal and liver diseases : JGLD 18: 469-472.
47. Kemp M (2010) Style and non-style in anatomical illustration: From Renaissance Humanism to Henry Gray. Journal of anatomy 216: 192-208.
48. Calkoen GThA (2012) Onder Studenten. Leidse aanstaande medici en de metamorfose van de geneeskunde in de negentiende eeuw (1838-1888).
49. Rosenstein S (1899) De vooruitgang der geneeskunde in de laatste vijftig jaren . Ned Tijdschr Geneeskd 43: 114-122.
50. MacGillavry TH (1879) Microscopisch onderzoek van leukaemisch menschenbloed. Ned Tijdschr Geneeskd 23: 1-4.
51. Lignac GOE (1944) Levensbericht N.Ph. Tendeloo. Jaarboek KNAW 1944-1945: 137-140.
52. Blok N, Jan Dröge, David Geneste, Petra Helwig, Corine Hendriks et al (2013) Vier eeuwen geschiedenis in steen.
53. Lignac GOE (1952) Quo Vadis? Ned Tijdsch Geneeskd 96: 2792-2797.

54. van Duijn P, Oostrom J, Wehberg BJ (1954) Histochemische contrastkleuring van desoxyribonucleinezuren en polysacchariden. Ned Tijdschr Geneeskd 98: 1075-1088.
55. Schaberg A (1994) In memoriam prof.dr.Th.G.van Rijssel. Ned Tijdschr Geneeskd 138: 1887.
56. Rodenburg CJ, Ploem-Zaaijer JJ, Cornelisse CJ, Mesker WE, Hermans J et al. (1987) Use of DNA image cytometry in addition to flow cytometry for the study of patients with advanced ovarian cancer. Cancer Res 47: 3938-3941.
57. Smeulders AW, Cornelisse CJ, Vossepoel AM, Ploem JS (1979) An image segmentation approach to the analysis of nuclear texture of cervical cells. Acta histochemica Supplementband 20: 217-222.
58. Cornelisse CJ, Ploem JS (1976) A new type of two·color fluorcscence staining for cytology specimens. J of Hist and Cytoch 24: 72-81.
59. Devilee P, Thierry RF, Kievits T, Kolluri R, Hopman AH et al. (1988) Detection of chromosome aneuploidy in interphase nuclei from human primary breast tumors using chromosome-specific repetitive DNA probes. Cancer Res 48: 5825-5830.
60. Smit VT, Wessels JW, Mollevanger P, Dauwerse JG, van Vliet M et al. (1991) Improved interpretation of complex chromosomal rearrangements by combined GTG banding and in situ suppression hybridization using chromosome-specific libraries and cosmid probes. Genes, chromosomes & cancer 3: 239-248.
61. Kibbelaar RE, van Kamp H, Dreef EJ, Wessels JW, Beverstock GC et al. (1991) Detection of trisomy 8 in hematological disorders by in situ hybridization. Cytogenetics and cell genetics 56: 132-136.
62. Kibbelaar RE, Mulder JW, Dreef EJ, van Kamp H, Fibbe WE et al. (1993) Detection of monosomy 7 and trisomy 8 in myeloid neoplasia: a comparison of banding and fluorescence in situ hybridization. Blood 82: 904-913.
63. Jiwa M, Steenbergen RD, Zwaan FE, Kluin PM, Raap AK et al. (1990) Three sensitive methods for the detection of cytomegalovirus in lung tissue of patients with interstitial pneumonitis. American journal of clinical pathology 93: 491-494.
64. Gruis NA, Abeln EC, Bardoel AF, Devilee P, Frants RR et al. (1993) PCR-based microsatellite polymorphisms in the detection of loss of heterozygosity in fresh and archival tumour tissue. Br J Cancer 68: 308-313.
65. Cornelis RS, Devilee P, van Vliet M, Kuipers-Dijkshoorn N, Kersenmaeker A et al. (1993) Allele loss patterns on chromosome 17q in 109 breast carcinomas indicate at least two distinct target regions. Oncogene 8: 781-785.
66. Abeln EC, Corver WE, Kuipers-Dijkshoorn NJ, Fleuren GJ, Cornelisse CJ (1994) Molecular genetic analysis of flow-sorted ovarian tumour cells: improved detection of loss of heterozygosity. Br J Cancer 70: 255-262.
67. Abeln EC, Kuipers-Dijkshoorn NJ, Berns EM, Henzen-Logmans SC, Fleuren GJ et al. (1995) Molecular genetic evidence for unifocal origin of advanced epithelial ovarian cancer and for minor clonal divergence. British journal of cancer 72: 1330-1336.

68. Kononen J, Bubendorf L, Kallioniemi A, Barlund M, Schraml P et al. (1998) Tissue microarrays for high-throughput molecular profiling of tumor specimens. Nat Med 4: 844-847.
69. Hendriks Y, Franken P, Dierssen JW, de Leeuw W, Wijnen J et al. (2003) Conventional and tissue microarray immunohistochemical expression analysis of mismatch repair in hereditary colorectal tumors. Am J Pathol 162: 469-477.
70. Van Wezel T, Lombaerts M, van Roon EH, Philippo K, Baelde HJ et al. (2005) Expression analysis of candidate breast tumour suppressor genes on chromosome 16q. Breast Cancer Res 7: R998-R1004.
71. Lips EH, Dierssen JW, Van Eijk R, Oosting J, Eilers PH et al. (2005) Reliable high-throughput genotyping and loss-of-heterozygosity detection in formalin-fixed, paraffin-embedded tumors using single nucleotide polymorphism arrays. Cancer Res 65: 10188-10191.
72. Corver WE, Middeldorp A, ter Haar NT, Jordanova ES, van PM et al. (2008) Genome-wide allelic state analysis on flow-sorted tumor fractions provides an accurate measure of chromosomal aberrations. Cancer Res 68: 10333-10340.
73. Hanahan D, Weinberg RA (2000) The hallmarks of cancer. Cell 100: 57-70.
74. Hanahan D, Weinberg RA (2011) Hallmarks of cancer: the next generation. Cell 144: 646-674.
75. Vogelstein B, Kinzler KW (2004) Cancer genes and the pathways they control. Nat Med 10: 789-799.
76. Newmark P (1989) Nobel for oncogenes. Nature 341: 475.
77. Stehelin D, Varmus HE, Bishop JM, Vogt PK (1976) DNA related to the transforming gene(s) of avian sarcoma viruses is present in normal avian DNA. Nature 260: 170-173.
78. Puls LN, Eadens M, Messersmith W (2011) Current status of SRC inhibitors in solid tumor malignancies. The oncologist 16: 566-578.
79. Nowell, Hungerford (1960) Chromosome studies on normal and leukemic human leukocytes. Journal of the National Cancer Institute 25: 85-109.
80. Pray LA (2008) Gleevec: the Breakthrough in Cancer Treatment. Nature Education 1.
81. Burkitt D (1958) A sarcoma involving the jaws in African children. The British journal of surgery 46: 218-223.
82. Tomita N (2011) BCL2 and MYC dual-hit lymphoma/leukemia. Journal of clinical and experimental hematopathology : JCEH 51: 7-12.
83. Knudson AG, Jr. (1971) Mutation and cancer: statistical study of retinoblastoma. Proc Natl Acad Sci U S A 68: 820-823.
84. Devilee P, Cleton-Jansen AM, Cornelisse CJ (2001) Ever since Knudson. Trends Genet 17: 569-573.
85. Baker SJ, Markowitz S, Fearon ER, Willson JK, Vogelstein B (1990) Suppression of human colorectal carcinoma cell growth by wild-type p53. Science (New York, N Y) 249: 912-915.
86. Smilenov LB (2006) Tumor development: haploinsufficiency and local network assembly. Cancer letters 240: 17-28.

87. Kinzler KW, Vogelstein B (1997) Gatekeepers and caretakers. Nature 386: 761-763.
88. Oliveira AM, Ross JS, Fletcher JA (2005) Tumor suppressor genes in breast cancer: the gatekeepers and the caretakers. American journal of clinical pathology 124 Suppl: S16-S28.
89. Pietras K, Ostman A (2010) Hallmarks of cancer: interactions with the tumor stroma. Experimental cell research 316: 1324-1331.
90. Hirsch FR, Varella-Garcia M, Bunn PA, Jr., Franklin WA, Dziadziuszko R et al. (2006) Molecular Predictors of Outcome With Gefitinib in a Phase III Placebo-Controlled Study in Advanced Non-Small-Cell Lung Cancer. J Clin Oncol 24: 5034-5042.
91. Zou ZQ, Zhang XH, Wang F, Shen QJ, Xu J et al. (2009) A novel dual PI3Kalpha/mTOR inhibitor PI-103 with high antitumor activity in non-small cell lung cancer cells. Int J Mol Med 24: 97-101.
92. Loupakis F, Ruzzo A, Cremolini C, Vincenzi B, Salvatore L et al. (2009) KRAS codon 61, 146 and BRAF mutations predict resistance to cetuximab plus irinotecan in KRAS codon 12 and 13 wild-type metastatic colorectal cancer. British journal of cancer 101: 715-721.
93. Karapetis CS (2008) K-ras mutations and benefit from cetuximab in advanced colorectal cancer. N Engl J Med 3: 1757-1765.
94. van Puijenbroek M, Nielsen M, Tops CM, Halfwerk H, Vasen HF et al. (2008) Identification of patients with (atypical) MUTYH-associated polyposis by KRAS2 c.34G > T prescreening followed by MUTYH hotspot analysis in formalin-fixed paraffin-embedded tissue. Clin Cancer Res 14: 139-142.
95. Vidwans SJ, Flaherty KT, Fisher DE, Tenenbaum JM, Travers MD et al. (2011) A Melanoma Molecular Disease Model. PLoS One 6: e18257.
96. Rubinstein JC, Sznol M, Pavlick AC, Ariyan S, Cheng E et al. (2010) Incidence of the V600K mutation among melanoma patients with BRAF mutations, and potential therapeutic response to the specific BRAF inhibitor PLX4032. Journal of translational medicine 8: 67.
97. Legakis I, Syrigos K (2011) Recent advances in molecular diagnosis of thyroid cancer. Journal of thyroid research 2011: 384213.
98. Gianoukakis AG, Giannelli SM, Salameh WA, McPhaul LW (2011) Well differentiated follicular thyroid neoplasia: impact of molecular and technological advances on detection, monitoring and treatment. Molecular and cellular endocrinology 332: 9-20.
99. Farina Sarasqueta A, Zeestraten ECM, van Wezel T, van Lijnschoten G, van Eijk R et al. (2011) PIK3CA kinase domain mutation identifies a subgroup of stage III colon cancer patients with poor prognosis. Cellular oncology (Dordrecht) 34: 523-531.
100. Fagin JA, Mitsiades N (2008) Molecular pathology of thyroid cancer: diagnostic and clinical implications. Best practice & research Clinical endocrinology & metabolism 22: 955-969.
101. Harbour JW (2012) The genetics of uveal melanoma: an emerging framework for targeted therapy. Pigment cell & melanoma research 25: 171-181.

102. Pansuriya TC, van Eijk R, d'Adamo P, van Ruler MAJH, Kuijjer ML et al. (2011) Somatic mosaic IDH1 and IDH2 mutations are associated with enchondroma and spindle cell hemangioma in Ollier disease and Maffucci syndrome. Nature genetics 43: 1256-1261.
103. Tabatabai G, Stupp R, van den Bent M, Hegi M, Tonn JC et al. (2010) Molecular diagnostics of gliomas: the clinical perspective. Acta Neuropathologica 120: 585-592.
104. Gazdar AF (2009) Activating and resistance mutations of EGFR in non-small-cell lung cancer: role in clinical response to EGFR tyrosine kinase inhibitors. Oncogene 28 Suppl 1: S24-S31.
105. Subramanian S, West RB, Corless CL, Ou W, Rubin BP et al. (2004) Gastrointestinal stromal tumors (GISTs) with KIT and PDGFRA mutations have distinct gene expression profiles. Oncogene 23: 7780-7790.
106. Lux ML, Rubin BP, Biase TL, Chen CJ, Maclure T et al. (2000) KIT extracellular and kinase domain mutations in gastrointestinal stromal tumors. The American journal of pathology 156: 791-795.
107. Romeo S, Debiec-Rychter M, Van Glabbeke M, Van Paassen H, Comite P et al. (2009) Cell cycle/apoptosis molecule expression correlates with imatinib response in patients with advanced gastrointestinal stromal tumors. Clinical cancer research : an official journal of the American Association for Cancer Research 15: 4191-4198.
108. Curtin JA, Busam K, Pinkel D, Bastian BC (2006) Somatic Activation of KIT in Distinct Subtypes of Melanoma. J Clin Oncol 24: 4340-4346.
109. da Costa CET, Szuhai K, van Eijk R, Hoogeboom M, Sciot R et al. (2009) No genomic aberrations in Langerhans cell histiocytosis as assessed by diverse molecular technologies. Genes, chromosomes & cancer 48: 239-249.
110. Domont J, Salas S, Lacroix L, Brouste V, Saulnier P et al. (2010) High frequency of beta-catenin heterozygous mutations in extra-abdominal fibromatosis: a potential molecular tool for disease management. British journal of cancer 102: 1032-1036.
111. Pritchard CC, Grady WM (2011) Colorectal cancer molecular biology moves into clinical practice. Gut 60: 116-129.
112. Walther A, Houlston R, Tomlinson I (2008) Association between chromosomal instability and prognosis in colorectal cancer: a meta-analysis. Gut 57: 941-950.
113. Popat S, Houlston RS (2005) A systematic review and meta-analysis of the relationship between chromosome 18q genotype, DCC status and colorectal cancer prognosis. Eur J Cancer 41: 2060-2070.
114. Jansen M, Yip S, Louis DN (2010) Molecular pathology in adult gliomas: diagnostic, prognostic, and predictive markers. Lancet neurology 9: 717-726.
115. Masui K, Cloughesy TF, Mischel PS (2011) Review: Molecular pathology in adult high-grade gliomas: from molecular diagnostics to target therapies. Neuropathology and Applied Neurobiology no.

116. Romei C, Elisei R (2012) RET/PTC Translocations and Clinico-Pathological Features in Human Papillary Thyroid Carcinoma. Frontiers in endocrinology 3: 54.
117. Peter M, Gilbert E, Delattre O (2001) A multiplex real-time pcr assay for the detection of gene fusions observed in solid tumors. Laboratory investigation; a journal of technical methods and pathology 81: 905-912.
118. Sasaki T, Rodig SJ, Chirieac LR, Janne PA (2010) The biology and treatment of EML4-ALK non-small cell lung cancer. European journal of cancer (Oxford, England : 1990) 46: 1773-1780.
119. Ju YS, Lee WC, Shin JY, Lee S, Bleazard T et al. (2012) A transforming KIF5B and RET gene fusion in lung adenocarcinoma revealed from whole-genome and transcriptome sequencing. Genome research 22: 436-445.
120. Lipson D, Capelletti M, Yelensky R, Otto G, Parker A et al. (2012) Identification of new ALK and RET gene fusions from colorectal and lung cancer biopsies. Nature medicine 18: 382-384.
121. Takeuchi K, Soda M, Togashi Y, Suzuki R, Sakata S et al. (2012) RET, ROS1 and ALK fusions in lung cancer. Nature medicine 18: 378-381.
122. Hatada I, Fukasawa M, Kimura M, Morita S, Yamada K et al. (2006) Genome-wide profiling of promoter methylation in human. Oncogene 25: 3059-3064.
123. Herman JG, Umar A, Polyak K, Graff JR, Ahuja N et al. (1998) Incidence and functional consequences of hMLH1 promoter hypermethylation in colorectal carcinoma. Proc Natl Acad Sci U S A 95: 6870-6875.
124. Esteller M, Garcia-Foncillas J, Andion E, Goodman SN, Hidalgo OF et al. (2000) Inactivation of the DNA-repair gene MGMT and the clinical response of gliomas to alkylating agents. N Engl J Med 343: 1350-1354.
125. Klopfleisch R (2006) Excavation of a buried treasure--DNA, mRNA, miRNA and protein analysis in formalin fixed, paraffin embedded tissues. 26 6: 797-810.
126. Gnanapragasam VJ (2010) Unlocking the molecular archive: the emerging use of formalin-fixed paraffin-embedded tissue for biomarker research in urological cancer. BJU international 105: 274-278.
127. Zsikla V, Baumann M, Cathomas G (2004) Effect of buffered formalin on amplification of DNA from paraffin wax embedded small biopsies using real-time PCR. Journal of clinical pathology 57: 654-656.
128. de Jong D, Verbeke SL, Meijer D, Hogendoorn PC, Bovee JV et al. (2011) Opening the archives for state of the art tumour genetic research: sample processing for array-CGH using decalcified, formalin-fixed, paraffin-embedded tissue-derived DNA samples. BMC research notes 4: 1.
129. Turashvili G, Yang W, McKinney S, Kalloger S, Gale N et al. (2012) Nucleic acid quantity and quality from paraffin blocks: Defining optimal fixation, processing and DNA/RNA extraction techniques. Experimental and molecular pathology 92: 33-43.
130. Srinivasan M, Sedmak D, Jewell S (2002) Effect of fixatives and tissue processing on the content and integrity of nucleic acids. The American journal of pathology 161: 1961-1971.

131. de Bruin EC, van de Pas S, Lips EH, Van Eijk R, van der Zee MM et al. (2005) Macrodissection versus microdissection of rectal carcinoma: minor influence of stroma cells to tumor cell gene expression profiles. BMC Genomics 6: 142.
132. Otsuka Y, Ichikawa Y, Kunisaki C, Matsuda G, Akiyama H et al. (2007) Correlating purity by microdissection with gene expression in gastric cancer tissue. Scandinavian journal of clinical and laboratory investigation 67: 367-379.
133. Fuller AP, Palmer-Toy D, Erlander MG, Sgroi DC (2003) Laser capture microdissection and advanced molecular analysis of human breast cancer. Journal of Mammary Gland Biology and Neoplasia 8: 335-345.
134. Emmert-Buck MR, Bonner RF, Smith PD, Chuaqui RF, Zhuang Z et al. (1996) Laser Capture Microdissection. Science 274: 998-1001.
135. Killian JK, Walker RL, Suuriniemi M, Jones L, Scurci S et al. (2010) Archival fine-needle aspiration cytopathology (FNAC) samples: untapped resource for clinical molecular profiling. The Journal of molecular diagnostics : JMD 12: 739-745.
136. van Eijk R, Licht J, Schrumpf M, Talebian Yazdi M, Ruano D et al. (2011) Rapid KRAS, EGFR, BRAF and PIK3CA Mutation Analysis of Fine Needle Aspirates from Non-Small-Cell Lung Cancer Using Allele-Specific qPCR. PLoS One 6: e17791.
137. Goelz SE, Hamilton SR, Vogelstein B (1985) Purification of DNA from formaldehyde fixed and paraffin embedded human tissue. Biochemical and Biophysical Research Communications 130: 118-126.
138. De Jong AE, van Puijenbroek M, Hendriks Y, Tops C, Wijnen J et al. (2004) Microsatellite Instability, Immunohistochemistry, and Additional PMS2 Staining in Suspected Hereditary Nonpolyposis Colorectal Cancer. Clin Cancer Res 10: 972-980.
139. Torrente MC, Rios C, Misad C, Ramirez R, Acuna M et al. (2010) DNA extraction from formalin-fixed laryngeal biopsies: Comparison of techniques. Acta Otolaryngol 131: 330-333.
140. Muñoz-Cadavid C, Rudd S, Zaki SR, Patel M, Moser SA et al. (2010) Improving Molecular Detection of Fungal DNA in Formalin-Fixed Paraffin-Embedded Tissues: Comparison of Five Tissue DNA Extraction Methods Using Panfungal PCR. Journal of Clinical Microbiology 48: 2147-2153.
141. Hennig G, Gehrmann M, Stropp U, Brauch H, Fritz P et al. (2010) Automated Extraction of DNA and RNA from a Single Formalin-Fixed Paraffin-Embedded Tissue Section for Analysis of Both Single-Nucleotide Polymorphisms and mRNA Expression. Clin Chem 56: 1845-1853.
142. van Eijk R, van PM, Chhatta AR, Gupta N, Vossen RH et al. (2010) Sensitive and specific KRAS somatic mutation analysis on whole-genome amplified DNA from archival tissues. J Mol Diagn 12: 27-34.
143. Gilbert MT, Haselkorn T, Bunce M, Sanchez JJ, Lucas SB et al. (2007) The isolation of nucleic acids from fixed, paraffin-embedded tissues-which methods are useful when? PLoS One 2: e537.

144. Lim EH, Zhang SL, Li JL, Yap WS, Howe TC et al. (2009) Using whole genome amplification (WGA) of low-volume biopsies to assess the prognostic role of EGFR, KRAS, p53, and CMET mutations in advanced-stage non-small cell lung cancer (NSCLC). J Thorac Oncol 4: 12-21.
145. Baak-Pablo R, Dezentje V, Guchelaar HJ, van der Straaten T (2010) Genotyping of DNA Samples Isolated from Formalin-Fixed Paraffin-Embedded Tissues Using Preamplification. The Journal of Molecular Diagnostics 12: 746-749.
146. Hughes S, Arneson N, Done S, Squire J (2005) The use of whole genome amplification in the study of human disease. Progress in biophysics and molecular biology 88: 173-189.
147. Berthier-Schaad Y, Kao WH, Coresh J, Zhang L, Ingersoll RG et al. (2007) Reliability of high-throughput genotyping of whole genome amplified DNA in SNP genotyping studies. Electrophoresis 28: 2812-2817.
148. Lage JM, Leamon JH, Pejovic T, Hamann S, Lacey M et al. (2003) Whole genome analysis of genetic alterations in small DNA samples using hyperbranched strand displacement amplification and array-CGH. Genome Res 13: 294-307.
149. Heinmoller E, Liu Q, Sun Y, Schlake G, Hill KA et al. (2002) Toward efficient analysis of mutations in single cells from ethanol-fixed, paraffin-embedded, and immunohistochemically stained tissues. Lab Invest 82: 443-453.
150. Bataille F, Rummele P, Dietmaier W, Gaag D, Klebl F et al. (2003) Alterations in p53 predict response to preoperative high dose chemotherapy in patients with gastric cancer. Mol Pathol 56: 286-292.
151. Wilfinger WW, Mackey K, Chomczynski P (1997) Effect of pH and ionic strength on the spectrophotometric assessment of nucleic acid purity. Biotechniques 22: 474-6, 478.
152. Singer VL, Jones LJ, Yue ST, Haugland RP (1997) Characterization of PicoGreen reagent and development of a fluorescence-based solution assay for double-stranded DNA quantitation. Analytical biochemistry 249: 228-238.
153. van Beers EH, Joosse SA, Ligtenberg MJ, Fles R, Hogervorst FB et al. (2006) A multiplex PCR predictor for aCGH success of FFPE samples. Br J Cancer 94: 333-337.
154. Van Eijk R, Lips EH, van Puijenbroek M, Middeldorp A, Morreau H, et al. (2010) Genotyping And LOH Analysis On Archival Tissue Using SNP Arrays. In: Starkey M, Elaswarapu R, editors. Genomics: Essential Methods. Chichester: John Wiley & Sons, Ltd.
155. Fumagalli D, Gavin PG, Taniyama Y, Kim SI, Choi HJ et al. (2010) A rapid, sensitive, reproducible and cost-effective method for mutation profiling of colon cancer and metastatic lymph nodes. BMC Cancer 10: 101.
156. Hurst CD, Zuiverloon TCM, Hafner C, Zwarthoff EC, Knowles MA (2009) A SNaPshot assay for the rapid and simple detection of four common hotspot codon mutations in the PIK3CA gene. BMC research notes 2: 66.

157. Spittle C, Ward MR, Nathanson KL, Gimotty PA, Rappaport E et al. (2007) Application of a BRAF Pyrosequencing Assay for Mutation Detection and Copy Number Analysis in Malignant Melanoma. The Journal of Molecular Diagnostics 9: 464-471.
158. Davidson CJ, Zeringer E, Champion KJ, Gauthier MP, Wang F et al. (2012) Improving the limit of detection for Sanger sequencing: a comparison of methodologies for KRAS variant detection. Biotechniques 53: 182-188.
159. Zuo Z, Chen SS, Chandra PK, Galbincea JM, Soape M et al. (2009) Application of COLD-PCR for improved detection of KRAS mutations in clinical samples. Mod Pathol 22: 1023-1031.
160. Wagner T, Stoppa-Lyonnet D, Fleischmann E, Muhr D, Pages S et al. (1999) Denaturing high-performance liquid chromatography detects reliably BRCA1 and BRCA2 mutations. Genomics 62: 369-376.
161. Lakhotia S, Somasundaram K (2003) Conformation-sensitive gel electrophoresis for detecting BRCA1 mutations. Methods in molecular biology (Clifton, N J) 223: 403-412.
162. Orita M, Iwahana H, Kanazawa H, Hayashi K, Sekiya T (1989) Detection of polymorphisms of human DNA by gel electrophoresis as single-strand conformation polymorphisms. Proceedings of the National Academy of Sciences of the United States of America 86: 2766-2770.
163. Pareek C, Smoczynski R, Tretyn A (2011) Sequencing technologies and genome sequencing. Journal of Applied Genetics 52: 413-435.
164. Desai AN, Jere A (2012) Next-generation sequencing: ready for the clinics? Clinical Genetics 81: 503-510.
165. Ansorge WJ (2009) Next-generation DNA sequencing techniques. New biotechnology 25: 195-203.
166. Higuchi R, Fockler C, Dollinger G, Watson R (1993) Kinetic PCR analysis: real-time monitoring of DNA amplification reactions. Bio/technology (Nature Publishing Company) 11: 1026-1030.
167. Smit ML, Giesendorf BA, Vet JA, Trijbels FJ, Blom HJ (2001) Semiautomated DNA mutation analysis using a robotic workstation and molecular beacons. Clin Chem 47: 739-744.
168. Arya M, Shergill IS, Williamson M, Gommersall L, Arya N et al. (2005) Basic principles of real-time quantitative PCR. Expert Rev Mol Diagn 5: 209-219.
169. Vandesompele J, De Preter K., Pattyn F, Poppe B, Van Roy N. et al. (2002) Accurate normalization of real-time quantitative RT-PCR data by geometric averaging of multiple internal control genes. Genome Biol 3: RESEARCH0034.
170. Bustin SA, Benes V, Garson JA, Hellemans J, Huggett J et al. (2009) The MIQE guidelines: minimum information for publication of quantitative real-time PCR experiments. Clin Chem 55: 611-622.
171. Wittwer CT, Reed GH, Gundry CN, Vandersteen JG, Pryor RJ (2003) High-resolution genotyping by amplicon melting analysis using LCGreen. Clin Chem 49: 853-860.

172. Vossen RH, Aten E, Roos A, den Dunnen JT (2009) High-Resolution Melting Analysis (HRMA)-More than just sequence variant screening. Hum Mutat 30: 860-866.
173. Erali M, Voelkerding KV, Wittwer CT (2008) High resolution melting applications for clinical laboratory medicine. Experimental and molecular pathology 85: 50-58.
174. Manaster C, Zheng W, Teuber M, Wachter S, Doring F et al. (2005) InSNP: a tool for automated detection and visualization of SNPs and InDels. Human mutation 26: 11-19.
175. den Dunnen JT, Antonarakis SE (2000) Mutation nomenclature extensions and suggestions to describe complex mutations: a discussion. Human mutation 15: 7-12.
176. Horaitis O, Cotton RGH (2004) The challenge of documenting mutation across the genome: the human genome variation society approach. Human mutation 23: 447-452.
177. Ogino S, Gulley ML, den Dunnen JT, Wilson RB (2007) Standard mutation nomenclature in molecular diagnostics: practical and educational challenges. The Journal of molecular diagnostics : JMD 9: 1-6.
178. Fokkema IFAC, den Dunnen JT, Taschner PEM (2005) LOVD: easy creation of a locus-specific sequence variation database using an “LSDB-in-a-box” approach. Human mutation 26: 63-68.
179. Fokkema IFAC, Taschner PEM, Schaafsma GCP, Celli J, Laros JFJ et al. (2011) LOVD v.2.0: the next generation in gene variant databases. Human mutation 32: 557-563.
180. LaFramboise T (2009) Single nucleotide polymorphism arrays: a decade of biological, computational and technological advances. Nucleic Acids Research 37: 4181-4193.
181. Szuhai K, Cleton-Jansen AM, Hogendoorn PCW, Bovee JVMG (2012) Molecular pathology and its diagnostic use in bone tumors. Cancer Genetics 205: 193-204.
182. Meldrum C, Doyle MA, Tothill RW (2011) Next-generation sequencing for cancer diagnostics: a practical perspective. The Clinical biochemist Reviews / Australian Association of Clinical Biochemists 32: 177-195.
183. Zhang C, Xing D (2007) Miniaturized PCR chips for nucleic acid amplification and analysis: latest advances and future trends. Nucleic Acids Research 35: 4223-4237.
184. Schouten JP, McElgunn CJ, Waaijer R, Zwijnenburg D, Diepvens F et al. (2002) Relative quantification of 40 nucleic acid sequences by multiplex ligation-dependent probe amplification. Nucleic Acids Res 30: e57.
185. Hermsen M, Coffa J, Ylstra B, Meijer G, Morreau H, et al. (2010) High-Resolution Analysis of Genomic Copy Number Changes. In: Starkey M, Elaswarapu R, editors. Genomics: Essential Methods. Chichester: John Wiley & Sons, Ltd. pp. 1-31.
186. Natte R, Van Eijk R, Eilers P, Cleton-Jansen AM, Oosting J et al. (2005) Multiplex ligation-dependent probe amplification for the detection of 1p and 19q chromosomal loss in oligodendroglial tumors. Brain Pathol 15: 192-197.

187. van Eijk R., Eilers PH, Natte R, Cleton-Jansen AM, Morreau H et al. (2010) MLPAinter for MLPA interpretation: an integrated approach for the analysis, visualisation and data management of Multiplex Ligation-dependent Probe Amplification. BMC Bioinformatics 11: 67.
188. Coffa J, van de Wiel MA, Diosdado B, Carvalho B, Schouten J et al. (2008) MLPAnalyzer: data analysis tool for reliable automated normalization of MLPA fragment data. Cell Oncol 30: 323-335.
189. Hardenbol P, Yu F, Belmont J, Mackenzie J, Bruckner C et al. (2005) Highly multiplexed molecular inversion probe genotyping: over 10,000 targeted SNPs genotyped in a single tube assay. Genome Res 15: 269-275.
190. Farina Sarasqueta A, Corver WE, Ruano D, Van Wezel T, Oosting J et al. (2012) *BRAF* V600E mutated colon carcinoma associated genomic profile differs from double wild type tumors genome. Submitted for publication .
191. Wang Y, Carlton VEH, Karlin-Neumann G, Sapolsky R, Zhang L et al. (2009) High quality copy number and genotype data from FFPE samples using Molecular Inversion Probe (MIP) microarrays. BMC medical genomics 2: 8.
192. Shen R, Fan JB, Campbell D, Chang W, Chen J et al. (2005) High-throughput SNP genotyping on universal bead arrays. Mutat Res 573: 70-82.
193. Kennedy GC, Matsuzaki H, Dong S, Liu WM, Huang J et al. (2003) Large-scale genotyping of complex DNA. Nat Biotechnol 21: 1233-1237.
194. Matsuzaki H, Loi H, Dong S, Tsai YY, Fang J et al. (2004) Parallel Genotyping of Over 10,000 SNPs Using a One-Primer Assay on a High-Density Oligonucleotide Array. Genome Res 14: 414-425.
195. Gunderson KL, Steemers FJ, Lee G, Mendoza LG, Chee MS (2005) A genome-wide scalable SNP genotyping assay using microarray technology. Nat Genet 37: 549-554.
196. Hua J, Craig DW, Brun M, Webster J, Zismann V et al. (2007) SNiPer-HD: improved genotype calling accuracy by an expectation-maximization algorithm for high-density SNP arrays. Bioinformatics 23: 57-63.
197. Hu G, Wang HY, Greenawalt DM, Azaro MA, Luo M et al. (2006) AccuTyping: new algorithms for automated analysis of data from high-throughput genotyping with oligonucleotide microarrays. Nucleic Acids Res 34: e116.
198. Scharpf RB, Ting JC, Pevsner J, Ruczinski I (2007) SNPchip : R classes and methods for SNP array data. Bioinformatics 23: 627-628.
199. Rabbee N, Speed TP (2006) A genotype calling algorithm for affymetrix SNP arrays. Bioinformatics 22: 7-12.
200. Shah SP (2009) Mutational evolution in a lobular breast tumour profiled at single nucleotide resolution. Nature 46: 809-813.
201. Ku CS, Naidoo N, Wu M, Soong R (2011) Studying the epigenome using next generation sequencing. Journal of medical genetics 48: 721-730.
202. Ku CS, Wu M, Cooper DN, Naidoo N, Pawitan Y et al. (2012) Technological advances in DNA sequence enrichment and sequencing for germline genetic diagnosis. Expert Rev Mol Diagn 12: 159-173.
203. Wong KM, Hudson TJ, McPherson JD (2011) Unraveling the genetics of cancer: genome sequencing and beyond. Annual review of genomics and human genetics 12: 407-430.

204. Jones S, Hruban RH, Kamiyama M, Borges M, Zhang X et al. (2009) Exomic sequencing identifies PALB2 as a pancreatic cancer susceptibility gene. Science (New York, N Y) 324: 217.
205. Loman NJ, Misra RV, Dallman TJ, Constantinidou C, Gharbia SE et al. (2012) Performance comparison of benchtop high-throughput sequencing platforms. Nat Biotech 30: 434-439.
206. Binladen J, Gilbert MT, Bollback JP, Panitz F, Bendixen C et al. (2007) The use of coded PCR primers enables high-throughput sequencing of multiple homolog amplification products by 454 parallel sequencing. PLoS One 2: e197.
207. Meyer M, Stenzel U, Myles S, Prufer K, Hofreiter M (2007) Targeted high-throughput sequencing of tagged nucleic acid samples. Nucleic Acids Research 35: e97.
208. Dahl F, Gullberg M, Stenberg J, Landegren U, Nilsson M (2005) Multiplex amplification enabled by selective circularization of large sets of genomic DNA fragments. Nucleic Acids Research 33: e71.
209. Tei Anim J. (2007) The Changing Role of the Pathologist. Bulletin of the Kuwait Institute for Medical Specialization 6: 8-12.
210. Hamilton SR (2012) Molecular pathology. Molecular oncology 6: 177-181.
211. Kirkham N (2000) The pathologist in the 21st century--generalist or specialist? Journal of clinical pathology 53: 7-9.

Chapter 2

Assessment of a Fully Automated High-Throughput DNA Extraction Method from Formalin-Fixed, Paraffin-Embedded Tissue for *KRAS,* and *BRAF* Somatic Mutation Analysis

Ronald van Eijk, Lisa Stevens, Hans Morreau, Tom van Wezel.

Department of Pathology
Leiden University Medical Center

Exp. Mol. Pathol. 94(1), 121 (2013) doi: 10.1016/j.yexmp.2012.06.004.

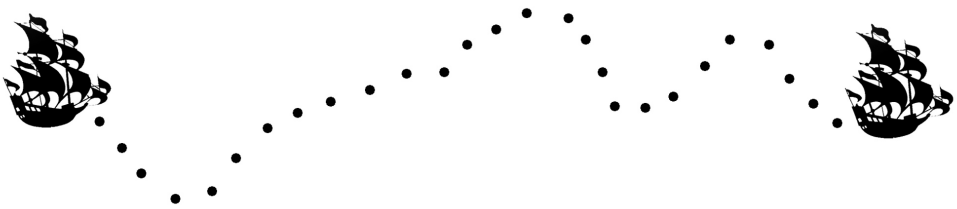

Abstract
Preoperative biopsies or imbedded cytological cells will become more and more a primary source of tissue for molecular diagnostic analyses as a result of novel neo-adjuvant treatment regimens for several cancer types. Furthermore there is a growing need to examine metastatic cancer tissue. Hence, nucleic acids need to be reliably isolated and analyzed from small amounts of formalin-fixed and paraffin-embedded (FFPE) tissue. The limited numbers of (tumor) cells in these samples make high quality and sensitive DNA isolation challenging. Also demands for faster turnaround times are growing. Therefore, we evaluated a fully automated DNA/RNA isolation system and compared this with a manual, classical routine molecular pathology method. We compared the quality of the isolates from both tissue cores and micro-dissection for detection of hotspot mutations in *KRAS*, *BRAF* applying hydrolysis probe assays. In addition we determined whether the automated method decreases the hands-on-time and turnaround times in routine molecular pathology workflow.
In conclusion, the automated method delivers high quality DNA from both small FFPE tissue cores and micro-dissected tissue material. In comparison to classical methods, less than 50% of starting tissue was sufficient as input for micro-dissection. Turnaround times decreased significantly and 50% less hands-on time was needed.

Introduction
Increasing numbers of cancer biomarkers have been implemented in molecular tumor diagnostics worldwide [1–4]. Mutations in *KRAS* predict for resistance to monoclonal antibody therapy in colon cancer patients [5]. In *BRAF,* the V600E and the rarer V600K variant are found in the majority of cutaneous melanoma, making the patients eligible for treatment with vemurafenib (PLX4032). [6] A subset of Non_Small_Cell_Lung_Cancers may harbour activating mutations in the *EGFR* kinase domain and might thereby respond to certain tyrosine kinase inhibitors [2]. Thus, based on these test results for *KRAS, BRAF and EGFR*, patients may be selected for guided treatment. Furthermore, a delay in the start of treatment of a cancer patient might influence the patient's life expectation (e.g., for the treatment of lung cancer with tyrosine kinase inhibitors). In addition, the amount of cancer material that is available for testing is decreasing as a result of the introduction of neo-adjuvant treatment protocols and the growing need to examine metastatic cancer tissue. Less invasive sampling procedures [7] may lead to little amounts of material.
The starting point in biomarker testing in pathological specimen is the efficient isolation of nucleic acids. These can be isolated from formalin-fixed, paraffin-embedded (FFPE) tissue from whole tumor sections, micro-dissected material, tissue cores or imbedded cytological material [8,9]. In FFPE tissue DNA degradation has already taken place resulting in a negative contribution to the quantity and quality of the DNA. [10,11] Several manual and semi-automated methods have been described for DNA extraction from FFPE tissue [12,13]. DNA quality and quantity obtained with these different techniques is variable. This

variability is primarily due to the quality of the material that has been used and not because of the quality of the isolation technique [14]. Nevertheless, all techniques described thus far require many hours of hands-on time and include operator- to-operator variation that might contribute to less reproducible and robust results [15]. Part of the hands-on time is due to the manual micro-dissection and lysis of the tumor tissue. However, deparaffinization is a crucial, time consuming step that can impact the quality and quantity of the extraction [16]. Moreover, this process often includes the use of toxic reagents such as xylene [17]. Additionally, in many cases, and specifically in micro-dissection, the final DNA yield is low and of reduced quality, thereby requiring additional steps such as whole genome amplification or other pre-amplification steps in order to obtain sufficient DNA for further molecular testing. [18–20]. Therefore, there is an increasing demand for fully automated, optimized and time-saving methods for the high quality DNA extraction from limited amounts of material.

Here we describe DNA extraction using a fully automated DNA/RNA extraction system which can process 48 tissue samples in 3 hours 15 min using silica-coated magnetic nanoparticles. The process integrates both lysis and deparaffinization by hydrophobic adsorption instead of offline xylene based deparaffinization [21,22]. We investigated if the quality of the isolated DNA from tissue cores and micro-dissected tissue obtained with this newly described method compares to our classical method. We also evaluated if the method decreases the turnover (turnaround) time for our most common molecular assays.

We determined that the fully automated method delivers high quality DNA from small tissue cores and micro-dissected material as compared to our classical method. For micro-dissection we found that only 20%- 50% of starting material was needed for the fully automated method when compared to the classical method. When the DNA is used in hydrolysis probes assays we achieved 24 hours faster turnover (turnaround) time with 50% less hands-on time being required.

Material and Methods

ETHICS STATEMENT

All samples used in this study were handled according to the medical ethical guidelines described in the Code Proper Secondary Use of Human Tissue established by the Dutch Federation of Medical Sciences (www.federa.org, accessed October 27, 2010). According to these guidelines, the specific need for the ethics committee's approval was not necessary for this study because all human material used in this study has been anonymized.

TEST MATERIAL

This study included formalin-fixed, paraffin-embedded tissue samples obtained from micro- dissected tissue from slides (10 µm) and tissue cores (0.3 mm diameter and variable length) of different tissue types (Supplementary table 1). Hematoxylin-eosin staining was performed on tissue sections to visualize presence of tumor cells. These were used to guide micro-dissection on hematoxilin-stained duplicate slides and to determine the area of the tissue cores.

DNA EXTRACTION

The classical method

Classical DNA extraction from FFPE material was performed according to the method described by de Jong [23]. In brief, the FFPE sections on slides or tissue cores were deparaffinized by two xylene and ethanol washing steps (process includes centrifugation and incubation steps as well). The sections and cores were collected in various amounts of PK1 buffer depending on the amount of material and then incubated overnight at 56°C in the presence of proteinase K and Chelex beads. If the volume of the PK1 buffer was under 15 µl no Chelex beads were added. The following day the samples were further incubated at 100°C for 10 minutes, centrifuged and then the supernatant was transferred to a clean tube.

The fully automated method

The fully automated DNA extraction from FFPE tissue (Tissue Preparation System with VERSANT Tissue Preparation Reagents, Siemens Healthcare Diagnostics, Tarrytown, NY) has been described previously, [21,22] In this method micro-dissected tissue or tissue cores were directly transferred into 1.5 ml tubes (Sarstedt, Nümbrecht, Germany) and subjected to automated total nucleic acid extraction. Samples were heat lysed in 150-µL FFPE buffer at 80°C for 30 minutes with shaking. After cooling, enzymatic lysis was carried out at 65°C for 30 minutes with proteinase K. Any residual tissue debris was then removed by the nonspecific binding to silica-coated iron oxide beads followed by subsequent magnetic separation. Deparaffinized and clarified lysates were transferred to new tubes and nucleic acids were bound to fresh silica-coated beads under chaotrophic conditions. Beads were washed 3 times and total nucleic acids were eluted with 100 µL of elution buffer at 70°C.

MOLECULAR ANALYSIS

Hydrolysis probes assays were performed as described elsewhere [7]. In this method 10µl qPCR reactions contained 5µl mastermix (FastStart Universal Probe Master, Roche Diagnostics, Almere, The Netherlands), 1µl of 10x primer and hydrolysis probe solutions and 2µl DNA solution or sterile water. qPCR was performed in a sealed 384 well plate in a qPCR instrument (CFX384, Bio-Rad, Veenendaal, The Netherlands), with an initial denaturation step of 10 minutes at 95°C follow by 40 cycles of 15 seconds at 92°C, 60 seconds at 60°C and 10 seconds at 72°C. In the experiments described below we used 8 different assays, 7 for *KRAS* p,G12S, p,G12R, p.G12C, p.G12D, p.G12A, p.G12V and p.G13D and one for the *BRAF* p.V600E variant.

Results

For molecular diagnostic analyses of hotspot mutations in *KRAS* and *BRAF* on DNA isolated from small tissue cores or micro-dissected tissue sections hydrolysis probes assays are often used.. As described, DNA isolation from FFPE tissue sections is possible with a fully automated system in the routine laboratory [22,24]. Since in our laboratory we isolate DNA in ~ 60% of the cases

from tissue cores, our first assessment of the fully automated system was to determine if DNA could be isolated from 0.3 mm tissue cores taken from tumor fields of FFPE tissue blocks. We used 3 tissue cores from 4 colon tumor / normal pairs, respectively for the classic and automated isolation methods as described in the material and methods. Final DNA was collected in 100 µl PK1 for the classic and 100 elution buffer for the automated method. To check for the quality of the material we performed the 8 hydrolysis probes assays with 2 µl of a 1:5 diluted stock of both eluates (Supplementary table 1). All 64 data-points were plotted in a scatterplot (Figure 1A). The mean Cq of the "Classic samples was 31.45 with a standard deviation of 1.55. The automated method had a mean Cq of 32.23 with a standard deviation of 1.96 demonstrating that Cq values obtained with the Classic method are in the same range as the Cq values obtained with the automated method.

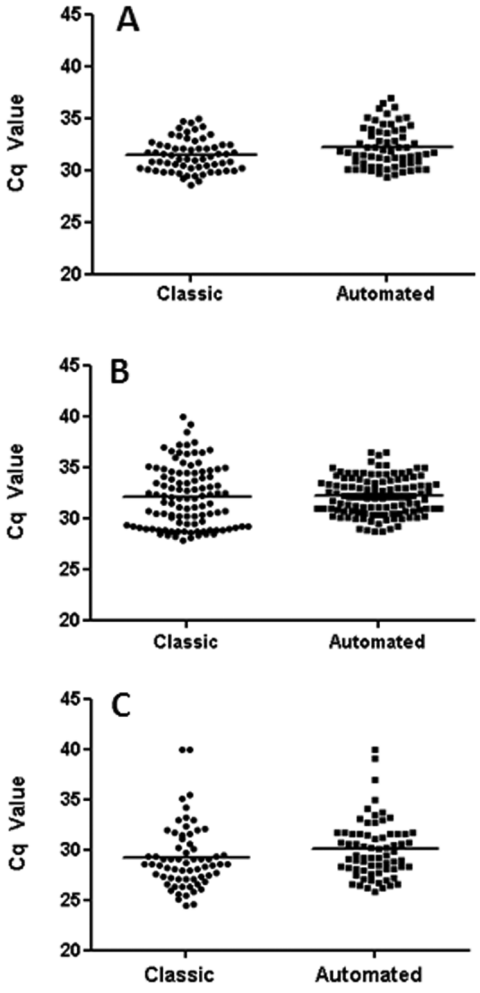

Figure 1. Scatter plots of hydrolysis probes assays Cq values over isolation type. Plot A shows the Cq values obtained in DNA isolated from tissue cores in equal amounts of DNA obtained with the classic and fully automated method with 8 different hydrolysis probes assays for *KRAS* and *BRAF*. Plot B shows the Cq values obtained with equal amounts of micro-dissected DNA in 8 different hydrolysis probes assays for KRAS and BRAF. Plot C shows the Cq values obtained with a BRAFV600E Hydrolysis probes assay on samples in two different, however comparable sets of samples tested in two different time intervals in molecular diagnostics

Micro-dissection.

In our laboratory micro-dissection for tumor cell enrichment, where 8 to 10 consecutive 10 micron sections are used as starting material, is required in about 40% of the cases. Deparaffinized and stained tumor containing fields are scraped off the different slides and pooled. This process, at about 5 minutes per slide, adds up to approximately 1 hour hands-on time.

We determined the threshold for the minimal input of the automated system by micro-dissecting in duplicate 1, 2 and 4 mm² tissue from deparaffinized and stained sections of a single 10 micron slide of a colon and a lung specimen. DNA was extracted with the automated method and eluted in a final volume of 100µl. Two µl of the eluate was used in the *KRAS* and the *BRAF* hydrolysis probes assay. Mean Cq values of 31.97 +/- 1.6, 31.45 +/- 1.5 and 29.93 +/- 1.3 were observed for the 1, 2 and 4 mm² tissue sections, respectively (Supplementary table 2). This demonstrates that as little as 1 mm² micro dissected tumor material of a single 10 µM slide can produce enough DNA to perform 50 qPCR reactions when using the automated extraction method. In the colon cancer specimen a *KRAS* c.34G>A mutation was clearly detectable in the 1, 2 and 4 mm² micro-dissected tissue sections. Remarkably the wild type allele tended to disappear in the 1 mm² .This may possibly be explained by the loss of the wild type allele or preferential amplification of the mutant allele. (Figure 2)

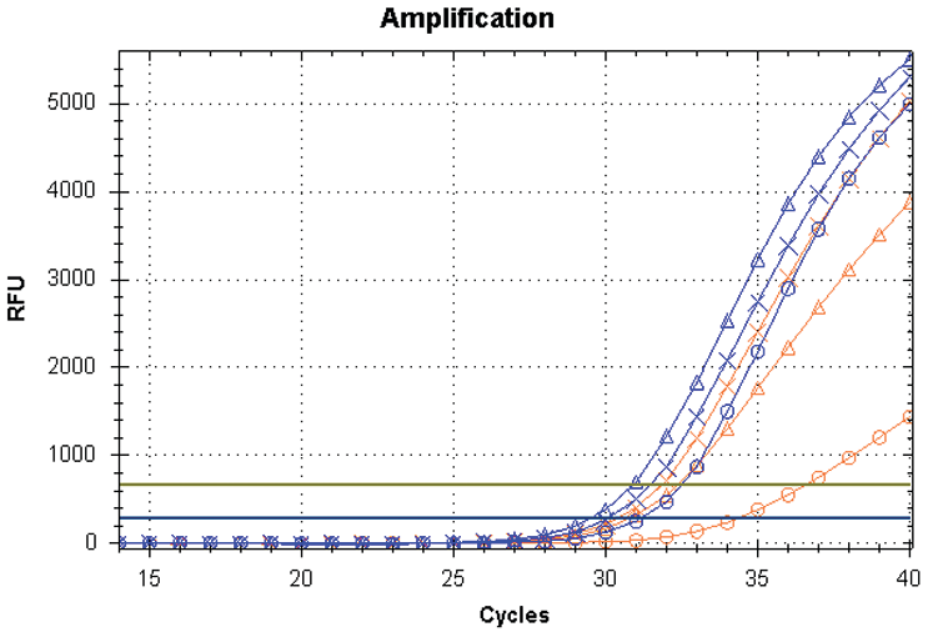

Figure 2. Minimal input testing in the fully automated system. Wild type (orange) and mutant (blue) amplification curves of 1mm² (Circle), 2mm² (Triangle) and 4mm² (Cross) micro-dissected tissue parts originating from one single 10 µM slice of a lung tumor harboring a *KRAS* c.34G>A p.G12S mutation.

Subsequently, micro-dissection was performed on 14 different tissue type specimen to enrich for tumor cells (Supplementary Table 3). Like in routine diagnostics, eight sections per specimen were used for the classic isolation with micro-dissection. These were compared to two sections per specimen for micro-dissection with the automated DNA isolation, thus 2x1 mm^2 or more tissue was available for processing. The classical isolates were eluted in PK1 varying from 12.5 to 75 µl depending on the amount of tumor material present (Supplementary table 3). DNA isolates from the classical method was diluted five times in sterile water prior to hydrolysis probes assays while 2 µl of undiluted DNA obtained with the automated method was always used. Eight assays detecting *KRAS* and *BRAF* hotspot mutations were performed and Cq values were compared. The mean Cq for the classical method was 32.10 +/- 2.9 and the automated method had a mean Cq of 32.18 +/- 1.9. This indicated that although 4 times less tissue was used for the automated method similar Cq's were obtained. (Figure 1B).

These results demonstrate that the automated method leads to at least the same quality DNA and detection rates of mutations as compared to the manual method while workload can be reduced and quicker turnover (turnaround) times can be achieved. In the classical protocol, micro dissecting ten replicates for each of 14 samples requires up to 7 hours hands-on time resulting in a total time including DNA extraction of about 28 hours before isolated DNA is available for assay (Figure 3). With the automated approach, micro dissecting only two replicates for each of 14 samples requires up to 2 hours hands-on time resulting in a total time including DNA extraction of about only 6 hours before isolated DNA is available for assay (Figure 3).
To determine if the automated approach will have a positive effect on both the hands-on time and turnover (turnaround) time we performed the automated approach for four consecutive weeks. Although the initial experiments demonstrated that micro-dissection on two slides generally yielded sufficient DNA for each test, we used 5 slides for micro-dissection in order to always guarantee sufficient DNA concentrations, accounting for very small tumors and/or much degraded tissues. Using 5 slides for microdissection still reduces the workload by half when compared to the classical method. To demonstrate that the hydrolysis probe assays perform equally well with DNA from both methods we compared the overall results from the four week interval with a previous four week interval in which samples were isolated with the classical method. In the first time interval, DNA from 66 samples was isolated using the classical method and Cq values for the *KRAS* and V600E assays were measured. In the second time interval, the identical assay was performed on 70 independent samples for which DNA was isolated using the fully automated method. In this way we compared a consecutive, representable series of DNA from tumor tissue cores or microdissected tumors from different tissue types (Supplementary Table 4). For the *BRAF* V600E assay the results are shown in figure 1C. The Mean Cq for the classical method was 29.20 +/- 3.14 and 30.03+/-2.88 for the automated method. This indicated that both methods compared well despite the different

amount of input DNA. (Figure 1C). For the 7 *KRAS* assays comparable results were obtained (Supplementary Figure 1).

Discussion

We demonstrated that a fully automated DNA isolation method is an excellent tool to obtain hands-on time reduction and lower turnover (turnaround) times in the daily practice of molecular tumor diagnostics. In an ideal situation the use of the fully automated system allowed for molecular test results to be delivered to the clinic about 24 hours earlier than when the classical DNA isolation method was used. However, it still remains to be seen if this gain in time can also be achieved in daily practice. (Figure 3)

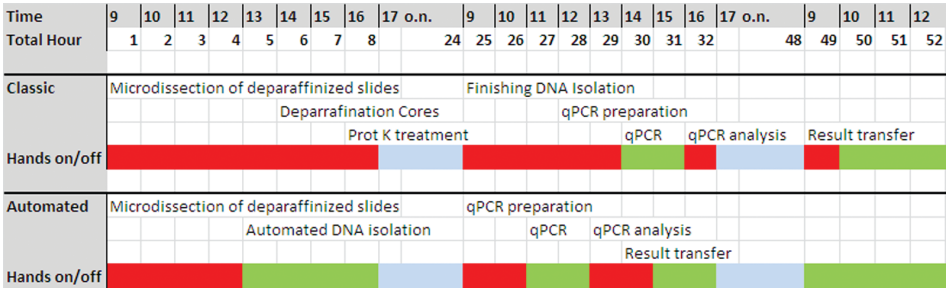

Figure 3. Laboratory implications for the fully automated method. Time evaluation of hands-on (red bar) and hands-off (green bar) workflow from tissue section to first molecular results. In the classical approach we start on Monday morning with the micro-dissection of 10 slides per sample request. One or two technicians work through this process until about the middle of the afternoon. In contrast, with the automated approach, micro-dissection is performed on only five tissue sections, and the work is finished around noon. Consequently, 50% of the hands-on time is saved. With the classical approach, on Monday afternoon the whole tissue sections or tissue cores are prepared and deparaffinized and an overnight Proteinase-K step is initiated. In the automated approach, the technician(s) finish the micro-dissection and start the DNA isolation around noon on Monday. At this point they can walk away from the system. The entire extraction is finished on the same day. On the following day (Tuesday) hours of hands-on time can be saved because the technician can immediately start with the qPCR processes instead of finishing the DNA isolation. This then results in the transfer of the results to the clinicians on Tuesday afternoon instead of Wednesday morning. In the near future it might be even possible to start the qPCR reaction on Monday afternoon which makes it possible to have the results reported to the clinic on Tuesday before noon. These results show that hands-on time, from tissue slide to first molecular results, can be reduced by approximately 50% . In addition, it is likely that the turnaround time can be further reduced to less than 24 hours in the near future. To make this process transparent to a broader public the department of Pathology made a video presentation of this process which can be viewed on http://www.scivee.tv/node/39348 (accessed February 24, 2012).

The isolated DNA is suitable for mutation detection by high throughput processes like routine hydrolysis probes assays. We demonstrated that in small deparaffinized tissue cores DNA of at least the same quality and quantity as with the classic method can be isolated. In many cases where micro-dissection is required the automated system provides significant added value in the whole process. Although deparaffinization and staining has already been performed before actual micro-dissection takes place at least 50% hands-on time can be saved by the fact that only 2mm^2 of material from a single 10µm slide is actually required for good quality DNA. Further, the consumption of rare and precious patient material is dramatically reduced. Thus, the automated extraction method can also decreases the burden on a patient by allowing for the isolation of DNA from minimal biopsies or other very small tissue fragments instead of larger tissue resections obtained by invasive surgery. DNA isolated with the automated system using nano-bead technology promises to be of sufficient quality and quantity for use in additional applications. It also potentially avoids pre-amplification protocols like whole genome amplification which again saves hands-on time, turnover (turnaround) time and costs.

The first results of using DNA obtained from the fully automated system in Sanger sequencing demonstrate that the overall quality of the sequences is higher than in the classical process (assessed by internal quality score; data not shown). Consequently, extra DNA treatment with whole genome amplification procedures can probably become obsolete for this application. Further validation of the automated extraction method should be performed for other types of assays such as Microsatellite Instability testing, clonality typing, MLPA, Maldi-tof, SNP arrays and high throughput and deep sequencing.

We conclude that the fully-automated IVD extraction system delivers sufficient and high quality DNA from precious FFPE tissue cores and micro-dissected tissue material. It significantly reduces the amount of starting tissue and labor and turnaround time. The automated and standardized extraction procedure can contribute to less operator-to-operator variability and reduces contamination risk between samples. In addition, the flexibility of the automated system including the ability to process between 1 and 48 samples per run and to select different protocols for both DNA and RNA while using the same reagents and protocol makes it very amenable for current and future high-throughput molecular laboratories.

Acknowledgements

LUMC department of Pathology: Sietske van Tol-Rensen, Rentia van Schaik-Ouwersloot, Natalja ter Haar, Brandt Meylis, Soheila Fallahi, Patrick Lelieveld, Melanie Schrumpf, Hans Baelde and Frans Prins.

Siemens Healthcare Diagnostics:Guido Hennig, Ton Raateland, Stephan de Gier, Carola van der Meer, Ellen Sampson

Conflict of Interest statement

RvE declares minor competing interests by being invited by Siemens Healthcare Diagnostics to deliver a presentation at a user meeting (travelling expenses paid). LS, HM,TvW declare no conflict of interests. Siemens Healthcare Diagnostics provided the necessary kits to evaluate the system in our laboratory, and supported to the preparation of this manuscript.

Reference List

1. Heinemann V, Stintzing S, Kirchner T, Boeck S, Jung A (2009) Clinical relevance of EGFR- and KRAS-status in colorectal cancer patients treated with monoclonal antibodies directed against the EGFR. Cancer Treatment Reviews 35: 262-271.
2. Gazdar AF (2009) Activating and resistance mutations of EGFR in non-small-cell lung cancer: role in clinical response to EGFR tyrosine kinase inhibitors. Oncogene 28 Suppl 1: S24-S31.
3. Wellbrock C, Ogilvie L, Hedley D, Karasarides M, Martin J et al. (2004) V599EB-RAF is an Oncogene in Melanocytes. Cancer Res 64: 2338-2342.
4. de Silva M, Reid R (2003) Gastrointestinal stromal tumors (GIST): C-kit mutations, CD117 expression, differential diagnosis and targeted cancer therapy with imatinib. Pathology & Oncology Research 9: 13-19.
5. Karapetis CS (2008) K-ras mutations and benefit from cetuximab in advanced colorectal cancer. N Engl J Med 3: 1757-1765.
6. Vidwans SJ, Flaherty KT, Fisher DE, Tenenbaum JM, Travers MD et al. (2011) A Melanoma Molecular Disease Model. PLoS One 6: e18257.
7. van Eijk R, Licht J, Schrumpf M, Talebian Yazdi M, Ruano D et al. (2011) Rapid KRAS, EGFR, BRAF and PIK3CA Mutation Analysis of Fine Needle Aspirates from Non-Small-Cell Lung Cancer Using Allele-Specific qPCR. PLoS One 6: e17791.
8. Boldrini L, Gisfredi S, Ursino S, Camacci T, Baldini E et al. (2007) Mutational analysis in cytological specimens of advanced lung adenocarcinoma: a sensitive method for molecular diagnosis. J Thorac Oncol 2: 1086-1090.
9. Hunt JL (2008) Molecular Testing in Solid Tumors: An Overview. Archives of Pathology & Laboratory Medicine 132: 164-167.
10. Ferrer I, Armstrong J, Capellari S, Parchi P, Arzberger T et al. (2007) Effects of Formalin Fixation, Paraffin Embedding, and Time of Storage on DNA Preservation in Brain Tissue: A BrainNet Europe Study. Brain Pathology 17: 297-303.
11. Klopfleisch R (2006) Excavation of a buried treasure--DNA, mRNA, miRNA and protein analysis in formalin fixed, paraffin embedded tissues. 26 6: 797-810.
12. Torrente MC, Rios C, Misad C, Ramirez R, Acuna M et al. (2010) DNA extraction from formalin-fixed laryngeal biopsies: Comparison of techniques. Acta Otolaryngol 131: 330-333.
13. C.Muñoz-Cadavid, Rudd S, Zaki SR, Patel M, Moser SA et al. (2010) Improving Molecular Detection of Fungal DNA in Formalin-Fixed Paraffin-Embedded Tissues: Comparison of Five Tissue DNA Extraction Methods Using Panfungal PCR. Journal of Clinical Microbiology 48: 2147-2153.
14. Gilbert MT, Haselkorn T, Bunce M, Sanchez JJ, Lucas SB et al. (2007) The isolation of nucleic acids from fixed, paraffin-embedded tissues-which methods are useful when? PLoS One 2: e537.

15. Bonin S, Hlubek F, Benhattar J, Denkert C, Dietel M et al. (2010) Multicentre validation study of nucleic acids extraction from FFPE tissues. Virchows Archiv : an international journal of pathology 457: 309-317.
16. Steinau M, Patel SS, Unger ER (2011) Efficient DNA extraction for HPV genotyping in formalin-fixed, paraffin-embedded tissues. The Journal of molecular diagnostics : JMD 13: 377-381.
17. Goelz SE, Hamilton SR, Vogelstein B (1985) Purification of DNA from formaldehyde fixed and paraffin embedded human tissue. Biochemical and Biophysical Research Communications 130: 118-126.
18. van Eijk R., van PM, Chhatta AR, Gupta N, Vossen RH et al. (2010) Sensitive and specific KRAS somatic mutation analysis on whole-genome amplified DNA from archival tissues. J Mol Diagn 12: 27-34.
19. Lim EH, Zhang SL, Li JL, Yap WS, Howe TC et al. (2009) Using whole genome amplification (WGA) of low-volume biopsies to assess the prognostic role of EGFR, KRAS, p53, and CMET mutations in advanced-stage non-small cell lung cancer (NSCLC). J Thorac Oncol 4: 12-21.
20. Baak-Pablo R, Dezentje V, Guchelaar HJ, van der Straaten T (2010) Genotyping of DNA Samples Isolated from Formalin-Fixed Paraffin-Embedded Tissues Using Preamplification. The Journal of Molecular Diagnostics 12: 746-749.
21. Bohmann K, Hennig G, Rogel U, Poremba C, Mueller BM et al. (2009) RNA Extraction from Archival Formalin-Fixed Paraffin-Embedded Tissue: A Comparison of Manual, Semiautomated, and Fully Automated Purification Methods. Clin Chem 55: 1719-1727.
22. Hennig G, Gehrmann M, Stropp U, Brauch H, Fritz P et al. (2010) Automated Extraction of DNA and RNA from a Single Formalin-Fixed Paraffin-Embedded Tissue Section for Analysis of Both Single-Nucleotide Polymorphisms and mRNA Expression. Clin Chem 56: 1845-1853.
23. De Jong AE, van Puijenbroek M, Hendriks Y, Tops C, Wijnen J et al. (2004) Microsatellite Instability, Immunohistochemistry, and Additional PMS2 Staining in Suspected Hereditary Nonpolyposis Colorectal Cancer. Clin Cancer Res 10: 972-980.
24. Lehmann A, Schewe C, Hennig G, Denkert C, Weichert W et al. (9000) Applicability of a System for Fully Automated Nucleic Acid Extraction From Formalin-fixed Paraffin-embedded Sections for Routine KRAS Mutation Testing. Diagnostic Molecular Pathology 21: 114-119.

Chapter 3

Multiplex Ligation-Dependent Probe Amplification for the Detection of 1p and 19q Chromosomal Loss in Oligodendroglial Tumors

Remco Natté[1]*, Ronald van Eijk[1*], Paul Eilers[2], Anne-Marie Cleton-Jansen[1], Jan Oosting[1], Mathilde Kouwenhove[3], Johan M. Kros[3], Sjoerd van Duinen[1]

*These authors contributed equally to this work
Department of Pathology[1] and Medical Statistics[2]
Leiden University Medical Center

Department of Pathology[3]
Erasmus Medical Center, Rotterdam

Brain Pathol. 15(3), 192 (2005) doi: 10.1111/j.1750-3639.2005.tb00520.x

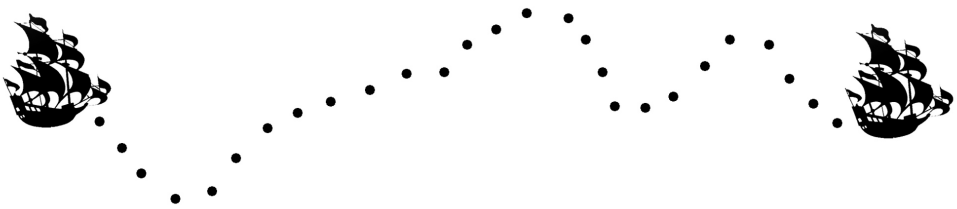

Abstract
Multiplex Ligation-Dependent Probe Amplification (MLPA) is a new assay for the detection of multiple chromosomal deletions in tumor tissue in a single experiment. Since genotyping of gliomas with oligodendroglial features by the detection of 1p/19q chromosomal deletions became essential for treatment decisions, we developed and validated an MLPA- based assay to determine these losses in formalin fixed and paraffin embedded oligodendroglial tumors (OG). Nineteen OG, and 10 control samples were analyzed by MLPA and the results were correlated with those obtained by fluorescent in situ hybridization (FISH). The MLPA results were reproducible in all samples in which repeated experiments were performed. In 18 of 19 OG MLPA and FISH were concordant for presence or absence of 1p deletion. In 3 OG, MLPA detected a 19q deletion not shown by FISH. For the other 15 OG MLPA and FISH were concordant. In one sample with 50-75% of tumor, MLPA failed to detect the 1p/19q deletions revealed by FISH (though with borderline values of significance). We conclude that MLPA is a valid and reproducible method for the detection of 1p/19q chromosomal deletions in OG stored on formalin fixed, paraffin embedded tissue.

Introduction
Gliomas are a group of primary brain tumors presumably originating from the astrocytic and/or oligodendroglial cell lineage. An oligodendroglial morphology in gliomas is associated with chemosensitivity and a relatively favorable prognosis, as well as deletions of the short arm of chromosome 1 and the long arm of chromosome 19 (1,2,8,10). More specific, chemosensitvity and 1p/19q deletions are most frequent in oligodendrogliomas, less frequent in gliomas showing both oligodendroglial and astrocytic phenotypes (oligo-astrocytomas) and least frequent in astrocytomas (8,10,13). The determination of 1p/19q deletions in gliomas is likely to result in a more reproducible and biologically and clinically more meaningful sub-classification of gliomas than the current classification, which is, to a large degree, based on subjective morphological criteria. Since the presence of 1p and/or 19q physical deletions in gliomas appears to be a better predictor for chemosensitivity and prognosis than morphology alone, there is growing need for a practical assay to determine these deletions in the routine clinical practice (3,11,13).
So far, a variety of methods for detection of 1p and 19q loss in gliomas have been used, like Fluorescent In Situ Hybridization (FISH) (10,12), detection of loss of heterozygosity (LOH) by microsatellite repeat analysis (5), and quantitative microsatellite analysis by real-time PCR (QUMA) (6).
Multiplex ligation dependent probe amplification (MLPA) is a recently developed technique for the relative quantification of DNA sequences that can detect chromosomal deletions or amplifications (4,7,9,14). The principle of MLPA is that two DNA oligonucleotides are directly adjacent hybridized to their complementary target sequences on the template DNA, followed by ligation of these two oligonucleotides. One oligonucleotide contains a target specific part with an M13 forward tail, the second probe contains a target specific part linked to a variable

length stuffer sequence and an M13 reversed tail. The two oligonucleotides can only be ligated together if both target specific parts are hybridized adjacently to their DNA template. PCR is then performed making use of the M13 primer sequences on the ligation product. PCR can only start after successful adjacent hybridization and ligation of both oligonucleotides, which ensures specificity of probe amplification. MLPA is thus characterized by PCR performed on the ligated two oligonucleotides (forming the probe) and not on the template DNA. The amount of ligated probes is related to the number of specific primer binding sites, making this method suitable for the detection of chromosomal deletions or amplifications.
MLPA has several advantages over currently used techniques: 1) up to 40 genomic loci can be analyzed in one reaction (9), 2) paired non-neoplastic tissue from the same patient is not needed and there are no non-informative loci, 3) requires only small amounts of DNA, (20ng is sufficient for 1 reaction in which 40 loci can be tested) (9), 4) is probably less sensitive to DNA degradation because probe target sequences are small (50-70bp) (9).
To the best of our knowledge, there are no reports about the feasibility of MLPA for the detection of 1p/19q deletions in oligodendroglial tumors (OG). The objective of the present study was to develop an MLPA based assay for the detection of 1p/19q chromosomal deletions in formalin fixed, paraffin embedded OG and to test the validity and reproducibility of this assay.

Materials and methods

Patients

Nineteen OG from 19 patients were analyzed. From all tumors FISH data were available. The tissue was obtained by stereo tactic biopsy or surgical excision and routinely formalin fixed (around 16 hours) and paraffin embedded (4-11 years). All tumors received a histological diagnosis according to the WHO criteria (JMK) (Table 2). Tumor percentages in isolated tissue were above 75% in 15 tumors, 50-75% in 3 tumors and around 50% in one tumor. Control brain tissue was obtained from microscopically unaffected brain areas of 3 of the above patients with an OG, 6 autopsy brains and 1 lymph node (5 of these autopsy brains were without abnormalities and 1 brain was from a patient with hereditary cerebral hemorrhage with amyloidosis, Dutch type). Autopsy brains were fixed for 24 hours (3X), 3 days (1X) or unknown (2X).

DNA isolation

Guided by the HE section, tumor or non-neoplastic tissue was punched from the paraffin embedded tissue blocks with a tissue array needle (Beecher Instruments, Silver Spring, MD) and deparaffinized by 2x 15 minutes incubation in xylol, followed by 2x 15 minutes incubation in ethanol. Tissue cores were resuspended in 128 μL of PK-1 lysis buffer [50 mM KCl, 10 mM Tris (pH 8.3), 2.5 mM MgCl2, 0.45% NP40, 0.45% Tween 20, 0.1 mg/mL gelatine] containing 5% Chelex beads (Biorad, Herculaes, USA) and 100 μg of proteinase K. The suspension was

Table 1. MLPA and FISH probes included in the analysis.

Probeset	Cyto pos	Map-view 31	probe number	PCR product length
FLJ10782-D01-247-M	01p36.33	01-002.45	16	247
FISH-probe D1S32	01p36			
TP73-D01-256-M	01p36	01-003.6	17	256
TNFRSF1B-D01-166-M	01p36.3	01-012.1	7	166
MUTYH-D02-310-M	01p34.3-1p32.1	01-044.8	23	310
BCAR3-D01-418-M	01p13.2	01-093.4	35	418
F3-D01-139-M	01p22-p21	01-094.2	2	139
BCAS2-D01-400-M	01p13.3	01-114.0	33	400
FISH-probe PUC 1.77	01cen			
TANK-D01x-220-M	02q24	02-160.6	13	220
CHL1-D01-265-M	03p26	03-000.3	18	265
MLH1-D13-355-M	03p21.3	03-036.3	28	355
MLH1-D17-436-M	03p21.3	03-036.3	37	436
APC-D09B-283-M	05q21-q22	05-112.6	20	283
APC-D01-175-M	05q21-q22	05-112.6	8	175
IL4-D01-154-M	05q31.1	05-132.5	5	154
IL12B-D01-382-M	05q31.1-q33.1	05-159.3	31	382
RAD54B-D01-292-M	08q21.3-q22	08-095.3	21	292
RB1-D03-193-M	13q14.3	13-043.0	10	193
RB1-D17B-160-M	13q14.3	13-043.0	6	160
FISH-Probe BAC2310A1	19p13			
BAX-D01-301-M	19q13.3	19-049.8	22	301
BAX-D02-211-M	19q13.3	19-049.8	12	211
FISH-probe BAC127F23	19q13			
KLK3-D02-391-M	19q13	19-051.7	32	391
LOC125905-D01-450-M	19q13.43	19-059.4	38	450

incubated for 12 h at 56 °C, 10 min at 100 °C and after 10 minutes centrifugation at 13.000g, the DNA containing supernatant was collected.

DNA quality

DNA concentration was measured with PICO green (Molecular Probes Europe BV, Leiden, the Netherlands) according to the manufacturers protocol. DNA concentration ranged from 5.2 – 154ng/ul, median 9.9 ng/ul. For testing tumor DNA quality, a PCR reaction was performed on P53 exon 8 generating a 239-basepair product in controls. The primer sequences were: ex8-forward, GTA GGA CCT GAT TTC CTT ACT GCC TCT TGC, ex8-reversed ATA ACT GCA CCC TTG GTC TCC TCC ACC GC. Each reaction was performed in 25 μL using AmpliTaq Gold ™ at 94 °C for 10 minutes initial denaturation followed by 35 cycles of 94 °C for 45 s, 57°C for 30 s and 72°C for 1 min. Products were analyzed on a 2% agarose gel to confirm size and quantity (data not shown).

MLPA detection

MLPA has previously been described (9). In brief, MLPA is based on the ligation of two DNA oligonucleotides that hybridize adjacently to DNA target sequence. The first oligonucleotide was synthesized with an on average 26bp (min: 21bp, max: 39bp) target specific part and a universal M13-forward tail. The second oligonucleotide was an M13-derived single stranded DNA containing an, on average, 42bp (min: 31bp, max: 50bp) target specific part, a stuffer sequence of variable length (130-480 base pairs) and an M13-reversed tail. Thus, a probe consists of two oligonucleotides of which the target specific parts hybridize adjacently and ligate. The M13 forward and reversed tails attached to all probes and the different length of each probe made it possible to perform a single primer multiplex PCR.

Twenty-two probes of the 40 probes in the kit were included for analysis and selected on the basis of localization on 1p or 19q (focus probes), likelihood to be unaltered in OG (1) (reference probes) and performance (Table 1). The MLPA kit was assembled by MRC-Holland (Amsterdam, the Netherlands). Details of MLPA and probes can be found at http://www.mlpa.com.

After denaturing 15-250ng DNA for 5 minutes at 95°C, the probe mix, containing all probe sets, was added. After overnight hybridization at 60°C the hybridized probes were ligated for 15 minutes at 54°C with a DNA-ligase. An aliquot was taken out of the ligation mix and the ligated products were amplified in a multiplex PCR with forward and reverse M13 primers for 20 sec at 95°C, 30 seconds at 60°C and 60 seconds at 72°C for 33 cycles in an Applied Biosystems® 9700 PCR machine. After PCR 3 μL of the PCR products were mixed with 1 μL 500 TAMRA (Applied Biosystems ®) internal size marker and 20μL deionised formamide and injected for 5 seconds in an ABI310® capillary filled with POP5 polymer. After a 30 minutes run the data were collected and analyzed with Genescan analysis and Genotyper software (Applied Biosystems®) (Figure 1). A Genotyper output file was generated combining probe set number, size and peak heights. This table was exported to a database where probe annotation is added to the data table. Subsequently normalization and diagnosis of the profiles were performed.

A

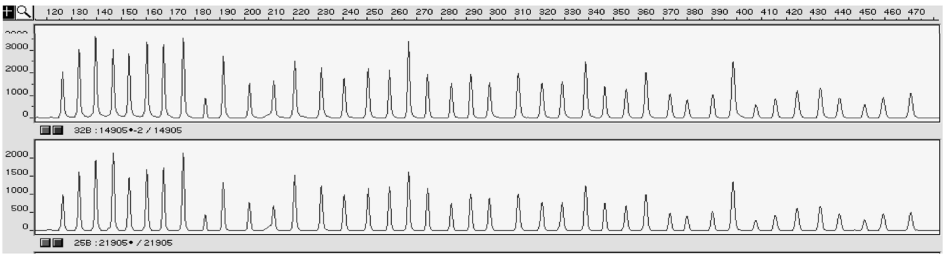

B

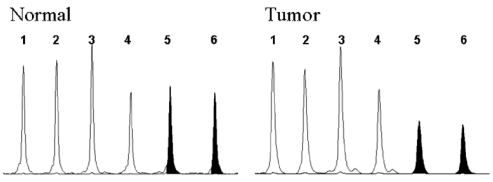

Probeset	Gene Name	Chr pos
1	CHL1	03p26
2	CDKN2A	09p21
3	APC	05q21-q22
4	RAD54B	08q21.3-q22
5	BAX	19q13.3
6	MUTYH	1p32.1

Figure 1. Examples of ABI electrophoresis signals in MLPA. A: Two control DNA samples showing reproducibility of MLPA patterns of all 40 probes in the kit, of which 22 were selected for analysis. Peakheight differences for the different loci are due to probe length (smaller probes give higher peaks/signals due to more efficient PCR) and differences in binding kinetics for each oligonucleotide. Differences in absolute peakheights between samples are probably due to differences in DNA concentration. B: Fragment of an MLPA pattern showing decreased peak heights of probes on 1p and 19q in an oligodendroglioma, indicating chromosomal loss.

Data analysis for MLPA

Normalization

Because MLPA traces analyzed with Genescan and Genotyper are not calibrated, raw data files had to be normalized. Peak heights were dependent on sample quality, DNA concentration, hybridisation parameters and instrument settings. Also peaks from different probe sets differed in magnitude in a systematic way (Figure 1). To calibrate the data, we used the following algorithm:

1. Distinguish focus probes (seven and four loci on chromosome 1p and 19q respectively) and reference probes (11 loci usually unaltered in OG).
2. Select the reference probes from the control (non-tumour) samples. Perform steps 3 to 5 with this subset of data.
3. Within each sample divide all peak heights by the median peak height of the concerning sample. This is to correct for the sample-to-sample variation.
4. Within each probe, divide all peak heights by the median peak height of the concerning probe. This is to correct for systematic differences between probes. The result of 3 and 4 we call normalized peak heights.
5. Determine which (reference) probes are most stable. Subtract 1 from each normalized peak height and take the absolute value. Compute the median of these numbers for each probe. This is the median of the absolute deviations: MAD.
6. Select the 5 reference probes with the lowest MAD. These 5 reference probes are named calibration probes and are used to normalize the complete experiment as described in step 7 and 8.
7. Within each sample (OG and normal control samples) divide all peak heights (focus and all reference probes) by the median peak height of the five calibration probes of the concerning sample. This is to correct for the sample-to-sample variation.
8. Within each probe (focus and reference probes), take the median peak height of the control samples. Then, within each probe (focus and reference probes) divide all peak heights (OG and normal control samples) by the median peak height of the concerning probe. This is to correct for systematic differences between probes.

Computing was initially performed in Matlab (The Mathworks inc., Natick, MA, USA). A Windows analysis interface was constructed using Delphi. The application is available on request (J.Oosting@lumc.nl).

Data visualization and interpretation.

Each experiment was normalized and analyzed separately. Heatmaps were generated for each experiment using Matlab (Figure 2) and scatter plots for each individual Tumor and Normal were generated in Matlab (Figure 3) and anonymized. Two authors (SvD an RN) independently decided if a scatter plot showed a deletion or not. The principle decision rule for a deletion was that for 1p at least 4 probes and for 19q at least 2 focus probes had normalized peak heights at least 0.25 below the median normalized peak height of the reference probes.

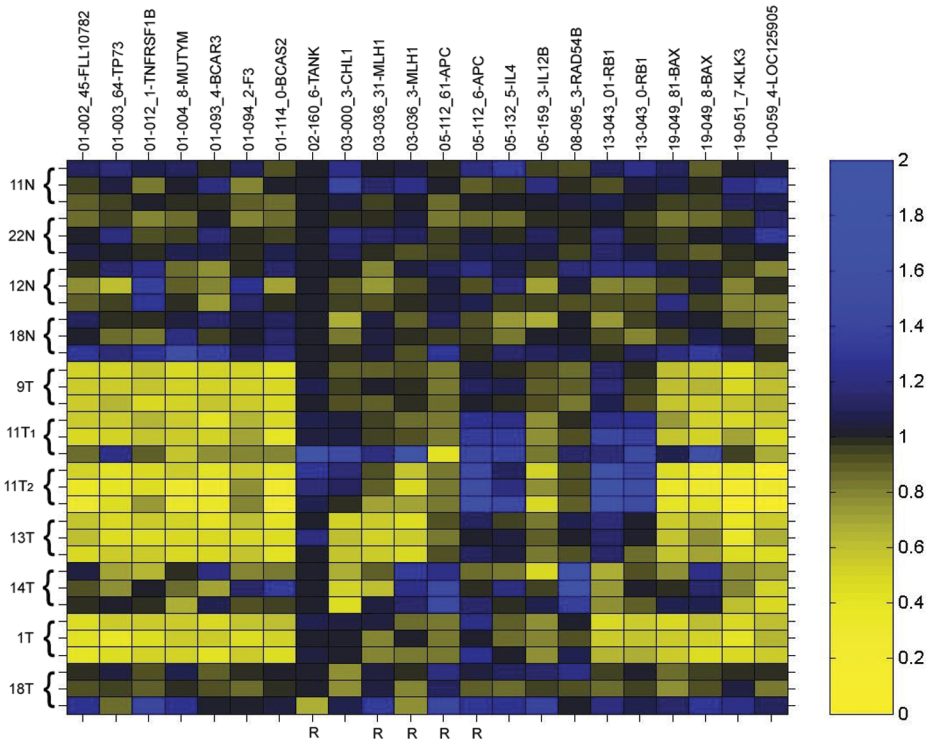

Figure 2. Heatmap representing an overview of a complete experiment. On the Y-axis samples are shown. The X-axis shows the different probes in chromosomal order. R indicates the 5 probes with least variance the Normal samples, and these were used for normalization. Chromosomal loss (yellow) or gain (blue) is shown.

FISH

The 1p and 19q status of all 19 OG was determined with fluorescence in situ hybridization on paraffin embedded, archival material using locus specific probes as earlier described (13). The cut off value to decide whether a 1p or 19q deletion was present or absent was 0.8.

Results

DNA quality was checked by a standard 239bp PCR, which was negative in 3 tumor and 2 control samples and weak in 4 tumor and 3 control samples. However, MLPA showed reproducible peak heights in these samples (Table 2). Electrophoresis was repeated once or twice in each experiment and gave highly reproducible results (Figure 2 and 3).

In 15 OG and 5 controls 2 to 4 experiments were performed. For all samples the different experiments showed consistent results, with little variation in the amount of focus probes with a normalized peak height of at least 0.25 below the median of the reference probes (Table 2).

In 18/19 OG, results of MLPA and FISH were concordant for presence or absence of a 1p deletion. In 15/19 OG, results of MLPA and FISH were concordant for a 19q deletion. In 3 OG, MLPA detected a 19q deletion, which was not shown by

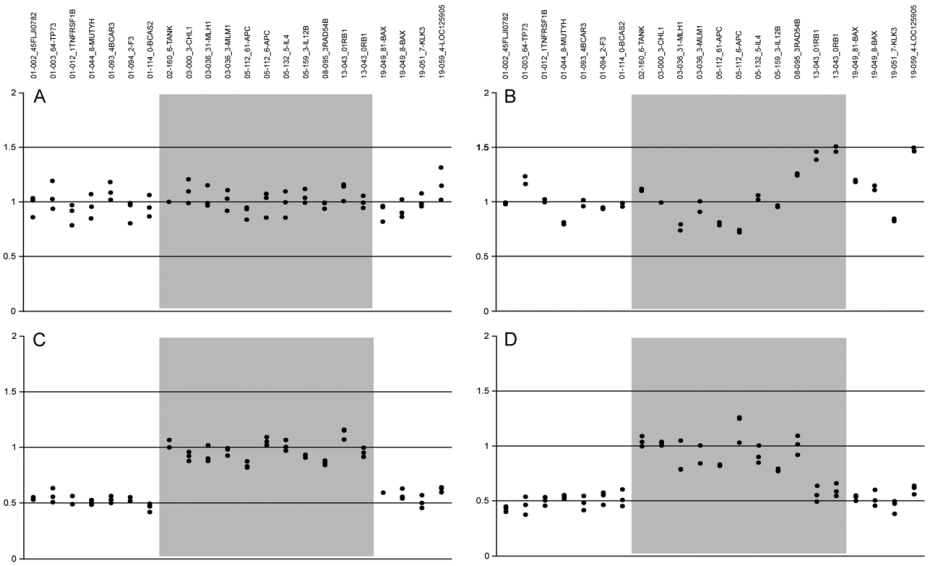

Figure 3. Representative scatterplots of normalized peakheights. Each plot represents one sample from one experiment with electroforesis in duplicate or triplicate. On the left in white 1p, on the right in white 19q, in grey the reference probes. A: Non-neoplastic brain tissue. B: Oligodendroglioma with FISH 0.99 for 1p and FISH 0.95 for 19q. C: Oligodendroglioma with FISH 0.59 for 1p and FISH 0.57 for 19q. D: Oligodendroglioma with FISH 0.54 for 1p and FISH 0.58 for 19q.

Table 2. MLPA and FISH results. PCR= standard polymerase chain reaction to test DNA quality, see “Methods”. Exp=number of MLPA experiments. N=non-neoplastic brain tissue. O=oligodendroglioma, AO=anaplastic oligodendroglioma. OA=oligoastrocytoma. AOA=anaplastic oligoastrocytoma. ret/del= retention/deletion of chromosome1p/19q. The principle decision rule for a deletion was that for 1p at least 4 (out of 7) focus probes and for 19q at least 2 (out of 4) probes had normalized peak heights at least 0.25 below the median normalized peak height of the reference probes. Numbers between brackets state for each MLPA experiment the number of focus probes with a normalized peak height of at least 0.25 below the median normalized peak height of the reference probes.

								MLPA/FISH concordant	
DNA-ID	Tissue	PCR	exp	MLPA 1p	MLPA 19q	FISH 1p	FISH 19q	1p	19q
109N	N	pos	1	ret (0)	ret (0)				
111N	N	pos	2	ret (0-0)	ret (0-0)				
113N	N	pos	1	ret (0)	ret (0)				
114N	N	pos	1	ret (0)	ret (0)				
115N	N	neg	1	ret (0)	ret (0)				
116N	N	weak	1	ret (0)	ret (0)				
122N	N	pos	2	ret (0-0)	ret (0-0)				
13N	N	weak	4	ret (1-0-0-0)	ret (0-0-0-0)				
15N	N	neg	3	ret (0-0-2)	ret (0-1-0)				
18N	N	weak	4	ret (1-0-0-0)	ret (0-0-0-0)				
1T	AO	pos	3	del (7-7-7)	del (4-4-4)	0.54	0.58	+	+
2T	OA	neg	1	ret (0)	ret (0)	1	1.05	+	+
3T	AO	pos	2	del (7-7)	del (4-4)	0.66	0.78	+	+
4T	AO	pos	2	del (7-7)	del (3-3)	0.67	0.75	+	+
5T	AO	neg	2	del (4-5)	del (2-2)	0.46	0.85	+	-
6T	AO	pos	2	del (7-7)	del (4-3)	0,68	0,60	+	+
7T	AO	pos	2	ret (0-0)	ret (0-0)	0.99	0.95	+	+
8T	AO	weak	1	ret (1)	ret (0)	1.06	0.89	+	+
9T	AO	pos	3	del (7-7-7)	del (4-4-4)	0.59	0.57	+	+
10T	AO	pos	2	ret (0-0)	ret (0-1)	1.06	1.04	+	+
11T	AO	pos	4	del (5-7-7-7)	del (4-4-4-4)	0.73	0.68	+	+
12T	AO	pos	2	del (7-7)	del (4-4)	0.67	0.64	+	+
13T	AO	weak	3	del (6-7-6)	del (3-4-4)	0.74	0.85	+	-
14T	OA	neg	3	ret (0-0-3)	ret (0-2-0)	1.02	1.06	+	+
15T	AOA	weak	1	ret (1)	ret (0)	0.95	0.97	+	+
16T	AO	pos	1	del (4)	del (3)	0.42	1.13	+	-
17T	AO	pos	2	del (4-7)	del (2-3)	0.66	0.59	+	+
18T	O	pos	3	ret (0-0-0)	ret (0-0-0)	0.73	0.79	-	-
19T	AO	pos	2	del (7-7)	del (4-4)	0.66	0.57	+	+

FISH. These 3 OG carried a 1p deletion according to both FISH and MLPA. In two of these samples, FISH results were close to the cut off value of 0.8. Only one sample showed inconsistent MLPA- and FISH results for both 1p and 19q status. This sample contained 50-75% tumor cells and the FISH results for 19q were close to the cut off value (Table 2, tumor 18T). None of the controls showed 1p/19q deletions. The amount of focus probes with a normalized peak height of at least 0.25 below the median of the reference probes is shown for each DNA sample and each experiment in Table 2. If not all focus probes in tumor samples with a deletion showed a normalized peak height of at least 0.25 below the median of the reference probes there was often a trend towards this value. The study was not designed for, and the data did not permit, the identification of breaking points.
The 3 tumor DNA's with negative control PCR all showed reproducible MLPA results consistent with FISH (Table 2).

Discussion

We showed that MLPA is a valid, reproducible, fast and simple method for the detection of physical 1p/19q deletions in DNA isolated from formalin fixed, paraffin embedded brain tissue. To the best of our knowledge, the use of MLPA for the detection of 1p/19q chromosomal loss in OG has not been described before.
MLPA is less limited by poor DNA integrity than conventional PCR because the probe target sequences (the combined binding specific domains of the 2 ligated oligonucleotides) are only 50-70bp (9). In the present study the use of formalin fixed, paraffin embedded material, even when stored for over 10 years (2 samples 11 years, 1 sample 10 years) and with only little amounts of DNA (as little as 15ng in the present series) yielded satisfactory results. Moreover, MLPA appeared to be more sensitive than conventional PCR. MLPA gave reproducible peak heights in 2 control- and 3 tumor DNA's with negative conventional PCR, normally generating a 239bp product.
MLPA is probably less sensitive to variations in DNA quality between samples than other techniques because, from the first round of amplification, ligated probes are amplified and not template DNA. Furthermore, the variable length of stuffer sequences in one of the probes permits the performance of multiplex PCR (40, and potentially more, reactions in one well), enabling the analysis of a large number of loci in a highly efficient way.
As compared to FISH, MLPA is performed in shorter time, is less elaborate and less dependent on individual interpretation. In addition, only one marker per experiment can be assessed using FISH. Tracing of chromosomal losses in individual tumor cells, for instance in infiltration margins of gliomas, is possible using FISH, but in the majority of studies FISH is used for detection of chromosomal aberrations in fields of tumor cells, not individual cells. For MLPA probably the majority of tissue needs to consist of tumor cells. In the present study we analyzed one tumor (tumor 18, table 2) with 50-75% of preexistent cells and were not able to detect a 1p or 19q deletion shown by FISH, although with borderline values of significance.

MLPA certainly has advantages over QUMA or LOH detection by microsatellite analysis. From the first round of amplification, PCR is performed on ligated probes instead of template DNA making PCR conditions more comparable between samples. Furthermore, MLPA is likely to work better on paraffin embedded material because probe target sequence (50-70bp) is smaller than the product lengths used in QUMA (in which expected product lengths length varied between 81-93bp and 145-157bp among the different probes) (6) or LOH (in which expected product lengths length varied between 69-110bp and 130-185bp among the different probes) (5). In addition, extended multiplexing with 40, and potentially more, loci in on reaction is possible, which is difficult with LOH detection by standard microsatellite markers or QUMA. To test the same amount of loci in conventional LOH or QUMA analysis is more elaborate and takes much more DNA. For QUMA it was reported that at least 15ng DNA per locus was required (6). In the present study, only 15ng of DNA was enough to determine the relative amount of DNA at all 22, and potentially more, loci. An additional major advantage of MPLA over LOH detection with microsatellite markers is that patient-matched normal DNA is not necessary. Any normal DNA can be used as a control. This is especially relevant for brain tumor biopsies and excisions in which 'normal' surrounding tissue is either not available or often contains variable amounts of infiltrating tumor cells.
We tested and validated a MLPA based assay for the detection of 1p/19q deletions in formalin fixed, paraffin embedded brain tissue. MLPA enables the introduction of many more probes in one reaction than presented in the present paper, potentially enabling the routine analysis of all clinically relevant or scientifically interesting chromosomal deletions and amplifications of oligodendrogliomas, oligo-astrocytomas and astrocytomas in one assay. It is likely that this information will improve classification of these tumors, enable a more reliable estimation on prognosis and guide therapeutic decisions. The present results suggest that MLPA on paraffin embedded tissue may also be used for clinically or scientifically relevant chromosomal deletions or amplifications in other malignancies like HER-2/neu amplification in breast cancer.

Acknowledgements
Jan Schouten, MRC Holland, Amsterdam, the Netherlands for supplying the MLPA kit.

Reference List

1. Bigner SH, Matthews MR, Rasheed BKA, Wiltshire RN, Friedman HS, Friedman AH, Stenzel TT, Dawes DM, McLendon RE, Bigner DD (1999) Molecular genetic aspects of oligodendrogliomas including analysis by comparative genomic hybridization. Am J Pathol 155:375-386.
2. Cairncross G, Macdonald D, Ludwin S, Lee D, Cascino T, Buckner J, Fulton D, Dropcho E, Stewart D, Schold C, Wainman N, Eisenhauer E (1994) Chemotherapy for Anaplastic Oligodendroglioma. J Clin Oncol 12:2013-2021.
3. Cairncross JG, Ueki K, Zlatescu MC, Lisle DK, Finkelstein DM, Hammond RR, Silver JS, Stark PC, Macdonald DR, Ino Y, Ramsay DA, Louis DN (1998) Specific genetic predictors of chemotherapeutic response and survival in patients with anaplastic oligodendrogliomas. J Natl Cancer Instit 90:1473-1479.
4. Gille JJ, Hogervorst FB, Pals G, Wijnen JT, van Schooten RJ, Dommering CJ, Meijer GA, Craanen ME, Nederlof PM, de Jong D, McElgunn CJ, Schouten JP, Menko FH (2002) Genomic deletions of MSH2 and MLH1 in colorectal cancer families detected by a novel mutation detection approach. Br J Cancer 87:892-897.
5. Hatanpaa KJ, Burger PC, Eshleman JR, Murphy KM, Berg KD (2003) Molecular diagnosis of oligodendroglioma in paraffin sections. Lab Invest 83:419-428.
6. Nigro JM, Takahashi MA, Ginzinger DG, Law M, Passe S, Jenkins RB, Aldape K (2001) Detection of 1p and 19q loss in oligodendroglioma by quantitative microsatellite analysis, a real-time quantitative polymerase chain reaction assay. Am J Pathol 158:1253-1262.
7. Postma C, Hermsen M, Coffa J, Baak J, Mueller J, Mueller E, Bethke B, Schouten J, Stolte M, Meijer G (2005) Chromosomal instability in flat adenomas and carcinomas of the colon. J Pathol 205:514-521.
8. Reifenberger J, Reifenberger G, Liu L, James CD, Wechsler W, Collins VP (1994) Molecular-genetic analysis of oligodendroglial tumors shows preferential allelic deletions on 19Q and 1P. Am J Pathol 145:1175-1190.
9. Schouten JP, McElgunn CJ, Waaijer R, Zwijnenburg D, Diepvens F, Pals G (2002) Relative quantification of 40 nucleic acid sequences by multiplex ligation-dependent probe amplification. Nucl Acids Res 30:e57
10. Smith JS, Alderete B, Minn Y, Borell TJ, Perry A, Mohapatra G, Hosek SM, Kimmel D, O'Fallon J, Yates A, Feuerstein BG, Burger PC, Scheithauer BW, Jenkins RB (1999) Localization of common deletion regions on 1p and 19q in human gliomas and their association with histological subtype. Oncogene 18:4144-4152.
11. Smith JS, Perry A, Borell TJ, Lee HK, O'Fallon J, Hosek SM, Kimmel D, Yates A, Burger PC, Scheithauer BW, Jenkins RB (2000) Alterations of chromosome arms 1p and 19q as predictors of survival in oligodendrogliomas, astrocytomas, and mixed oligoastrocytomas. J Clin Oncol 18:636-645.

12. Stock C, Ambros IM, Mann G, Gadner H, Amann G, Ambros PF (1993) Detection of Ip36 Deletions in paraffin sections of neuroblastoma tissues. Genes Chrom Cancer 6:1-9.
13. Van Den Bent MJ, Looijenga LHJ, Langenberg K, Dinjens W, Graveland W, Uytdewilligen L, Smitt PAS, Jenkins RB, Kros JM (2003) Chromosomal anomalies in oligodendroglial tumors are correlated with clinical features. Cancer 97:1276-1284.
14. Worsham MJ, Pals G, Schouten JP, Van Spaendonk RM, Concus A, Carey TE, Benninger MS (2003) Delineating genetic pathways of disease progression in head and neck squamous cell carcinoma. Arch Otolaryngol Head Neck Surg 129:702-708.

Chapter 4

MLPAinter for MLPA interpretation: an integrated approach for the analysis, visualisation and data management of Multiplex Ligation-dependent Probe Amplification

Ronald van Eijk[1], Paul H. C. Eilers[2], Remco Natté[1], Anne-Marie Cleton-Jansen[1], Hans Morreau[1], Tom van Wezel[1] and Jan Oosting[1]

[1] Department of Pathology
Leiden University Medical Center
[2] Department of Biostatistics
Erasmus University Medical Center, Rotterdam

BMC Bioinformatics. 11, 67, (2010) doi: 0.1186/1471-2105-11-67.

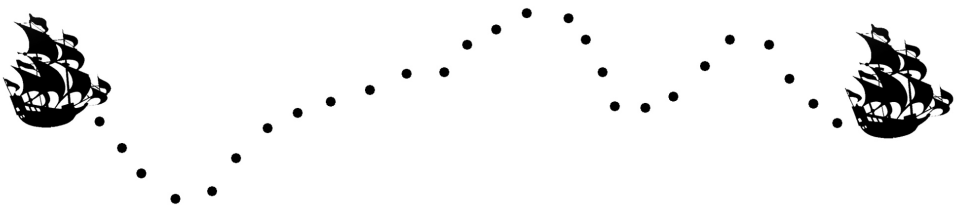

ABSTRACT

Background

Multiplex Ligation-Dependent Probe Amplification (MLPA) is an application that can be used for the detection of multiple chromosomal aberrations in a single experiment. In one reaction, up to 50 different genomic sequences can be analysed. For a reliable work-flow, tools are needed for administrative support, data management, normalisation, visualisation, reporting and interpretation.

Results

Here, we developed a data management system, *MLPAInter* for MLPA interpretation, that is windows executable and has a stand-alone database for monitoring and interpreting the MLPA data stream that is generated from the experimental setup to analysis, quality control and visualisation. A statistical approach is applied for the normalisation and analysis of large series of MLPA traces, making use of multiple control samples and internal controls.

Conclusions

MLPAinter visualises MLPA data in plots with information about sample replicates, normalisation settings, and sample characteristics. This integrated approach helps in the automated handling of large series of MLPA data and guarantees a quick and streamlined dataflow from the beginning of an experiment to an authorised report.

BACKGROUND

In medical research, knowledge of chromosomal deletions or amplifications is of great importance. For example, it can help us better understand the genetic causes of certain diseases and as a consequence, improve the treatment and prognosis of individual patients. Classic techniques for the detection of chromosomal abnormalities include karyotyping, Southern blotting, Fluorescent In Situ Hybridisation (FISH), CA-repeat analysis and quantitative micro satellite analysis by real-time PCR [1-4]. In recent years, high-throughput methods based on BAC arrays, SNP arrays and related techniques have gained prominence [5,6]. Although these are excellent tools for whole genome analysis, these techniques are laborious, time-consuming, difficult to implement, expensive and generate large data sets. The management and interpretation of such voluminous data is not a light task. Multiplex Ligation-dependent Probe Amplification (MLPA) [7] has been introduced as a relatively cheap and fast method to perform quantitative chromosomal analysis of up to about 50 genomic DNA or RNA sequences, which is able to distinguish sequences differing in only one nucleotide. This technique fills the gap between the methods that investigate a single locus and the techniques that interrogate thousands of loci.

MLPA is a quick and cost effective approach to testing for the presence of gene deletions or obtaining tumour profiles on multiple loci in a single tube, which can easily be applied in molecular pathology. Furthermore, MLPA only requires small amounts of DNA. Moreover, DNA obtained from formalin fixed paraffin

embedded material can be used. Currently, MLPA is used for the validation of array-based comparative genomic hybridisation (array-CGH) and SNP arrays. [7-12]. Other applications for MLPA include methylation status determination, copy number analysis in segmentally duplicated regions, expression profiling, and transgene genotyping [13]. The principle of MLPA is that for each locus, two DNA oligonucleotides (probes) must hybridise to their complementary target sequences on the template DNA for ligation to occur. Subsequently a PCR reaction is performed on the ligated probes. After PCR, an aliquot of the PCR product is combined with an internal size marker and deionised formamide. The sample is then injected into a capillary of an automated sequencer, where after a 30 minutes run, the data are subsequently collected for further analysis. Since, the amount of ligated probes is dependent on the number of specific primer binding sites, this method is suitable for the detection of chromosomal deletions or amplifications [7]

The analysis, visualisation and data management of hundreds of samples with many different probes per reaction can be cumbersome. Like in many modern techniques, the results of an MLPA analysis are delivered as lists of values that can be easily imported into spreadsheet applications. Large collections of individual spreadsheets are not the best way to collect and analyse data, especially in an environment where a controlled work flow has to be guaranteed. A database system offers advantages such as the tracking of material used in the tests and consistency in the handling of test results. Some of the information that needs to be managed includes: the origin of normal and test samples, the experimental setup, the identity of the probes, and the quality settings. Normalisation has to be performed within and between samples and results have to be visualised and stored. Sophisticated tools are needed to facilitate the reliable use of MLPA [7,9,14-16]. In this paper, we present a statistical technique for the normalisation of MLPA data and the software component that we have developed to make MLPA a simple, effective, and attractive tool. Here we describe *MLPAinter,* for MLPA interpretation, a system that stores results, instrument settings and sample descriptions in a Microsoft Access database. A special front-end, written in the Borland Delphi language, allows the user to interrogate the database, normalise data and visualise results as heat maps and specialised plots.

IMPLEMENTATION

MLPA probe kits are obtained from MRC-Holland (Amsterdam, The Netherlands). All assays are performed according to the manufacturers' protocols on an ABI DNA sequencer (Applied Bio Systems, Foster City, CA, USA). *MLPAinter* was constructed using Delphi 2009 (Embarcadero, San Francisco, CA, USA) for the GUI, and Microsoft Office Access 2003 (Microsoft, Seattle, WA, USA) for the standalone database. The runtime requirements for the application are Windows XP or newer. Statistics used in *MLPAinter* as described below, were validated in a series of oligodendroglial tumours as previously described [9]. The source code and a step by step protocol to use *MLPAinter* together with showcase sample files and analysis tables can be obtained from http://code.google.com/p/mlpainter/

RESULTS

Data pre-processing

MLPAinter can not handle the raw electrophoresis signal and therefore requires that the MLPA amplification product peaks have already been linked to the corresponding MLPA probes of the used MLPA kit. After electrophoresis, all MLPA sample trace files should be pre-processed in standard software for basic analysis of MLPA traces. Subsequently, the report files can be imported. Here we used GeneMapper (Applied Bio Systems, Foster City, CA, USA) for *MLPAinter*, but the system can also import data from the combination Genescan Analysis and Genotyper software (Applied Bio Systems, Foster City, CA, USA). Adaptations to other software programs like Genemarker (Softgenetics, State College, PA, USA) should be straightforward. A step-by-step vignette for Genemapper settings can be found at http://code.google.com/p/mlpainter/. Briefly, the product lengths of the ligated probes are defined with an internal size standard. The peak height and area are calculated for every peak present in the trace. Any undefined peaks are discarded from further analysis. Data tables are then automatically generated with length, height and area of all recognised peaks. These tables are exported from the Genemapper software package and imported into *MLPAinter* for specific analysis of the raw data. Protocols for linking output files from other software packages are planned for future versions.

Data management

Here, we developed a relational database using Microsoft Access to manage all pertinent information for MLPA experiments and created a front end with Borland Delphi to guide laboratory workflow and data analysis. Characteristics such as the sample number and status, e.g., tumour or normal, DNA concentration and, if available, tumour percentages that are relevant for the performance of the MLPA should be stored in a database. Annotation information like the chromosomal position and gene names of the different probes in a kit should be available for the interpretation of the results in output tables, heat maps, and plots. To assist the laboratory work-flow, electronic and paper sample sheets can be prepared for the automated sequencer. The raw data of the sequencing reports are imported into the database for subsequent quality control steps and analysis.

The relational database contains three hierarchies which are interconnected. The hierarchies are MLPA kits and probes, electrophoresis results, and analyses. In the database tables, next to the specific Kit information, you can find gene and probe names, as well as the physical and cytogenetic location of the probes. All probes in a particular kit are numbered from 1, for the probe with the smallest product size to n, for the probe with the largest product size. Every kit contains a number of probes that can be used for a quality check of the trace. The corresponding products are named based on their size in base pairs. The different kits as defined by MRC-Holland, can be imported from www.mlpa.com.

Both the MLPA run and analysis hierarchy use the samples table. This table contains clinical information like the origin of the used DNA, e.g., if the DNA is isolated from whole blood, fresh frozen tissue or formalin fixed paraffin embedded

tissue. Every sample is labelled with an N for Normal, T for Test or the Tumour origin of the tissue. Normal samples are treated differently from test samples in the normalisation and analysis steps as described in the normalisation section. An electrophoresis run typically consists of a sample plate to be processed by the sequencer. The sample, the kit, and a unique name for the plate are recorded for each position on the sample plate. Different types of kits can be used within one run. From this information a sample sheet or configuration file is created for the sequencer. The resulting peak heights and peak areas of an MLPA run are imported for all of the probes in a kit and the analysis settings can be set to analyse peak heights or peak areas.
During analysis, specific MLPA runs can be combined from one or more electrophoresis runs. A group of reference probes can be copied from another analysis with the same kit, and can be adapted to suit the needs of the specific analysis. However, to avoid inter experimental differences, values from experiments performed at a different time should not be used. Probes can also be excluded from the analysis. Successful analysis can be finalised by authorising the results. After authorising the analysis, all options are fixed except for visualisation and sorting options.

Quality control
MLPAinter presents three data quality indicators, Q1, Q2 and Q3, (Figure 1A) to assist with the decision of whether to include a trace in the analysis.
The first indicator (Q1) is the ratio between the ligation dependent peak at 94 base pairs and the median of the DNA dependent 64, 70, 76 and 82 peaks (Figure 2). Van Dijk et al. [10] state that this ratio should be greater than 5 to obtain good and reproducible results. Nonetheless, we have observed that in some cases, lower ratios can also give reliable peak patterns (Figure 2).
The second quality indicator (Q2) is the median peak height of the probe signals present in the kit. If the median of the first 20 ligated probe peak heights is below 450 relative fluorescent units (RFU), the trace quality is considered low. Moreover, because of the limits in the detection optics of the instrument, a median peak height over 4000 RFU is indicative that the trace quality is low (Figure 2) [14].
For the last indicator (Q3) all analysis peaks are split in 2 parts based on sequence length. The value is computed as the median signal of the longest probes divided by the median signal of the shortest probes. Often the longest probes show lower signals, however in high quality traces this indicator is usually over 0.5.
Other factors that are important for the assessment of quality, which can optionally be stored into the database, are the DNA concentration of the sample, the tumour percentage of the tumour specimens and the intrinsic DNA quality of the sample. The combination of these quality parameters allows the user to decide on inclusion or exclusion of a trace from the analysis.

Normalisation
Raw MLPA results are not calibrated. Peak areas or heights are dependent on sample quality, hybridisation parameters and instrument settings. To analyse the

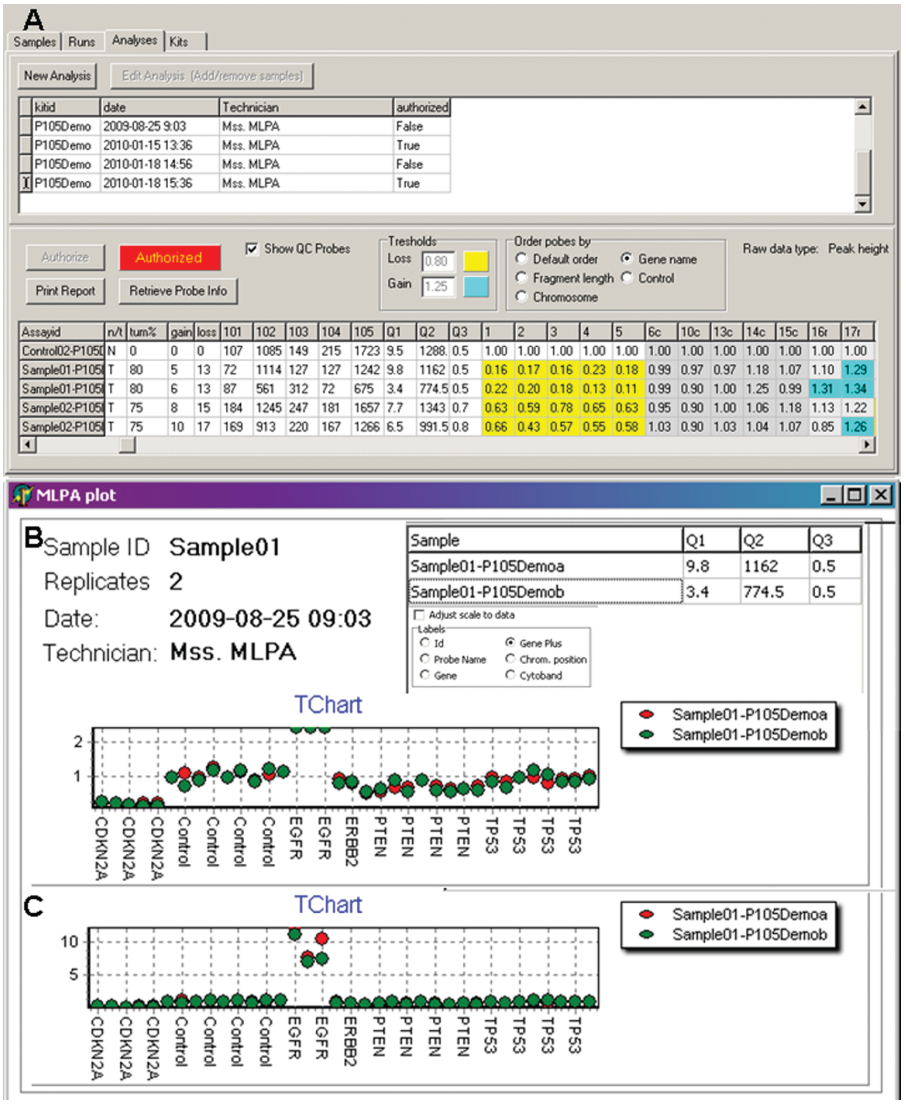

Figure 1. MLPAinter for MLPA interpretation. Panel A: Heat map of an authorised series of samples after normalisation. The probes are sorted by the name of the gene. The gain and loss columns show the total number of probes with gain or loss. Q1-3 show the different quality scores calculated from the DNA dependent probes (marked 101-104) and the ligation dependent probe (105) and as explained in the text. Dark grey cells: calibration probes, the id has a suffix 'c'. Light grey cells: reference probes, the id has a suffix 'r'. Yellow cells: probes with loss of one allele (< 0.8). Blue cells: probes with gain of one allele (>1.25). Panel B: Sample plot of an individual sample after normalisation. The quality indices for each replicate are shown. Replicates are visualised in different colours. Probes are sorted by the gene name combined with the chromosomal position. The standard scale can be adjusted in case of samples with amplified probes (see panel C).

MLPA traces, internal and external control loci are used for the normalisation of the data. External controls, e.g., normal tissue in tumour analysis, have to be present in every experiment for the pattern comparison. Internal controls for the calibration of the samples are present in every kit and are supposed to be non-altered or reference probes in a tumour sample. These reference probes are compared to the probes where DNA changes are expected.

The top trace in Figure 2 shows a normal sample. It is evident that peak heights or areas differ between probes; and these differences have to be corrected. Also the average peak areas or heights may differ from sample to sample. Therefore, sample calibration and probe calibration have to be performed. Consider the data as a matrix *Y*, with columns for the probes and rows for the sample. Then, we need to apply normalisation to both rows and columns. Normalisation is implemented as division by row parameters $r_i, i = 1 \ldots m$ and column parameters c_j, $j = 1 \ldots n$, such that a matrix $X = [x_{ij}]$ results, with $x_{ij} = y_{ij} / (r_i c_j)$. We prefer to work on the original scale instead of with logarithms because loss and gain correspond to integer ratios (including zero) on the original scale.

A simple approach would be to take row and column medians for *r* and *c, respectively*. This could work well if the number of deletions or amplifications is relatively small. However, for samples with a large number of deletions (more than 50%), the corresponding row median might become a number near zero and normalisation by dividing with this small number would give a completely wrong result.

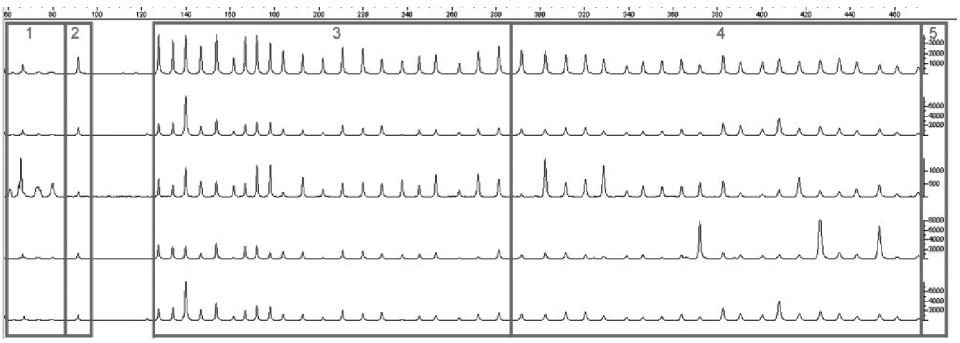

Figure 2. MLPA sample trace files. Overview of 5 different sample traces obtained with MLPA kit P105 (Oligodendroglioma-2) showing the necessity of data normalisation. Differences in and between samples are hard to distinguish. Quality aspects of every trace are visible. Probe lengths in base pairs are shown on the x-axis. Box 1: four no template control peaks of 64, 70, 76 and 82 bases, respectively. Box 2: a 94 base pair ligation control peak. Box 3 and 4: larger peaks in the first half than in the second half of the sample trace. Box 5: peak heights are noted on the y-axis

To improve normalisation and obtain calibration factors, we use only a subset of the samples and probes. Specifically, we use normal samples, and only a subset of the probes, where copy number changes are unlikely, even in tumour samples. We use the following algorithm:

1. To correct for the sample-to-sample variation, divide the peak heights or areas of all the probes in each sample by their median. This gives provisional row parameters, *ř* for the normal samples, and provisional normalisation of the normal samples.
2. To correct for systematic differences between probes, divide the peak heights or areas of all the probes within a MLPA run by their median. This results in the *normalised peak areas or heights*, and represents the column parameters *c* for all probes. The average of all probes is now close to 1.
3. Select the probes that have a small probability of change in copy number. Call these *the reference probes*. The remaining probes are called the *focus probes*, since we look for changes in these. The description file for commercial kits includes this information, and the program uses these probes by default.
4. Select the part of the data that represents the normal control or non-tumour samples and the reference probes.
5. Redo steps 1 and 2 for the subsets of reference samples and reference probes.
6. Determine which probes are most stable. Subtract 1 from each normalised peak height or area and take the absolute value. Compute for integrated MLPA analysis the median of these numbers for each probe. This is the median of the absolute deviations: MAD.
7. The reference probes with the lowest MAD are most stable. Select the five probes closest to zero. These are the probes that we call the *calibration probes*.
8. Compute the median peak height or area of the 5 calibration probes for each sample (normal and test samples or tumours and non-tumours). Divide all peak heights or areas as computed in step 2 in each sample by this value. This gives the final row parameters *r* for all samples, and their final normalisation.

Reference probe selection

As in quantitative RT-PCR, the selection of reference probes is a critical element of the analysis [17]. MLPA kits contain about 10 reference probes that are included for normalisation purposes because they are not involved in the experimental hypothesis/diagnostic question. Alternatively, one can usually find a subset of probes in existing kits that are known not to be involved in the hypothesis. The procedure selects the most stable probes from the reference probes to calibrate the data. The number of calibration probes used (five, in this instance) did not significantly influence the results (data not shown). However, the number is configurable in the program. If probes show high variability between replicates or between normal samples, they should be excluded from the analysis.

Visualisation

We have designed a number of visualisations to interpret the results after the normalisation and quality control of the data set. The first visualisation is a heat map that shows all of the data in an experiment. Deletions and gains are colour-coded with configurable thresholds. Probes can be sorted by locus names or chromosomal position. The reference and calibration probes are clearly differentiated by a grey-shade (Figure 1). Another visualisation shows the normalised values of all replicates of one sample in a plot (Figure 1). Technical replicates are shown in different colours. On the x-axis, the different probes are shown in the selected probe order. The y-axis is on a scale from 0 to 2.5, where 0 stands for absent probes. Ideally probes at genomic loci with loss of a single allele show values around 0.5. Unaltered probes are visualised around 1.0. Probes with DNA gains have values around 1.5 or above. In tumour samples contaminated with normal DNA these values are usually not that outspoken. The researcher should keep this in mind during the interpretation. Information about sample characteristics and probes used are also shown in the plots.

Future developments

Currently the system is suited for the analysis, visualisation and data management of MLPA. However, all of the information generated during an experiment is still not fully integrated in the data analysis. For instance, tumour percentages can be stored in the database and will be displayed, but it is up to the user to incorporate this information into the interpretation. We plan to include the tumour percentage and probably the DNA index for automated identification of the allelic state of the chromosomal aberrations in the analysed sample ([18]).

Another worthwhile improvement would be to remove the dependency on an external program to do the peak detection.

DISCUSSION

MLPA has a variety of applications for the detection of changes in dosage at a single locus, e.g., a subtelomeric locus, to those with multiple changes. Up to 50 different probes (genomic sequences) can be interrogated in one single reaction. Advantages are that only small amounts of DNA are needed and that DNA isolated from formalin fixed paraffin embedded material can be used. As it stands, currently available software tools for MLPA analysis do not integrate data management, normalisation and visualisation, and do not always perform adequate data normalisation between and within traces. In these packages, the quality aspects of the analysis are not always taken into consideration. Therefore, we have developed a method for MLPA data interpreting, *MLPAinter*, in which sample information can be stored, and where the laboratory and analysis workflow is assisted. Experiments are prepared by selecting samples and MLPA kits. Then sample sheets for automated sequencers are generated, which can easily be imported in the sequencer, avoiding manual input and typing errors. Analysis tables can then be imported from standard DNA analysis programs. Given the sensitivity and reproducibility of this methodology, the requirements

for proper internal controls for normalisation have to be stringent [17]. For that reason, in each kit, the manufacturer has provided sets of reference probes for sample data. However, for the analysis of unpredictable (tumour) samples, these provided reference probes may be inadequate. Thus, we created an algorithm that will select the 5 most stable reference probes and suggest that these probes be used for the normalisation of the traces. The user has full control over the settings of the analysis, and changes like including or excluding samples or designating probes as reference probes result in immediate recalculations. All calculations can be visualised in plots. By authorising the results, the analysis settings are definitively linked to the analysis and can no longer be changed.
MLPA results are, in general, very reproducible. Still, we perform all tests at least in duplicate, especially in a diagnostic setting. *MLPAinter* supports the handling of replicates in the analysis. We previously validated the statistics used for *MLPAinter* on a series of DNAs that were obtained from formalin fixed and paraffin embedded oligodendroglial tumours by correlating the results with those obtained by fluorescent in situ hybridisation (FISH). The MLPA results were reproducible in all samples in which repeated experiments were performed. [9]

CONCLUSIONS

We have combined the analysis, visualisation and data management for MLPA in a tool, *MLPAinter* for MLPA interpretation, which makes use of a relational database with a Delphi front end. This integrated approach helps in the automated handling of large series of MLPA data and helps to guarantee a quick and streamlined dataflow from the initiation of an experiment to the generation of authorised report. *MLPAinter* has been successfully used in our lab for over two years to manage over 3000 samples. Moreover, different MLPA kits have been successfully used for this type of analysis, e.g., Kit P088 and P105 for the analysis of Oligodendrogliomas, P024 for CDKN2A/B and P036 for subtelomeric regions.

AVAILIABILITY AND REQUIREMENTS

Project name: MLPAinter
Project home page: http://code.google.com/p/mlpainter/
Operating system(s): Windows XP or higher
Programming language: Delphi
Other requirements: no
Licence: GNU GPL 3.0
Any restrictions to use by non-academics: no

ABBREVIATIONS

MLPA: Multiplex Legation-Dependent Probe Amplification, RFU: relative fluorescent units, RT-PCR: Real Time-PCR, MAD: median of the absolute deviations.

AUTHORS' CONTRIBUTIONS

RvE specified MLPAinter functionalities and drafted the main parts of this manuscript. PHCE developed the statistics for normalisation of the MLPA data. RN validated statistics on a series of oligodendrogliomas. AMCJ, TvW and JM participated in the study design and supervised the implementation of MLPAinter in molecular diagnostics. JO developed the software and supervised the drafting of the manuscript. All authors read and approved the final manuscript.

ACKNOWLEDGEMENTS

We thank the technicians at the Molecular Diagnostics group in the LUMC department of Pathology for testing the tool in different biological settings and Tanaka Moyo for troubleshooting.

Reference List

1. Petrij-Bosch A, Peelen T, van Vliet M, van Eijk R, Olmer R, Drusedau M, Hogervorst FB, Hageman S, Arts PJ, Ligtenberg MJ et al.: BRCA1 genomic deletions are major founder mutations in Dutch breast cancer patients. *Nat Genet* 1997, 17:341-345.
2. Klinger K, Landes G, Shook D, Harvey R, Lopez L, Locke P, Lerner T, Osathanondh R, Leverone B, Houseal T et al.: Rapid detection of chromosome aneuploidies in uncultured amniocytes by using fluorescence in situ hybridization (FISH). *Am J Hum Genet* 1992, 51:55-65.
3. Devilee P, Cleton-Jansen AM, Cornelisse CJ: Ever since Knudson. *Trends Genet* 2001, 17:569-573.
4. Nigro JM, Takahashi MA, Ginzinger DG, Law M, Passe S, Jenkins RB, Aldape K: Detection of 1p and 19q loss in oligodendroglioma by quantitative microsatellite analysis, a real-time quantitative polymerase chain reaction assay. *Am J Pathol* 2001, 158:1253-1262.
5. Douglas EJ, Fiegler H, Rowan A, Halford S, Bicknell DC, Bodmer W, Tomlinson IP, Carter NP: Array comparative genomic hybridization analysis of colorectal cancer cell lines and primary carcinomas. *Cancer Res* 2004, 64:4817-4825.
6. Lips EH, Dierssen JW, van Eijk R, Oosting J, Eilers PH, Tollenaar RA, de Graaf EJ, van't Slot R, Wijmenga C, Morreau H et al.: Reliable high-throughput genotyping and loss-of-heterozygosity detection in formalin-fixed, paraffin-embedded tumors using single nucleotide polymorphism arrays. *Cancer Res* 2005, 65:10188-10191.
7. Schouten JP, McElgunn CJ, Waaijer R, Zwijnenburg D, Diepvens F, Pals G: Relative quantification of 40 nucleic acid sequences by multiplex ligation-dependent probe amplification. *Nucleic Acids Res* 2002, 30:e57.
8. Erlandson A, Samuelsson L, Hagberg B, Kyllerman M, Vujic M, Wahlstrom J: Multiplex ligation-dependent probe amplification (MLPA) detects large deletions in the MECP2 gene of Swedish Rett syndrome patients. *Genet Test* 2003, 7:329-332.
9. Natte R, van Eijk R, Eilers P, Cleton-Jansen AM, Oosting J, Kouwenhove M, Kros JM, van Duinen S: Multiplex ligation-dependent probe amplification for the detection of 1p and 19q chromosomal loss in oligodendroglial tumors. *Brain Pathol* 2005, 15:192-197.
10. van Dijk MC, Rombout PD, Boots-Sprenger SH, Straatman H, Bernsen MR, Ruiter DJ, Jeuken JW: Multiplex ligation-dependent probe amplification for the detection of chromosomal gains and losses in formalin-fixed tissue. *Diagn Mol Pathol* 2005, 14:9-16.
11. Hameetman L, Szuhai K, Yavas A, Knijnenburg J, van Duin M, van Dekken H, Taminiau AH, Cleton-Jansen AM, Bovee JV, Hogendoorn PC: The role of EXT1 in nonhereditary osteochondroma: identification of homozygous deletions. *J Natl Cancer Inst* 2007, 99:396-406.

12. Kantarci S, Donahoe PK: Congenital diaphragmatic hernia (CDH) etiology as revealed by pathway genetics. *Am J Med Genet C Semin Med Genet* 2007, 145:217-226.
13. Kozlowski P, Jasinska AJ, Kwiatkowski DJ: New applications and developments in the use of multiplex ligation-dependent probe amplification. *Electrophoresis* 2008, 29:4627-4636.
14. Gerdes T, Kirchhoff M, Bryndorf T: Automatic analysis of multiplex ligation-dependent probe amplification products (exemplified by a commercial kit for prenatal aneuploidy detection). *Electrophoresis* 2005, 26:4327-4332.
15. Ahn JW, Ogilvie CM, Welch A, Thomas H, Madula R, Hills A, Donaghue C, Mann K: Detection of subtelomere imbalance using MLPA: validation, development of an analysis protocol, and application in a diagnostic centre. *BMC Med Genet* 2007, 8:9.
16. Coffa J, van de Wiel MA, Diosdado B, Carvalho B, Schouten J, Meijer GA: MLPAnalyzer: data analysis tool for reliable automated normalization of MLPA fragment data. *Cell Oncol* 2008, 30:323-335.
17. Vandesompele J, De Preter K, Pattyn F, Poppe B, Van Roy N, De Paepe A, Speleman F: Accurate normalization of real-time quantitative RT-PCR data by geometric averaging of multiple internal control genes. *Genome Biol* 2002, 3:RESEARCH0034.
18. Corver WE, Middeldorp A, ter Haar NT, Jordanova ES, van Puijenbroek M, van Eijk R, Cornelisse CJ, Fleuren GJ, Morreau H, Oosting J, van Wezel T: Genome-wide allelic state analysis on flow-sorted tumor fractions provides an accurate measure of chromosomal aberrations. *Cancer Res* 2008, 68:10333-10340.

Chapter 5

Sensitive and Specific KRAS Somatic Mutation Analysis on Whole Genome Amplified DNA from Archival Tissues

Ronald van Eijk[1], Marjo van Puijenbroek[1], Amiet R. Chhatta[1], Nisha Gupta[1], Rolf H.A.M. Vossen[2], Esther H. Lips[1], Anne-Marie Cleton-Jansen[1], Hans Morreau[1] and Tom van Wezel[1]

[1] Department of Pathology
[2] The Leiden Genome Technology Center at the Department of Human Genetics Leiden University Medical Center

J Mol Diagn. 12, 270 (2010) doi: 10.2353/jmoldx.2010.090028.

This work was supported by Dutch Cancer Society grant UL 2003-2807. The funders had no role in study design, data collection and analysis, decision to publish, or preparation of the manuscript. The resulting method is the subject of European patent application number 08075728.9 / EPO 8075728.

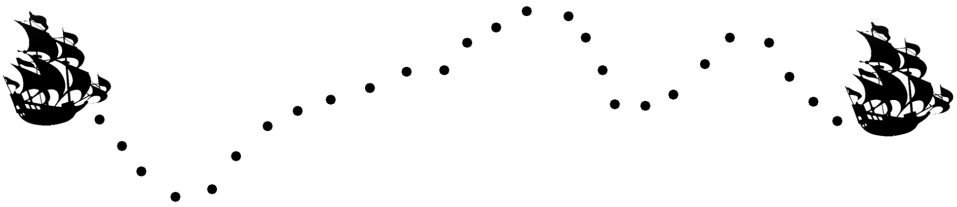

Abstract
KRAS is a small GTPase that plays a key role in Ras/MAPK signaling; somatic mutations in *KRAS* are frequently found in many cancers. The most common *KRAS* mutations result in a constitutively active protein. Accurate detection of *KRAS* mutations is pivotal to the molecular diagnosis of cancer and may guide proper treatment selection.
We describe a two-step *KRAS* mutation screening protocol that combines whole genome amplification (WGA), high resolution melting analysis (HRM) as a prescreen method for mutation carrying samples, and direct Sanger sequencing of DNA from formalin-fixed, paraffin-embedded (FFPE) tissue, from which limited amounts of DNA are available. We developed target-specific primers, thereby avoiding amplification of homologous *KRAS* sequences. The addition of Herring Sperm DNA facilitated WGA in DNA samples isolated from as few as 100 cells.
We show that *KRAS* mutation screening using HRM on wgaDNA from FFPE tissue is highly sensitive and specific; additionally, this method is feasible for screening of clinical specimens, as illustrated by our analysis of pancreatic cancers. Furthermore, PCR on wgaDNA does not introduce genotypic changes, as opposed to unamplified genomic DNA. This method can, after validation, be applied to virtually any potentially mutated region in the genome.

Introduction
Kirsten RAS *(KRAS)* is a member of the *Ras* gene family, which encodes small G proteins with intrinsic GTPase activity. These proteins play a key role in Ras/MAPK signaling, which is involved in multiple pathways including proliferation, differentiation, and apoptosis. It has been suggested that *KRAS* mutations are related with a random CpG island methylation pattern which may lead to CpG island methylator phenotype (CIMP)-low tumors (1). *KRAS* is an important etiological factor in many cancers. Somatic mutations in *KRAS* are found in 75-90% of pancreatic adenocarcinomas, 35-50% of colorectal carcinomas, and 30% of lung adenocarcinomas. In other cancers, *KRAS* mutations are less frequent or only present in specific subsets, such as subsets of bladder, endometrial, thyroid, and liver cancers (2-5). Mutations in *KRAS* negatively predict success of anti-EGFR therapies. Gain-of-function *KRAS* mutations lead to EGFR independent activation of intracellular signaling pathways, resulting in tumor cell proliferation, protection against apoptosis, increased invasion and metastasis, and activation of tumor induced angiogenesis (6).
The most common *KRAS* mutations are found in exon 2 (codons 12 and 13) and, more rarely, in exon 3 (codons 59 and 61). These mutations alter the conformation of *KRAS,* causing impaired GTPase activity that results in constitutive activation of the protein (7). Accurate detection of *KRAS* mutations is pivotal to the molecular diagnosis of cancer and may guide proper treatment selection. *KRAS* mutation analysis has been shown to be important for disease stratification in clinical trials of EGFR inhibitors (8;9), and for the detection of *MUTYH* mutants after *KRAS* mutation pre-screening (10). In the near future, it is expected that at least 50% of all recurrent colorectal tumors will be screened for *KRAS* mutations.

Various methods have been described for the detection of *KRAS* mutations, such as a mutagenic PCR assay (11), pyrosequencing (12), and real time PCR (13); however, Sanger sequencing on PCR products remains the golden standard. (6;14;15) Recently, high-resolution melting analysis (HRM) was added as a method for mutation scanning and genotyping (16-18), including analysis of *KRAS* mutations in heterogenic tumor populations. This method is a valuable addition to Sanger based sequencing, as it detects heterozygous genetic changes in samples containing only 10% of mutant cells (19-21), whereas direct Sanger sequencing requires the mutation to be present at a level of 20% of the sample. (20) HRM has also been described for methylation detection and the detection of internal tandem duplications (22;23). In addition, HRM has a high sensitivity and specificity for the detection of variants in a background of normal DNA (24;25).
For mutation analysis, the majority of tissues are available as formalin-fixed, paraffin-embedded (FFPE) material. The genomic DNA (gDNA) that can be isolated from FFPE tissue is usually fragmented due to formalin fixation. At the same time, for most cases, including pre-operative biopsies, the available (FFPE) tissue, and thus gDNA, is limiting. As a result, the number of genetic assays that can be performed is restricted (26;27).
One approach designed to overcome this limitation is whole genome amplification (WGA), which ideally generates a new whole genome sample of amplified DNA (wgaDNA) that is indistinguishable from the original, but with a higher DNA concentration (28). We used a primer extension pre-amplification (PEP) method that has been successfully applied to formalin-fixed paraffin-embedded (FFPE) tissue (29;30). We have studied HRM as a pre-screening method for somatic mutation detection in combination with WGA on gDNA from FFPE tissue. This approach is sensitive and specific and can open the archives for large scale mutation analysis (31-34).

Materials and methods

Samples

We previously performed somatic *KRAS* mutation analyses in a series of colorectal cancers (35). A subset of 60 tumors (14 FF and 46 FFPE) was used to determine the sensitivity and specificity of the assay on FF and FFPE tissue. The tumor cell percentage in the series was 50-80%. Additionally we isolated gDNA from five pre-operative biopsies from pancreatic adeno-carcinomas and three 0.3 mm tissue punch cores that were isolated from matching resection specimens. Guided by an H&E stained section, the extremely small tumor fields were dissected from the biopsies.
DNA was extracted using a standard proteinase K method as described elsewhere (36). All samples were handled according to the medical ethical guidelines described in the Code Proper Secondary Use of Human Tissue established by the Dutch Federation of Medical Sciences (www.federa.org, accessed June 2, 2009).

gDNA concentrations were measured using PICOgreen (Invitrogen/Molecular Probes, Leiden, The Netherlands) according to the manufacturer's protocol. For WGA and PCR, gDNA is brought to a standard concentration of 5 ng/µL in 10 mM Tris, pH 8.0, 0.1 mM EDTA, and is stored in 2D bar-coded sample tubes (Thermo Fisher Scientific, NH, USA) for process standardization and robotic analysis.

Whole genome amplification

Primer extension pre-amplification (PEP) WGA using thermo stable DNA polymerases (Kbioscience, UK) was carried out according to the manufacturer's protocol using 25 ng gDNA in a final reaction volume of 25 µL. For FFPE samples and other samples from which limited gDNA was available, herring-sperm DNA (Promega) was added to a final concentration of 2 ng/µL per reaction. Thermal cycling was performed in a Biorad I-cycler. After an initial denaturation step of 10 minutes at 94^{o}C, 40 cycles of 30 seconds at 94^{o}C, 30 seconds at 37^{o}C, and ramping at a speed of 0.1^{o}C /sec to 55^{o}C, and 4 minutes at 55^{o}C were performed.

Mutation scanning and detection

Oligonucleotides were obtained from Operon (Germany). The primer sequences for the amplification of *KRAS* codons 12 and 13 were KRAS_C1213_M13F 5'-(*TGT AAA ACG ACG GCC AGT*-TCG ACC CAG GAT CCA ACT T-**GCT GAA AAT GAC TGA ATA TAA ACT TG)-3'** and KRAS_C1213_M13R 5'-(*CAG GAA ACA GCT ATG ACC ATG A*-TCC AGT ACT TGA GAG AAT TCC ATC-**TAG CTG TAT CGT CAA GGC ACT C)-3'**. Stuffer sequences (underlined), were added between M13 tails (*in italics*) and the *KRAS*-specific part (**bold**) of the primer. The total length of the amplicon, inclusive of the M13 tails and stuffers, is 166 base pairs.

Duplicate PCR reactions were carried out in 10 µL reactions in white 96 well plates (AB0800/W, ABgene) that are suitable for HRM. The reactions included iQ Supermix (Bio-Rad, cat nr 170-8860), 2 pmol primers and 1 µM SYTO9 (Invitrogen). PCR reactions were performed with an initial denaturation step of 10 minutes at 95^{o}C, followed by 40 cycles of 5 seconds at 95^{o}C, 10 seconds at 60^{o}C, and 10 seconds at 72^{o}C, and a final elongation step of 10 minutes at 72^{o}C. Sanger DNA sequencing was performed on gDNA and wgaDNA at the sequence core of the Leiden Genome Technology Center, using the same PCR products as those submitted to HRM. Prior to Sanger sequencing PCR fragments were purified using a filter system according to the manufacturer's protocol (Montage, Millipore). DNA was eluted in 25 µL of sterile water. Sanger sequencing was subsequently performed with 5-10 ng of DNA and 6 pmol of an M13 primer (PR_M13F TGTAAAACGACGGCCAGT and PR_M13R CAGGAAACAGCTATGACC) on an ABI 3700 DNA Analyzer using Big Dye Terminator Chemistry (Applied Biosystems). All sequences were visually analyzed with Mutation Surveyor^{TM} DNA variant analysis software (version 2.61 Softgenetics, State College, PA).

HRM was performed in a LightScanner (Idaho Technology) after the addition of 15 µL of mineral oil (Sigma); Light Scanner software (version 1.1.0.566, Idaho Technology) was used for analysis. High salt addition (24); 1.5 µL of 1M KCl

and 0.5M Tris-HCl, pH 8.0, was added post-PCR to the 10 µL PCR products followed by 4 additional temperature cycles (30 seconds 94˚C, 30 seconds 72˚C). The sensitivity and specificity of the HRM were calculated. The sensitivity was determined as the number of true positives divided by the sum of the true positive and false negative samples. The specificity of the samples was determined as the number of true negatives divided by the sum of the true negatives and false positives. Mineral oil overlay, high salt addition, and PCR product purification was performed in a post-PCR setting.

Results

Detection of *KRAS* mutations in genomic DNA using HRM

KRAS PCR and HRM analyses were performed on gDNA in duplicate before and after the addition of high salt. All duplicate samples with an aberrant melting pattern were identified as carrying a possible mutation. The data were compared with the Sanger sequencing results. An overview of the results is shown in Table 1. `Six FFPE samples (5%) failed to give an interpretable HRM pattern in one of the duplicates. None of these gave contradictory sequence results and were included in further analysis. (Supplementary table 1 at http://jmd.amjpathol.org)
In the set of 60 tumors we observed an overall sensitivity of 100% (33/33) and a specificity of 81% (22/27) for the detection of *KRAS* codon 12 or 13 variations. The specificity of gDNA from FFPE tissue (75%; 15/20) was lower than in FF tissue (100%; 7/7), probably as a result of poor gDNA quality intrinsic to the material (Table 2).

HRM on whole genome amplified (WGA) DNA from archival tissues

To evaluate the sensitivity and specificity of HRM on WGA-treated DNA from tumor specimens of different origins and quality, we performed WGA on the gDNA samples with known *KRAS* mutation status. To assess the DNA quality pre- and post-WGA, a multiplex PCR containing 3 fragments (150, 255, and 511 base pairs) was carried out. In all of the samples at least the 255-bp band was visible (data not shown).
Herring Sperm DNA was added up to 50 ng to all samples prior to WGA as driver DNA to prevent the amplification of excess small random PCR products
After WGA, 1:1, 1:5, and 1:10 dilutions of the wgaDNA were made to determine the amount of input wgaDNA that was required for HRM PCR. The addition of 2 µl of the 1:5 dilution to a 10 µl PCR gave the best results and we were able to detect the different mutations in control samples (Figure 1).
We combined 25 ng gDNA with 25 ng Herring Sperm DNA in each WGA reaction for the subset of 60 tumors. In these experiments, the researchers were blinded to the HRM and Sanger sequence results obtained for the gDNA samples. Subsequently, *KRAS* PCR was performed in duplicate, and HRM analysis was performed before and after high salt addition. Three samples (2.5%) failed to give an interpretable HRM pattern in one set of the duplicates. For each product, one of the duplicates was purified and Sanger sequenced. HRM and re-sequencing of the WGA PCR samples revealed no discrepancies with the original samples

Table 1. False positives and false negatives in *KRAS* (wga) HRM and sequencing. Overview of false positives (FP) and false negatives (FN) in HRM performed with or without WGA. In the wgaDNA column, the HRM results on samples without the addition of high salt are shown between brackets. HRM results after the addition of a high salt solution on samples performed in duplicate (results for samples marked with * are based on a single result). The last column shows the concordant gDNA and wgaDNA results of Sanger sequencing on one of the duplicates. The complete overview of all tested samples is listed in Supplementary Table 1. FF; Freshly Frozen tissue, FFPE; formalin fixed paraffin embedded tissue, Var; KRAS-variant, WT; KRAS wild-type.

ID	Type	gDNA	wgaDNA (no salt)	(g-wga)DNA Sequencing
972	FF	Var	Var (FN)	c12. GGT>GTT
755	FF	WT	FP (WT*)	WT
819	FF	WT	WT (FP)	WT
826	FF	WT	WT (FP)	WT
977	FFPE	Var	Var (FN)	c13. GGC>GAC
998	FFPE	Var	Var (FN*)	c13. GGC>GAC
811	FFPE	Var	Var (FN)	c12. GGT>GAT
761	FFPE	Var	Var (FN)	c12. GGT>GTT
768	FFPE	Var	Var (FN)	c12. GGT>GTT
785	FFPE	Var	Var (FN)	c12. GGT>GTT
806	FFPE	Var	Var (FN*)	c12. GGT>GTT
013	FFPE	FP	WT (WT)	WT
023	FFPE	FP	WT (WT)	WT
750	FFPE	FP*	WT (FP)	WT
958	FFPE	FP	WT (WT)	WT
975	FFPE	FP*	WT (WT)	WT

Table 2. Sensitivity and specificity in (wga)HRM. Sensitivity and specificity calculated for HRM in FFPE, Freshly Frozen (FF) and combined FFPE and FF gDNA and wgaDNA samples in the presence of high salt. In the wgaDNA columns, HRM results on samples without the addition of high salt are shown between brackets. FP, false positives; FN, false negatives; Var, KRAS-variant; WT, KRAS wild-type.

	FFPE	FFPE	FF	FF	Com - bined	
DNA type	**gDNA**	**wgaDNA**	**gDNA**	**wgaDNA**	**gDNA**	**wgaDNA**
WT	15	20 (19)	7	6 (5)	22	26 (24)
Var	26	26 (19)	7	7 (6)	33	33 (25)
FN	0	0 (7)	0	0 (1)	0	0 (8)
FP	5	0 (1)	0	1 (2)	5	1 (3)
overall	46		14		60	
% Sensitivity	100	100 (73)	100	100 (86)	100	100 (76)
% Specificity	75	100 (95)	100	86 (71)	81	100 (89)

(Table 1 and Supplementary table 1 at http://jmd.amjpathol.org). The sensitivity and specificity of the HRM was calculated. WGA-HRM proved to be 100% (33/33) sensitive and 96% (26/27) specific in the presence of post-PCR high salt. Without high salt, the sensitivity and specificity were lower (76% (25/33) and 89% (24/27), respectively).(Table 2)

Detection limits for HRM of wgaDNA

To determine the limits of HRM to detect a possible *KRAS* mutation in wgaDNA from FFPE tissue, we performed WGA on a two-fold serial dilution of gDNA carrying a g.35GGT>GTT (p.12G>V) mutation. The gDNA input ranged from 10 ng to 0.08 ng, the latter corresponding to the gDNA equivalent of approximately 10-12 cells. After WGA, HRM was performed in duplicate on WGA samples diluted 1:5. A mutant allele was detected in WGA products corresponding with 600 pg (equivalent to approximately 100 cells) or higher. HRM on wgaDNA originating from lower input gDNA resulted in low fluorescence of the mutant allele, thus impairing the analysis and interpretation. We performed direct Sanger sequencing on all wgaDNA samples. The *KRAS* mutation was found in all dilutions, although the mutant allele was difficult to identify due to background noise in samples with lower than 600 pg input gDNA. *KRAS* mutations were easily detected in sequences from WGA PCR isolates corresponding to 100 cells or more (Figure 2) (29).

***KRAS* mutation detection in pancreatic adenocarcinomas**

We further evaluated *KRAS* HRM and Sanger sequencing in wgaDNA from archived clinical specimens. gDNA from pancreatic adenocarcinomas was isolated from a single slide (samples 1a-4a) and from four combined slides (1b-4b). For comparison, we also isolated gDNA from three 0.3 mm tissue punch cores that were isolated from matching resection specimens. After gDNA isolation, this sample was split into a minor (5f) and major (5p) fraction; the major fraction contained a 6-fold higher gDNA concentration. As expected, the gDNA concentrations of the isolates were low or not measurable (Table 3). Subsequently, WGA was performed on the fractions, and, HRM and Sanger sequencing were performed on the wgaDNA. For the samples 1b and fp, gDNA was also tested.

WGA was performed on 10 ng gDNA and adjusted to 50 ng with Herring Sperm DNA. For samples where the gDNA concentration was not measurable 15 µl of the raw isolate was added to the WGA reaction together with 50 ng with Herring Sperm DNA. HRM revealed concordant *KRAS*-variant curves in samples 5f and 5p, while samples 1a and 1b gave contradictory results for HRM. The variant curves for sample 3b were interpretable, while the signals for samples 2a, 2b, 3a, 4a, and 4b were low and could not be interpreted. Purification and re-sequencing of all of the HRM PCR products was possible in all cases, and revealed that samples 2 and 5 carried the g.35G>A (p.G12D) mutation, sample 3 was a g.35G>T (p.G12V) mutant, and samples 1 and 4 were wild-type. These results indicated that the HRM results for sample 1a were false positive (Table 3).

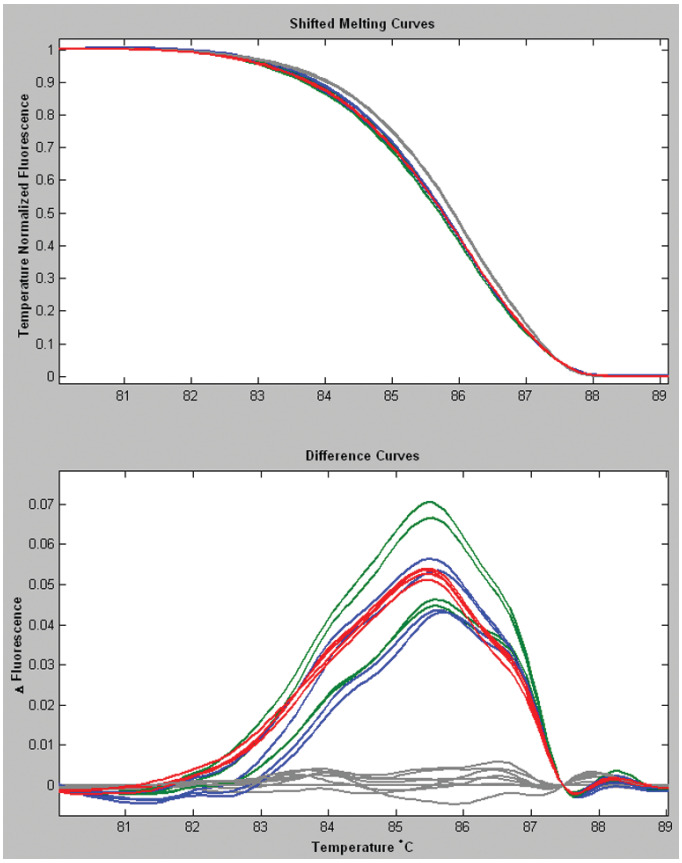

Figure 1. HRM curves in samples treated with or without WGA. HRM shifted melting curves and difference curves of 3 different *KRAS* codon 12 and 13 mutations in duplicate, with or without WGA treatment. g.35G>A (p.12G>D) DNA lower green, wgaDNA upper green; g.38G>A (p.13G>D) DNA lower blue, wgaDNA upper blue; g.35G>T (p.12G>V) red; and a series of 8 wild-type samples (gray).

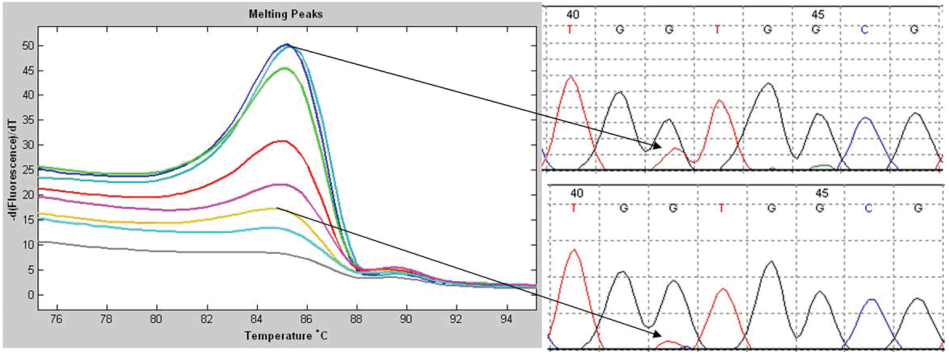

Figure 2. Detection limit of *KRAS* mutations in a PCR of serial diluted wgaDNA. Left panel: 2-fold serial dilution of gDNA starting with 0.08 ng input (lowest curve) to 10 ng (upper curve) shows the detection limit for *KRAS* mutations in a PCR on wgaDNA. Upper right panel: Sanger sequence on wgaDNA corresponds with 10 ng gDNA input in the WGA. Lower right panel: Sanger sequence on wgaDNA corresponds with 0.625 ng (+/- 100 cells) gDNA input in the WGA.

Table 3. WGA HRM results in histological specimens from pancreatic adenocarcinomas. Concentration measurements are performed on gDNA isolates from a single slide (samples 1a-4a), from four combined slides (samples 1b-4b), and from a matching resection specimen with minor (5f) and major fractions (5p). For a number of samples the gDNA concentration was not measurable (low). WGA is performed on all samples. HRM results in the presence of high salt. Samples marked Low Signal had an unclear HRM pattern. The last column shows the *KRAS* Sanger sequencing results on the purified HRM sample.

Sample	Tumour Sections	Concentration gDNA (ng/µl)	wgaDNA HRM+HighSalt	wgaDNA Sequence
1a	1	2.2	VAR	WT
1b	4	9.9	WT	WT
2a	1	<2	Low Signal	c12. GGT>GAT
2b	4	2.9	Low Signal	c12. GGT>GAT
3a	1	<2	Low Signal	c12. GGT>GTT
3b	4	3.3	VAR	c12. GGT>GTT
4a	1	<2	Low Signal	WT
4b	4	<2	Low Signal	WT
5f	fraction	<2	VAR	c12. GGT>GAT
5p	3 punches	12.1	VAR	c12. GGT>GAT

Discussion

Accurate detection of *KRAS* mutations is pivotal to the molecular diagnosis of cancer and may guide proper treatment selection. We have developed a standard WGA and PCR protocol for *KRAS* mutation detection in gDNA derived from FFPE tissue, for which limited amounts of gDNA are available. High resolution melting analysis (HRM) is used for mutation prescreening and Sanger sequencing is used for mutation detection.

The most frequently mutated codons, 12 and 13, in exon 2, are located in a region that is highly homologous to regions on chromosomes 6 and 16. To prevent the amplification of pseudogene sequences we used primers based on non-homologous nucleotides (10;37;38). Addition of universal M13 tails to the primers increased the specificity and fidelity of the PCR (10;39) and allows the use of uniform sequencing primers. Since the *KRAS* amplicon length is only 75 nucleotides and short PCR fragments can be difficult to sequence, we added additional stuffer sequences to the primers, between the M13 tails and the *KRAS*-specific part of the primer. These stuffers bear no homology to any known human sequence. Since the amplicons are very small, the length of each step of the PCR cycle was shortened, resulting in a 40 cycle PCR that lasted just over 1 hour.

We evaluated LCGreen and SYTO9 for HRM and found that both dyes were capable of detecting different *KRAS* variations. SYTO9 has been reported to have some advantages in terms of dye stability, dye-dependent PCR inhibition, and selective detection of amplicons during DNA melting curve analysis of multiplex

PCR (40). In our experiments, SYTO9 appeared to improve the quality of the melting curves, since the fluorescence signal was approximately 50% higher and the duplicate curves fit more tightly together. Therefore, we decided to use SYTO9 in subsequent experiments (Supplementary Figure S1 http://jmd.amjpathol.org). It has been reported that high-resolution analysis of amplicon melting is limited by any T_m variance, including differences in salt concentrations (arising from evaporation during processing or differences in buffers used for DNA preparation), and any variation in instrument temperature (41). Furthermore, poor DNA quality, low input, and positional effects of the samples on the microtiter plate might lead to false positive or false negative HRM measurements (42). Therefore, all samples were analyzed in duplicate. For calibration, at least two wild-type samples were analyzed in each experiment.

We observed an overall sensitivity of 100% (33/33) and a specificity of 81% (22/27) for the detection of *KRAS* codon 12 or 13 variations. However the specificity of gDNA from FFPE tissue (75%,15/20) was lower than in FF tissue (100%, 7/7), probably as a result of poor gDNA quality intrinsic to the material (Table 2). From the melting curve behavior, it was not possible to determine the specific mutation, likely due to tumor percentage and tumor heterogeneity. Consequently, all samples with possible mutations were Sanger sequenced in order to identify the nature of the mutation. Sanger sequencing was directly performed on the purified HRM PCR product without repeating the PCR, which is time, and costs saving.

KRAS mutations are frequently found in ductal pancreatic cancers (4) making it important in clinical practice to identify *KRAS* mutations in cytological, pancreatic juice with only minimal amounts of cells and limiting (FFPE) gDNA (26;27;43). One approach designed to overcome the limited number of assays possible on this material is whole genome amplification (WGA). Different types of WGA methods are available. Strand displacement amplification (SDA or MDA) has been described as most reliable for genotyping, giving highest call rates, best genomic coverage and lowest amplification bias. However this method has the disadvantage that the specific performance largely depends on input DNA quality making it less suitable to efficiently amplify DNA extracted from FFPE material (44). Primer extension pre-amplification PEP based WGA has been successfully applied to FFPE tissue. (29;30) although some bias as result of the WGA has been observed (12). We used a PEP based WGA method that is known to have high sequencing accuracy and is less dependent upon the quality of the input DNA (45) however we observed that, with low amounts of input (< 10 ng) gDNA and with poor quality FFPE samples, the random primers in the WGA produce excess random wgaDNA and primer dimer products. These additional products impaired HRM and subsequent Sanger sequencing. Therefore, we added non homologous Herring Sperm to the human DNA, for all samples prior to WGA to suppress primer dimer formation. The combined human and herring DNA input in the WGA reaction was approximately 50 ng. Herring Sperm DNA has low homology to human *KRAS* and we did not detect any PCR product with the described primers in a control PCR. Therefore, herring sperm DNA addition should not interfere with *KRAS* HRM or Sanger sequencing. We compared the Sanger

sequencing results on gDNA and wgaDNA. This did not reveal any discrepancies and showed that *KRAS* mutation screening using HRM on wgaDNA from FFPE tissue is concordant with the non-wgaDNA results. With this approach, we were able to WGA minimal amounts of gDNA with reliable results. We observed that with less than 2 ng of FFPE-derived gDNA input in the WGA reaction HRM on wgaDNA becomes unreliable. The PCR products still produced reliable Sanger sequences. This was also demonstrated by the pancreatic adenocarcinomas which failed for HRM but gave good Sanger sequence results. This showed that HRM is very sensitive for DNA variants, however, to obtain interpretable results higher amounts of DNA are required in the HRM than in Sanger sequencing (Table 3).

We optimized HRM in wgaDNA by the post-PCR addition of high salt (24). This resulted in enhanced heteroduplex formation, better discrimination of the mutation carrier during analysis, and 100% sensitivity and 96% specificity. Cho et al 2008 (34) reported that HRM on wgaDNA results in a higher fals positive rate and reduced sensitivity and specificity. We show that high-salt addition prior to analysis overcomes this problem, thereby making this approach suitable for high throughput mutation pre-screening.

A potential disadvantage of our method could be that PCR plates need to be opened prior to analysis, to add mineral oil and high salt solution, although opening the plates for PCR cleanup prior to sequencing is standard practice. To minimize the chance of PCR amplicon contamination pre, and post PCR rooms were strictly separated and we used a direct PCR reaction to avoid pseudogene amplification rather than nested PCR for *KRAS* mutation detection (37;46).

Another factor to consider is tumor heterogeneity. In samples with lower tumor percentage and low amount of the mutated allele, automated Sanger sequence analysis could miss variants while HRM could still detect mutations in gDNA and wgaDNA from samples with low tumor percentages. Vossen et al show that DNA variations could be detected in sample mixtures with as little as 5% variation fraction, although 30% and higher gave more reliable results in HRM (24). Because HRM in samples with unknown tumor percentage is limited in predicting the exact *KRAS* variant, samples with HRM variations have to be sequenced for variant determination. A combination of low tumor percentage and low input concentrations in the WGA might cause HRM dropout or contradictory results in the duplicate reactions, making careful (re)analysis of the Sanger sequencing indispensable (Figure 2). For this type of samples alternative mutation detection after HRM pre-screening should be considered such as pyrosequencing which is known to be more sensitive than Sanger sequencing (12). Allele specific real time PCR is also a very sensitive method but it has the disadvantage of detection known (*KRAS*) variants only while our approach envisions application for denovo mutation screening (47). For this type of samples sensitivity and specificity have to be calculated in relation to results obtained with pyrosequencing or real time PCR.

One can argue that the majority of laboratories can obtain a sufficient amount of DNA for *KRAS* mutation screening from even tiny biopsies without the WGA step.

This assertion might be true in some cases. However, in a time when personalized medicine is the norm, *KRAS* mutation detection may be one test in a series of many and in that respect, WGA may be an excellent method by which to increase the initial amount of DNA that can be used for the analysis of any potentially mutated region in the genome. (48)
Finally, the required equipment for this approach is limited to two standard thermal cyclers (one dedicated to WGA and another in a separate room for PCR), dedicated HRM equipment, and a sequencing facility. HRM on wgaDNA from FFPE origin can be a cost effective pre-screening method, since only potential variants found after HRM need re-sequencing. Therefore, HRM, in combination with WGA and sequencing, is a strong tool for *KRAS* mutation screening of samples with partially degraded or low yield DNA, as is often found in pathology archives.

Acknowledgements
KBioscience kindly provided the WGA kit.

Reference List

1. Nosho K, Irahara N, Shima K, Kure S, Kirkner GJ, Schernhammer ES, Hazra A, Hunter DJ, Quackenbush J, Spiegelman D, Giovannucci EL, Fuchs CS, and Ogino S: Comprehensive biostatistical analysis of CpG island methylator phenotype in colorectal cancer using a large population-based sample 9. PLoS ONE 2008, 3: e3698
2. Fearon ER: K-ras gene mutation as a pathogenetic and diagnostic marker in human cancer. J Natl Cancer Inst 1993, 85: 1978-1980
3. Barault L, Veyrie N, Jooste V, Lecorre D, Chapusot C, Ferraz JM, Lievre A, Cortet M, Bouvier AM, Rat P, Roignot P, Faivre J, Laurent-Puig P, and Piard F: Mutations in the RAS-MAPK, PI(3)K (phosphatidylinositol-3-OH kinase) signaling network correlate with poor survival in a population-based series of colon cancers. Int J Cancer 2008, 122: 2255-2259
4. Shibata D, Capella G, and Perucho M: Mutational activation of the c-K-ras gene in human pancreatic carcinoma. Baillieres Clin Gastroenterol 1990, 4: 151-169
5. Di Nicolantonio F, Martini M, Molinari F, Sartore-Bianchi A, Arena S, Saletti P, De Dosso S, Mazzucchelli L, Frattini M, Siena S, and Bardelli A: Wild-type BRAF is required for response to panitumumab or cetuximab in metastatic colorectal cancer. J Clin Oncol 2008, 26: 5705-5712
6. van Krieken JH, Jung A, Kirchner T, Carneiro F, Seruca R, Bosman FT, Quirke P, Flejou JF, Hansen TP, de Hertogh G, Jares P, Langner C, Hoefler G, Ligtenberg M, Tiniakos D, Tejpar S, Bevilacqua G, and Ensari A: KRAS mutation testing for predicting response to anti-EGFR therapy for colorectal carcinoma: proposal for an European quality assurance program. Virchows Arch 2009, 454: 233-235
7. Bos JL: ras oncogenes in human cancer: a review. Cancer Res 1989, 49: 4682-4689
8. Spano JP, Milano G, Vignot S, and Khayat D: Potential predictive markers of response to EGFR-targeted therapies in colorectal cancer. Crit Rev Oncol Hematol 2008, 66: 21-30
9. Lievre A, Bachet JB, Le Corre D, Boige V, Landi B, Emile JF, Cote JF, Tomasic G, Penna C, Ducreux M, Rougier P, Penault-Llorca F, and Laurent-Puig P: KRAS mutation status is predictive of response to cetuximab therapy in colorectal cancer. Cancer Res 2006, 66: 3992-3995
10. van Puijenbroek M, Nielsen M, Tops CM, Halfwerk H, Vasen HF, Weiss MM, van Wezel T, Hes FJ, and Morreau H: Identification of patients with (atypical) MUTYH-associated polyposis by KRAS2 c.34G > T prescreening followed by MUTYH hotspot analysis in formalin-fixed paraffin-embedded tissue. Clin Cancer Res 2008, 14: 139-142
11. Boldrini L, Gisfredi S, Ursino S, Camacci T, Baldini E, Melfi F, and Fontanini G: Mutational analysis in cytological specimens of advanced lung adenocarcinoma: a sensitive method for molecular diagnosis. J Thorac Oncol 2007, 2: 1086-1090

12. Ogino S, Kawasaki T, Brahmandam M, Yan L, Cantor M, Namgyal C, Mino-Kenudson M, Lauwers GY, Loda M, and Fuchs CS: Sensitive sequencing method for KRAS mutation detection by Pyrosequencing. J Mol Diagn 2005, 7: 413-421
13. Amicarelli G, Shehi E, Makrigiorgos GM, and Adlerstein D: FLAG assay as a novel method for real-time signal generation during PCR: application to detection and genotyping of KRAS codon 12 mutations. Nucleic Acids Res 2007, 35: e131
14. Brink M, de Goeij AF, Weijenberg MP, Roemen GM, Lentjes MH, Pachen MM, Smits KM, de Bruine AP, Goldbohm RA, and van den Brandt PA: K-ras oncogene mutations in sporadic colorectal cancer in The Netherlands Cohort Study. Carcinogenesis 2003, 24: 703-710
15. Chien CC, Chen SH, Liu CC, Lee CL, Yang RN, Yang SH, and Huang CJ: Correlation of K-ras codon 12 mutations in human feces and ages of patients with colorectal cancer (CRC). Transl Res 2007, 149: 96-102
16. Gundry CN, Vandersteen JG, Reed GH, Pryor RJ, Chen J, and Wittwer CT: Amplicon melting analysis with labeled primers: a closed-tube method for differentiating homozygotes and heterozygotes. Clin Chem 2003, 49: 396-406
17. Zhou L, Wang L, Palais R, Pryor R, and Wittwer CT: High-resolution DNA melting analysis for simultaneous mutation scanning and genotyping in solution. Clin Chem 2005, 51: 1770-1777
18. Ririe KM, Rasmussen RP, and Wittwer CT: Product differentiation by analysis of DNA melting curves during the polymerase chain reaction. Anal Biochem 1997, 245: 154-160
19. Nomoto K, Tsuta K, Takano T, Fukui T, Fukui T, Yokozawa K, Sakamoto H, Yoshida T, Maeshima AM, Shibata T, Furuta K, Ohe Y, and Matsuno Y: Detection of EGFR mutations in archived cytologic specimens of non-small cell lung cancer using high-resolution melting analysis. Am J Clin Pathol 2006, 126: 608-615
20. Do H, Krypuy M, Mitchell PL, Fox SB, and Dobrovic A: High resolution melting analysis for rapid and sensitive EGFR and KRAS mutation detection in formalin fixed paraffin embedded biopsies. BMC Cancer 2008, 8: 142
21. Krypuy M, Ahmed AA, Etemadmoghadam D, Hyland SJ, DeFazio A, Fox SB, Brenton JD, Bowtell DD, and Dobrovic A: High resolution melting for mutation scanning of TP53 exons 5-8. BMC Cancer 2007, 7: 168
22. Wojdacz TK and Dobrovic A: Methylation-sensitive high resolution melting (MS-HRM): a new approach for sensitive and high-throughput assessment of methylation. Nucleic Acids Res 2007,
23. Vaughn CP and Elenitoba-Johnson KS: High-resolution melting analysis for detection of internal tandem duplications. J Mol Diagn 2004, 6: 211-216
24. Vossen RH, Aten E, Roos A, and den Dunnen JT: High-Resolution Melting Analysis (HRMA)-More than just sequence variant screening 4. Hum Mutat 2009, 30: 860-866

25. Krypuy M, Newnham GM, Thomas DM, Conron M, and Dobrovic A: High resolution melting analysis for the rapid and sensitive detection of mutations in clinical samples: KRAS codon 12 and 13 mutations in non-small cell lung cancer. BMC Cancer 2006, 6: 295
26. Marchetti A, Merlo G, Buttitta F, Pellegrini S, Callahan R, Bistocchi M, and Squartini F: Detection of DNA mutations in acid formalin-fixed paraffin-embedded archival tumor specimens by polymerase chain reaction-single strand conformation polymorphism analysis. Cancer Detect Prev 1995, 19: 278-281
27. Farrand K, Jovanovic L, Delahunt B, McIver B, Hay ID, Eberhardt NL, and Grebe SK: Loss of heterozygosity studies revisited: prior quantification of the amplifiable DNA content of archival samples improves efficiency and reliability. J Mol Diagn 2002, 4: 150-158
28. Hughes S, Arneson N, Done S, and Squire J: The use of whole genome amplification in the study of human disease. Prog Biophys Mol Biol 2005, 88: 173-189
29. Heinmoller E, Liu Q, Sun Y, Schlake G, Hill KA, Weiss LM, and Sommer SS: Toward efficient analysis of mutations in single cells from ethanol-fixed, paraffin-embedded, and immunohistochemically stained tissues. Lab Invest 2002, 82: 443-453
30. Bataille F, Rummele P, Dietmaier W, Gaag D, Klebl F, Reichle A, Wild P, Hofstadter F, and Hartmann A: Alterations in p53 predict response to preoperative high dose chemotherapy in patients with gastric cancer. Mol Pathol 2003, 56: 286-292
31. Willmore C, Holden JA, Zhou L, Tripp S, Wittwer CT, and Layfield LJ: Detection of c-kit-activating mutations in gastrointestinal stromal tumors by high-resolution amplicon melting analysis. Am J Clin Pathol 2004, 122: 206-216
32. Willmore-Payne C, Holden JA, Tripp S, and Layfield LJ: Human malignant melanoma: detection of BRAF- and c-kit-activating mutations by high-resolution amplicon melting analysis. Hum Pathol 2005, 36: 486-493
33. Bastien R, Lewis TB, Hawkes JE, Quackenbush JF, Robbins TC, Palazzo J, Perou CM, and Bernard PS: High-throughput amplicon scanning of the TP53 gene in breast cancer using high-resolution fluorescent melting curve analyses and automatic mutation calling. Hum Mutat 2008, 29: 757-764
34. Cho MH, Ciulla D, Klanderman BJ, Raby BA, and Silverman EK: High-resolution melting curve analysis of genomic and whole-genome amplified DNA. Clin Chem 2008, 54: 2055-2058
35. Lips EH, van Eijk R, de Graaf EJ, Doornebosch PG, de Miranda NF, Oosting J, Karsten T, Eilers PH, Tollenaar RA, van Wezel T, and Morreau H: Progression and tumor heterogeneity analysis in early rectal cancer. Clin Cancer Res 2008, 14: 772-781

36. Lips EH, Dierssen JW, van Eijk R, Oosting J, Eilers PH, Tollenaar RA, de Graaf EJ, van't Slot R, Wijmenga C, Morreau H, and van Wezel T: Reliable high-throughput genotyping and loss-of-heterozygosity detection in formalin-fixed, paraffin-embedded tumors using single nucleotide polymorphism arrays. Cancer Res 2005, 65: 10188-10191
37. Sommerer F, Vieth M, Markwarth A, Rohrich K, Vomschloss S, May A, Ell C, Stolte M, Hengge UR, Wittekind C, and Tannapfel A: Mutations of BRAF and KRAS2 in the development of Barrett's adenocarcinoma. Oncogene 2004, 23: 554-558
38. van Puijenbroek M, van Asperen CJ, van Mil A, Devilee P, van Wezel T, and Morreau H: Homozygosity for a CHEK2*1100delC mutation identified in familial colorectal cancer does not lead to a severe clinical phenotype. J Pathol 2005, 206: 198-204
39. Boutin-Ganache I, Raposo M, Raymond M, and Deschepper CF: M13-tailed primers improve the readability and usability of microsatellite analyses performed with two different allele-sizing methods. Biotechniques 2001, 31: 24-6, 28
40. Herrmann MG, Durtschi JD, Bromley LK, Wittwer CT, and Voelkerding KV: Amplicon DNA melting analysis for mutation scanning and genotyping: cross-platform comparison of instruments and dyes. Clin Chem 2006, 52: 494-503
41. Seipp MT, Pattison D, Durtschi JD, Jama M, Voelkerding KV, and Wittwer CT: Quadruplex genotyping of F5, F2, and MTHFR variants in a single closed tube by high-resolution amplicon melting. Clin Chem 2008, 54: 108-115
42. Sieben NL, ter Haar NT, Cornelisse CJ, Fleuren GJ, and Cleton-Jansen AM: PCR artifacts in LOH and MSI analysis of microdissected tumor cells. Hum Pathol 2000, 31: 1414-1419
43. Shi C, Fukushima N, Abe T, Bian Y, Hua L, Wendelburg BJ, Yeo CJ, Hruban RH, Goggins MG, and Eshleman JR: Sensitive and quantitative detection of KRAS2 gene mutations in pancreatic duct juice differentiates patients with pancreatic cancer from chronic pancreatitis, potential for early detection. Cancer Biol Ther 2008, 7: 353-360
44. Lage JM, Leamon JH, Pejovic T, Hamann S, Lacey M, Dillon D, Segraves R, Vossbrinck B, Gonzalez A, Pinkel D, Albertson DG, Costa J, and Lizardi PM: Whole genome analysis of genetic alterations in small DNA samples using hyperbranched strand displacement amplification and array-CGH. Genome Res 2003, 13: 294-307
45. Dietmaier W, Hartmann A, Wallinger S, Heinmoller E, Kerner T, Endl E, Jauch KW, Hofstadter F, and Ruschoff J: Multiple mutation analyses in single tumor cells with improved whole genome amplification. Am J Pathol 1999, 154: 83-95
46. van Puijenbroek M, van Asperen CJ, van Mil A, Devilee P, van Wezel T, and Morreau H: Homozygosity for a CHEK2*1100delC mutation identified in familial colorectal cancer does not lead to a severe clinical phenotype. J Pathol 2005, 206: 198-204

47. Gibson NJ: The use of real-time PCR methods in DNA sequence variation analysis. Clin Chim Acta 2006, 363: 32-47
48. Lim EH, Zhang SL, Li JL, Yap WS, Howe TC, Tan BP, Lee YS, Wong D, Khoo KL, Seto KY, Tan L, Agasthian T, Koong HN, Tam J, Tan C, Caleb M, Chang A, Ng A, and Tan P: Using whole genome amplification (WGA) of low-volume biopsies to assess the prognostic role of EGFR, KRAS, p53, and CMET mutations in advanced-stage non-small cell lung cancer (NSCLC). J Thorac Oncol 2009, 4: 12-21

Chapter 6

Rapid *KRAS*, *EGFR*, *BRAF* and *PIK3CA* Mutation Analysis of Fine Needle Aspirates from Non-Small-Cell Lung Cancer using allele-specific qPCR

Ronald van Eijk[1]*, Jappe Licht[1]*, Melanie Schrumpf[1], Mehrdad Talebian Yazdi[2], Dina Ruano[1], Giusi I. Forte[1,4], Petra M. Nederlof[3], Maud Veselic[1], Klaus F. Rabe[2], Jouke T. Annema[2], Vincent Smit[1], Hans Morreau[1], Tom van Wezel[1]

* These authors contributed equally to this work.
[1] Departments of Pathology and [2]Pulmonology Leiden University Medical Center
[3] Department of Pathology
Netherlands Cancer Institute NKI-AVL, Amsterdam
[4] Current address; Department di Biopatologia e Biotecnologie Mediche e Forensi
Università di Palermo, Italy

PLoS ONE. 8;6(3):e17791 (2011) doi: 10.1371/journal.pone.0017791.

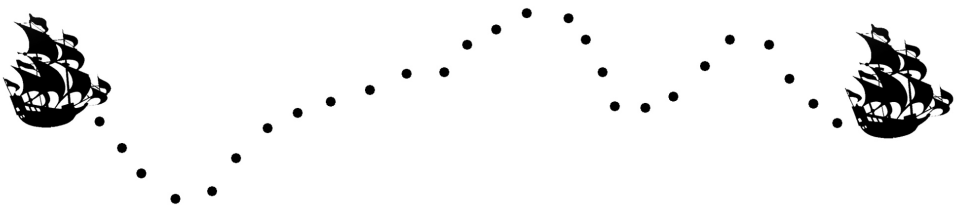

Abstract
Endobronchial Ultrasound Guided Transbronchial Needle Aspiration (EBUS-TBNA) and Trans-esophageal Ultrasound Scanning with Fine Needle Aspiration (EUS-FNA) are important, novel techniques for the diagnosis and staging of non-small cell lung cancer (NSCLC) that have been incorporated into lung cancer staging guidelines. To guide and optimize treatment decisions, especially for NSCLC patients in stage III and IV, *EGFR* and *KRAS* mutation status is often required. The concordance rate of the mutation analysis between these cytological aspirates and histological samples obtained by surgical staging is unknown. Therefore, we studied the extent to which allele-specific quantitative real-time PCR with hydrolysis probes could be reliably performed on EBUS and EUS fine needle aspirates by comparing the results with histological material from the same patient. We analyzed a series of 43 NSCLC patients for whom cytological and histological material was available. We demonstrated that these standard molecular techniques can be accurately applied on fine needle cytological aspirates from NSCLC patients. Importantly, we show that all mutations detected in the histological material of primary tumor were also identified in the cytological samples. We conclude that molecular profiling can be reliably performed on fine needle cytology aspirates from NSCLC patients.

Keywords
Lung cancer; Molecular diagnosis; Methodology; NSCLC; EBUS-TBNA; EUS-FNA; *EGFR; KRAS; PIK3CA; BRAF;* FFPE; qPCR, Personalized medicine

Introduction
Lung cancer is the leading cause of cancer mortality in the Western world [1]. For clinical and therapeutic purposes, lung cancer is traditionally subdivided into small cell (SCLC) and non-small cell lung cancer (NSCLC). Whereas SCLC is treated by chemo- and/or radiotherapy, NSCLC is primarily treated through resection; however, only 30% of NSCLC patients have a resectable disease (stage I/II) at the time of presentation [2]. This underscores the importance of accurate, preoperative mediastinal staging in preventing unnecessary resections. Preoperative staging can be performed through the transbronchial (EBUS-TBNA) or transesophageal (EUS-FNA) aspiration of the mediastinal lymph nodes. These cytological procedures are less invasive than routine mediastinoscopy followed by biopsy of the lymph nodes, but similar high specificity and sensitivity [3–9] are achieved. Endosonography has been incorporated into lung cancer staging guidelines as an alternative for the surgical staging of the mediastinum [10,11].
In many cases, the increased use of these minimally invasive techniques is sufficient to diagnose and stage the patient correctly. Although the amount of cellular material obtained by these procedures is relatively small, the information requested by the clinicians is rapidly growing, e.g., for NSCLC, immunohistochemistry and molecular pathology have become part of the standard care [12].

In addition to this change in staging procedures, the rapid development of new medical treatments for NSCLC patients has taken place. A subset of NSCLC cancers may harbor an activating mutation in the EGFR kinase domain [13]. Tumors with these mutations are frequently sensitive to tyrosine kinase inhibitors (TKIs). On the other hand, activating mutations in *KRAS* are associated with resistance to TKIs. Although most publications report that these mutations are mutually exclusive [14–19], evidence suggests [20] that a tumor can simultaneously harbor an activating *EGFR* mutation and mutations downstream in the pathway in the *KRAS* gene, which means that upstream inhibition of EGFR will have no therapeutic effect in these cases. Also, mutations in *BRAF* and *PIK3CA* are reported in NSCLC. However, further research is required to determine the extent to which these mutations can have consequences for treatment [21,22].

Due to these developments and the desire of patients and clinicians to minimize the delay of treatment, rapid and sensitive molecular techniques are needed. Preferably, these techniques should be applicable on formalin-fixed, paraffin-embedded (FFPE) cytological samples [23–25] because EBUS-TBNA and EUS-FNA aspiration samples are often the first material that is acquired from patients with NSCLC. Allele-specific quantitative real-time PCR (qPCR) with hydrolysis probes is a reliable and sensitive technique that can be used for this purpose. Detecting mutations in *EGFR*, *KRAS*, *BRAF* and *PIK3CA* with hydrolysis probes has been previously described in NSCLC patients [23–26]. The sensitivity of the assays also surpasses the 1% sensitivity proposal set for *KRAS* mutation testing [27] .

The majority of *EGFR* mutations are p.L858R, the hotspot mutation in exon 21 and deletions in exon 19, which are reported to comprise up to 36% of all activating mutations [15,28]. *KRAS* is mutated in 10%–30% of lung carcinomas and over 95% of all activating mutations in *KRAS* are located in exon 1 (codons 12 and 13) [28,29]. The *BRAF* p.V600E hotspot mutation is reported in 3% of NSCLC and alters residues important in AKT-mediated BRAF phosphorylation, suggesting that the disruption of AKT-induced BRAF inhibition plays a role in malignant transformation [28,30]. Three hotspot mutations in *PIK3CA* may be another cause of the over-activation of the PI3K–AKT pathway, which promotes the malignant transformation of human airway epithelial cells and has been reported in approximately 4% of lung carcinomas [28,31].

In the current study, we compared allele-specific qPCR assays for the most frequent activating mutations in *EGFR*, *KRAS*, *BRAF* and *PIK3CA* in tumor-positive fine needle cytological aspirates against histological material of primary tumors.

With this approach, we aimed to determine the extent to which allele-specific qPCR with hydrolysis probes can be performed on cytological aspiration material by comparing the mutation status and then observing the concordance rate between the cytological and histological material and between primary tumors and metastases.

Materials and methods

Ethics Statement

Specific need for ethics committee's approval was not necessary for this study. All samples were handled according to the medical ethical guidelines described in the Code Proper Secondary Use of Human Tissue established by the Dutch Federation of Medical Sciences (www.federa.org, accessed October 27, 2010). Accordingly to these guidelines all human material used in this study has been anonymized since clinical data were not used. Because of this anonymization procedure individual patients' permission is not needed.

Sample selection

Material from 43 patients with NSCLC for which both tumor-positive cytological and histological material was available were selected from the Department of Pathology in the Leiden University Medical Center (LUMC) and identified through a PALGA database search; non-gynecologic cytological samples between 2005 and 2009 were searched using the search-strings "lung, malignant cells and non small cell lung cancer" and "mediastinum, malignant cells and non small cell lung cancer". From the 447 unique cytological samples, we selected cases for which tumor-positive histological material of the primary tumor was also available (Supplementary Table S1). Of the 43 patients, 33 patients were subtyped: 14 squamous cell carcinomas, 15 adenocarcinomas, 3 adenosquamous carcinomas and 1 large cell carcinoma. The remaining 10 patients had been classified NSCLC only.

DNA from 42 control FFPE samples was obtained from the Molecular Diagnostics (MD) section of the Department of Pathology in the LUMC. For validation purposes, a series of 10 DNA samples, of which 9 had a demonstrated *EGFR* exon 19 deletion by DNA sequencing, was provided by the Netherlands Cancer Institute **-** Antoni van Leeuwenhoek Hospital.

DNA isolation

Prior to DNA isolation, tumor cells were enriched to obtain tumor cell percentages > 70% (Figure 1). The FFPE tumor blocks were enriched for tumor cells guided by a hematoxylin and eosin (H&E)-stained slide taking 0.6-mm tissue punches from the tumor focus in the FFPE block by using a tissue microarrayer (Beecher Instruments, Sun Prairie, WI, USA). Prior to DNA isolation, the tissue was deparaffinized in xylene and washed in 70% ethanol. For the cell blocks, 10 slides of 10 μm were stained with hematoxylin. Tumor cells were marked by guiding with a 5-μm H&E slide and the corresponding tumor fields on the hematoxylin slides were microdissected.

For the cytology smears, microdissection was initiated by marking the tumor foci with a diamond needle on the back side of the Giemsa-stained slide. Subsequently, cover slips were removed by incubating in xylene at room temperature in separate 50-ml tubes to avoid contamination. Incubation was performed overnight or until the cover slip was removed (sometimes up to a week). Subsequently, the slides were washed in alcohol, three times in 100%, once in 70% and once in 50%, to

rehydrate the tissue. Using a scalpel blade, the tumor foci from the marked areas were scraped and collected in micro tubes for DNA isolation.
DNA was isolated using the NucleoSpin Tissue XS Genomic DNA Purification kit (Machery-Nagel, Düren, Germany) according to the manufacturer's instructions. The average DNA yield from the cytological smears and cell blocks was 282 ng and 280 ng, respectively. However, cytology smears were fixed using methanol rather than formalin, so the isolated DNA was expected to be of higher quality. The average DNA yield from the biopsies was considerably higher (985 ng).
Prior to analysis, the DNA samples were diluted by 5 or 15 times. We observed that DNA diluted over 15 times generally gave a quantification cycle (Cq) > 35 (data not shown); therefore, in the subsequent assays, we used 5x stock DNA dilutions in sterile water.

Mutation detection
The assays for the detection of seven different *KRAS*, three *PIK3CA* and one *BRAF* variant were obtained through the Custom TaqMan® Assay Design Tool (Applied Biosystems, Nieuwerkerk a/d IJssel, NL). Hydrolysis probes were designed with minor grove binder (MGB) modifications at the 3′-end. These modified probes have the advantage that relatively short probes can be designed with higher melting temperature (Tm) and increased duplex stability and specificity in comparison to conventional probes [32]. The *EGFR* assays were described previously [33]. qPCR reactions were performed in 10-µl reactions containing 5 µl of FastStart Universal Probe Master (Roche Applied Science), 1 µl of 10x primer and hydrolysis probe solutions, 2 µl of 5x diluted DNA and 2 µl of sterile water in a sealed LightCycler 480 Multiwell Plate 384 (Roche Applied Science) in a LightCycler 480 system (Roche Diagnostics) as follows: 10 minutes at 95 °C and 45 cycles of 15 seconds at 92 °C, 60 seconds at 60 °C and 10 seconds at 72 °C. For validation, we performed direct Sanger sequencing using M13 primers as described previously [34] at the sequencing core of the Leiden Genome Technology Center. Primer sequences are listed in Supplementary Table S2. All DNA Sequencing was completed on known genes and no new sequencing was completed.
Raw data from the LC480 software were imported into an in-house–created Microsoft Excel 2003 spreadsheet to define the mutation status. The quantification cycle (Cq) was used for quality assessment and samples with Cq values exceeding 35 (Cq>35) in the wild-type channel were rejected and excluded for further analysis. To determine the presence or absence of a mutation, the endpoint fluorescence ratio R_m/R_{wt} was calculated after subtracting the average background signal from three negative controls. The spreadsheet is available upon request. For *BRAF*, *PIK3CA* and *EGFR* p.L858R, mutation status was directly discriminated (Figure 2a). Mutations were identified when the R_m/R_{wt} ratio was higher than 0.7, while a ratio lower than 0.3 indicated the absence of a mutation. No intermediate values were observed. In *KRAS* wild-type samples, an increased background signal was observed for the c.34G>T (R_m/R_{wt}±0.4) and c.38G>C (R_m/R_{wt}±0.6) assay in the mutant probe channel. This was probably

caused by imperfect hybridization of these probes to the wild-type allele. The setting to identify the mutation correctly was c.34G>T R_m/R_{wt}>0.7, while the c.38G>T mutant was identified when an R_m/R_{wt} ratio cut-off of 0.8 was used. The *EGFR* exon 19 deletion probe resulted in a drop in endpoint fluorescence, while in a wild-type sample, both probes gave a signal. To analyze *EGFR* exon 19 deletions, R_m/R_{wt}>0.8 and Cq<32 were considered wild-type and R_m/R_{wt}≤0.6 and Cq<32 indicated a deletion. Intermediate values, with R_m/R_{wt} ratio between 0.6 and 0.8 and Cq<35, required confirmation using Sanger sequencing.

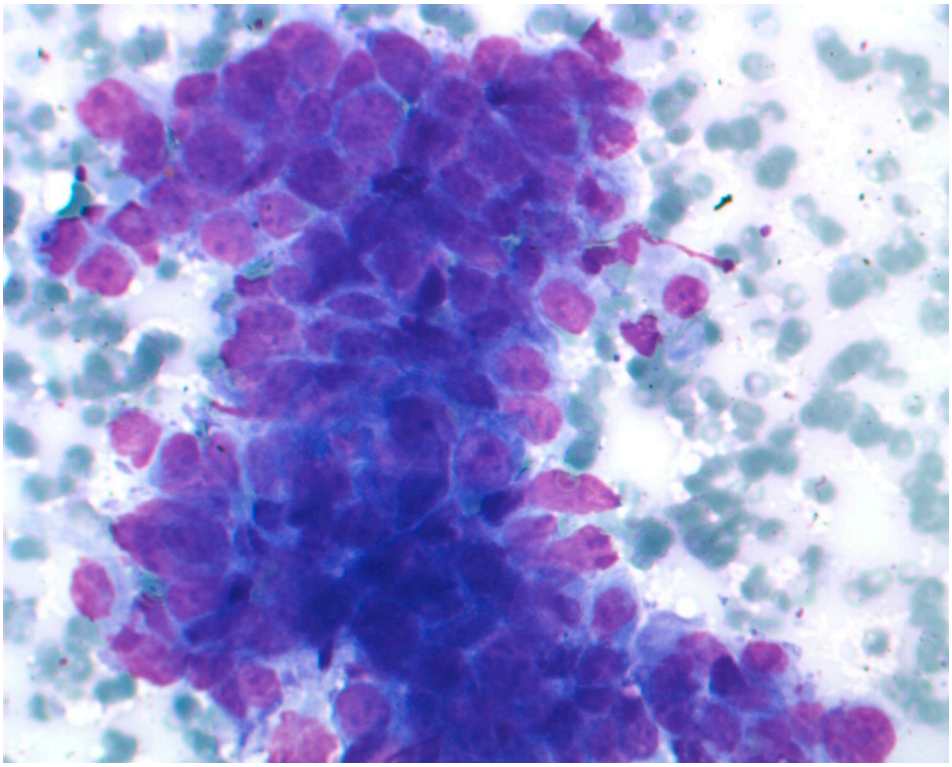

Figure 1. Mediastinal lymph node cytology of a NSCLC patient. Microscopical detail of a cytological smear obtained through fine needle aspiration of a meadiastinal lymph node from a NSCLC patient. The tumor foci are marked on the backside of each slide with a diamond tip. Subsequently the coverslips are removed and tumor foci are scraped from the slide using a scalpel blade (not shown).

Results and discussion

Assay design and validation

For *BRAF*, a single assay was designed that detects the activating hotspot mutation p.V600E, which results from the c.1799T>A substitution [35]. For *PIK3CA*, we designed probes for the three most common substitutions [36]: c.1624G>A (p.E542K), c.1633G>A (p.E545K) and c.3140A>G (p.H1047R). Although these three assays detected over 85% of all mutations in NSCLC, some of the infrequent substitutions in the hotspot regions were potentially missed. For *KRAS*, we designed assays for the seven most frequent base pair substitutions in codons 12 and 13: c.34G>A (p.G12S), c.34G>C, (p.G12R), c.34G>T, (p.G12C), c.35G>A, (p.G12D), c.35G>C, (p.G12A), c.35G>T (p.G12V) and c.38G>A (p.G13D). Together, these assays detect almost all substitutions in *KRAS*, although some rare variants might be missed. To detect the p.L858R hotspot and exon 19 deletions in *EGFR* we used previously reported assays [33]. The *EGFR* p.L858R mutation was detected using a probe mix containing a wild-type probe and two different mutant probes: one for the most common variant (c.2573T>G) and one for the rare complex c.2573_2574TG>GT inversion.

Hotspot mutation analysis in cytology material from NSCLC patients

To address the extent to which the mutation analysis can be reliably performed on EBUS-TBNA and EUS-FNA aspiration material, we performed the 13 assays on 43 patients with NSCLC for which both primary tumor (either biopsies or histological material from resections) and tumor-positive cytological material had been collected. The material from the 43 patients represents 29 tissue cores from histological excisions, 23 microdissected biopsies and 3 whole-section biopsies which were compared to 45 microdissected cytological smears and 17 microdissected cell blocks (Supplementary Table S1).

Six patients presented with a *KRAS* mutation: c.34G>T (N=2), c.34G>A, c.35G>A, c.35G>C and c.38G>A. One patient carried a deletion in exon 19 of *EGFR* (c.2238_2252del15) and two patients showed *PIK3CA* mutations: c.1633G>A and c.3140A>G. The latter case showed an additional *KRAS* mutation (p.34G>T). No mutations in *BRAF* were observed.

For some patients, multiple histological and/or cytological samples were analyzed. In different samples for the same patient, conflicting results for the same type of material were never observed. Therefore in table 1 each patient is represented only once, where for each type of material the information from all the patient's samples is merged. This means that the clearest signal for each assay took precedence. In table 1, the remaining missing calls, due to low signals are indicated by "?".

The overall call rate in the 13 assays, after merging, amounts to 95% (58 undetermined results out of 1118 tests). The call rate for histological material is substantially higher at 99% (8 undetermined out of 559) than for cytological material at 91% (48 out of 559). Within the cytological material, the call rate for primary tumors is lower (84%) than for metastases (96%). Note that these observations remain if the patient with the lowest quality results (sample 21) is

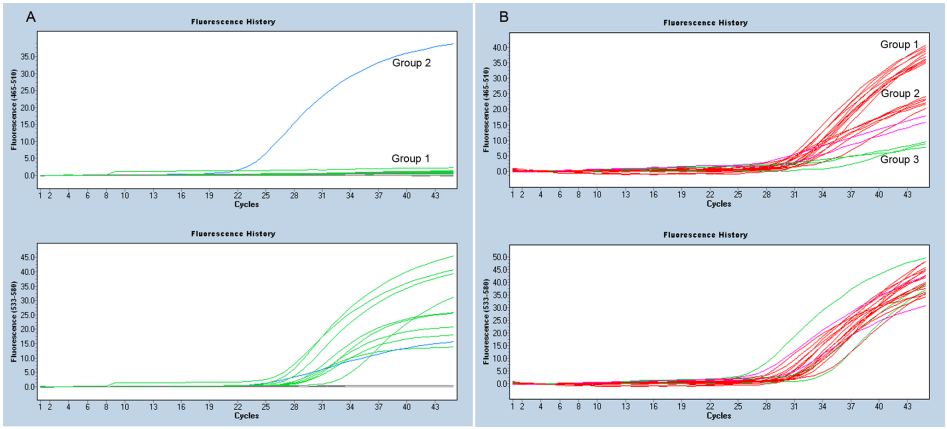

Figure 2. qPCR Results for the EGFR assays. Panel A shows the EGFR p.L858R assay. All samples show a wild type (control) signal, VIC, lower panel (green and blue lines) while only group 2 (blue line) shows a mutant FAM signal. Panel B shows the EGFR exon 19 mutation assay. The lower panel shows the wildtype VIC signal for all samples (red, green and purple lines). The top panels shows the mutant FAM signal. Group 1 (red lines) shows the wildtype signal, Group 2 (red and purple) shows possible mutants with decreased fluorescence, group 3 (green line) show an almost completely disappeared signal indicating a deletion. The images are obtained from the LC480 software release 1.5.0.The y-axis shows the relative fluorescence for the FAM (465-510 nm) and VIC (533-580nm) probes, x-axis shows the PCR cycles.

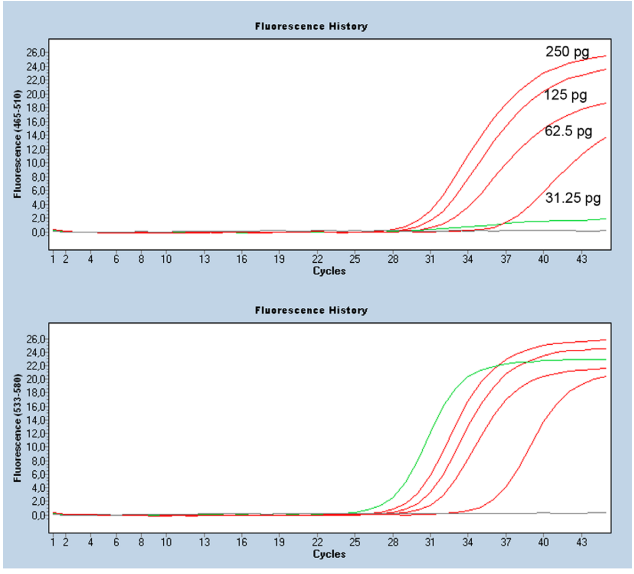

Figure 3. Effect of the DNA concentration on the c.34G>T KRAS assay. The top panel shows the mutant (FAM) signal for a range of different amounts of input DNA in pg carrying the c.34G>T KRAS mutation. No "mutant" signal is observed in a wildtype DNA (green line) and water control (grey line). In the wildtype (VIC) panel all DNA's show a wildtype signal while the water control is negative (grey line). The images are obtained from the LC480 software release 1.5.0. The y-axis shows the relative fluorescence for the FAM (465-510 nm) and VIC (533-580nm) probes, x-axis shows the PCR cycles.

removed. Within the histological material the same difference in call rate can be observed, but in a much lower degree (98% for primary tumors versus 99% for metastases). When comparing call rates per assay, we observed that the three assays on the *PIK3CA* gene performed less (between 88 and 91%) than the other 10 assays (between 94 and 99%).
As could be observed, when cytological material was obtained from primary tumors, the mutation results for histology and cytology were concordant in all cases where both results were determined. When cytological material was obtained from metastasis, in one patient (nr 40) with an adenocarcinoma/ bronchoalveolar cell carcinoma (BAC), a KRAS c.34G>A mutation was identified in the mediastinal lymph node which was not detected in the primary tumor. This could be explained by the commonly observed genetic divergence of metastasis from its primary tumor. In this case the time-span is 18 years between the primary tumor and the metastasis. Overall, the discordance rate is only 0.20% (1 assay out of 503 where both histological and cytological results are determined).

Tumor cell percentage and DNA quality
From biopsies and cytology, only small tumor foci can be microdissected. This results in a low DNA yield that, in case of formalin fixation, is also partially degraded. To study the quality of the DNA, we compared the DNA yield to assay performance. We observed that the average amount of DNA isolated (295 ng) was lower in the group (n=15) where two or more assays failed [as compared to the group without failing assays (n=102, 2973 ng)]. Nevertheless, in the latter group, 44% of the samples (n=45) also had a DNA amount of lower than 295 ng. This indicates that Cq values are a better indicator of DNA quality and performance than DNA concentration measurements.
Allele-specific qPCR with hydrolysis probes has been reported to surpass the 1% sensitivity level [27]. However, considering that the qPCR efficiency also depends on DNA fragmentation, the DNA isolated from FFPE samples could accurately be analyzed at a sensitivity level of 10% [26]. We determined the detection limit in serial dilutions of DNA from two tumors carrying a *KRAS* c.34G>T or a c.35G>A mutation. This showed that the minimal DNA input must be at least 32 pg, the equivalent of 4–6 cells of high molecular DNA, to give Cq values <35 (Figure 3).
Furthermore, we validated the assays in a series of DNA isolates from microdissected FFPE samples with known *KRAS*, *PIK3CA*, *BRAF* or EFGR variants as determined by Sanger sequencing. We found a 100% correlation with the hydrolysis probe assays.
We validated the assay for *EGFR* exon 19 in a series of 10 samples with possible sequence verified exon 19 deletions and a tumor percentage of more than 50%. The samples were tested without prior knowledge of the mutation status. The hydrolysis assay results were compared with the DNA sequence results and all nine samples containing an exon 19 deletion were correctly identified and distinguished from the wild-type specimen (Figure 2b). In one case, there was an 18-bp insertion in exon 19. Because this fell outside the detection area of the probes, the mutant was not detected by the deletion assay (SampleID 1012

Table 1. Results of mutation analysis for the 13 assays for 43 NSCLC subjects. For each subject the origin of the cytological material and the mutational status for each of the 13 assays are indicated. Only one subject (40) shows a discordance on a single assay (boxed cell), which may be explained from the commonly observed genetic divergence of metastasis from its primary tumor. **'P'**, primary tumor; '**M'**, metastasis; '**√**', concordance of wildtype result from mutation analysis between histology and cytology; **'mut'**, concordant samples with a somatic mutation; '**-/+**', discordant result, mutation in the cytological and wildtype in the histological material; **'-/?**', wildtype signal in the histology with discordancy in the cytological material because of low signal; '**?/-**', Low signal in the histological material and wildtype signal in the cytology.

	KRAS							*EGFR*		*BRAF*	*PIK3CA*		
SAMPLE	**p.G12S**	**p.G12R**	**p.G12C**	**p.G12D**	**p.G12A**	**p.G12V**	**p.G13D**	**deletion**	**p.L858R**	**p.V600E**	**p.E542K**	**p.E545K**	**p.H1047R**
ORIGIN	**c.34G>A**	**c.34G>C**	**c.34G>T**	**c.35G>A**	**c.35G>C**	**c.35G>T**	**c.38G>A**	**exon 19**	**exon 21**	**c.1799T>A**	**c.1624G>A**	**c.1633G>A**	**c.3140A>G**
1-M	√	√	√	√	√	√	√	√	√	√	√	√	√
2-M	√	√	√	mut	√	√	√	√	√	√	√	√	√
3-P	√	√	√	√	- / ?	√	- / ?	- / ?	√	- / ?	- / ?	- / ?	- / ?
4-M	√	√	√	√	√	√	√	√	√	√	√	√	√
5-M	√	√	√	√	√	√	√	√	√	? / -	? / -	√	? / -
6-M	? / -	√	√	√	√	√	√	√	√	√	√	√	√
7-M	√	√	√	√	√	√	√	√	√	√	√	√	√
8-M	√	√	√	√	√	√	√	√	√	√	√	√	√
9-M	√	√	√	√	√	√	√	√	√	√	- / ?	- / ?	- / ?
10-M	√	√	√	√	√	√	√	√	√	√	√	√	√
11-M	√	√	√	- / ?	- / ?	√	√	√	√	√	√	√	√
12-M	√	√	√	√	√	√	√	√	√	√	√	√	√
13-M	√	√	√	√	√	√	√	√	√	√	√	√	√
14-M	√	√	√	√	√	√	√	√	√	√	√	√	√
15-M	√	√	√	√	√	√	√	√	√	√	√	√	√
16-M	√	√	√	√	√	√	√	√	√	√	√	√	√
17-M	√	√	√	√	√	√	√	√	√	√	- / ?	- / ?	- / ?

18-M	√	√	√	√	√	√	√	√	√	√	√	√	√
19-P	√	√	√	√	√	√	√	mut	√	√	√	√	√
20-P	√	√	√	√	√	√	√	√	√	√	√	√	√
21-P	- / ?	- / ?	- / ?	- / ?	- / ?	- / ?	√	- / ?	√	- / ?	- / ?	- / ?	- / ?
22-P	√	√	√	√	√	√	√	√	√	√	√	√	√
23-P	√	√	√	√	√	√	√	√	- / ?	√	- / ?	- / ?	√
24-P	√	√	√	√	√	√	√	√	- / ?	√	- / ?	- / ?	- / ?
25-P	√	√	√	√	√	√	√	? / -	√	? / -	? / -	√	? / -
26-P	√	√	mut	√	√	√	√	√	√	√	√	√	√
27-P	√	√	√	√	√	√	√	√	√	√	√	√	√
28-P	√	√	√	√	√	√	√	- / ?	√	√	- / ?	- / ?	- / ?
29-P	√	√	√	√	√	√	mut	√	√	√	√	√	√
30-P	√	√	√	√	√	√	√	√	√	√	√	mut	√
31-M	√	√	√	√	√	√	√	√	√	√	√	√	√
32-M	√	√	mut	√	√	√	√	√	√	√	√	√	√
33-M	√	√	√	√	√	√	√	√	√	√	√	√	√
34-M	√	√	√	√	√	√	√	√	√	√	√	√	√
35-P	√	√	mut	- / ?	- / ?	- / ?	√	√	√	√	√	√	mut
36-M	√	√	√	√	√	√	√	√	√	√	√	√	√
37-M	√	- / ?	√	- / ?	√	√	- / ?	- / ?	√	- / ?	√	√	√
38-P	√	√	√	√	√	√	√	√	√	√	√	√	√
39-M	√	√	mut	√	√	√	√	√	√	√	√	√	√
40-M	- / +	√	√	√	√	√	√	√	√	√	√	√	√
41-M	√	√	√	√	√	√	√	√	√	√	- / ?	- / ?	- / ?
42-M	√	√	√	√	√	√	√	√	√	√	√	√	√
43-M	√	√	√	√	√	√	√	√	√	√	√	√	√

in Supplementary Table S3). These results show that all hotspot mutations and *EGFR* exon 19 deletions can be detected using the hydrolysis probes.

Cross-reactivity

Mutations in *KRAS* and *PIK3CA* cluster in hotspots. For *KRAS*, all seven assays hybridized to codons 12 and 13 (nucleotides c.34G, c.35G and c.38G), while for *PIK3CA* two assays detected exon 9 changes (c.1624G>A and c.1633G>A). As the probes potentially hybridized in the same region, cross-reactivity between the different *KRAS* or *PIK3CA* assays might be observed as a result of increased fluorescence readings from imperfectly matched probes or primers [26]. Additionally, cross-reactivity might result from (rare) base pair substitutions that are not covered by the used assays.

Cross-reactivity was studied in a series of 42 MD samples carrying a *KRAS* mutation at position 34, 35 or 38. A total of 294 assays (42x7) were performed. The correct mutation status was identified when an R_m/R_{wt} ratio cut-off >0.7 was used; however, in 68 assays, a cross-reactivity signal was observed. Five cross-reactivity signals had R_m/R_{wt}>0.7, but in these cases, the assay for the genuine mutation had R_m/R_{wt}>1.0. Cross-reactivity was only observed for probes covering the same base pair position (at position 34 or 35). Cross-reactivity between signals from base pair 34 or 35 and position 38 was not observed (Supplementary Table S4). Therefore, it is probable that no cross-reactivity effects were observed for the two different *PIK3CA* probes.

Clinical practice

The described methods can be implemented in clinical practice. The molecular diagnostics test results can be generated in a short time. In daily practice, the cytological EBUS-TBNA or EUS-FNA aspiration material is morphologically typed by pathologists. Subsequently, samples are clustered for microdissection on a weekly basis. Microdissection is essential to obtain high tumor cell percentages to detect the EGFR exon 19 deletion, and to allow other analyses with lower sensitivity than the described method, e.g Sanger sequencing. After DNA isolation, the hydrolysis probe assays are performed on the DNA dilutions. At the end of the second day, the qPCR results are analyzed in an in-house–developed Microsoft Excel–based analysis tool to interpret the results, e.g., determine the mutation status of each probe and interpret the effect of cross-reactivity. The results are subsequently reported to the clinic. A limitation of hotspot analysis is, by definition, that only the hotspot mutations are detected, while Sanger sequencing can identify all mutations in the PCR amplicon. In some cases, in which the mutation analysis does not meet the quality settings, Sanger sequencing will be performed. For Sanger sequencing, extra PCR reactions, reaction product purifications and electrophoresis must be performed, which will require two extra days in the analysis pipeline.

Conclusion

We conclude that somatic mutation hotspot analysis for *KRAS*, *PIK3CA*, *BRAF* and *EGFR* of fine needle aspirations of mediastinal lymph nodes in NSCLC patients is accurate and reliable. Somatic hotspot mutation analysis for *KRAS*, *PIK3CA*, *BRAF* and *EGFR* can reliably be performed using allele-specific qPCR with hydrolysis probes; the mutation results from cytological specimens and the primary tumors are highly concordant.

Somatic mutation analysis in NSCLC for molecular staging and the guidance of treatment decisions can be performed on EBUS and EUS fine needle aspirates, procedures that are less invasive for the patient than routine mediastinoscopy.

Our findings indicate that the molecular genetic analysis of NSCLC should be incorporated with the standard EBUS and EUS procedures. This combined approach will result in the accurate diagnosing and staging of those patients and will also help to guide the optimal treatment decisions, especially in stage III and IV NSCLC.

Acknowledgements

We thank the technicians at the Molecular Diagnostics group in the LUMC Department of Pathology for testing the protocols in different biological settings and troubleshooting the various aspects of the study.

Reference List

1. Parkin DM, Bray F, Ferlay J, Pisani P (2005) Global Cancer Statistics, 2002. CA Cancer J Clin 55: 74-108.
2. Molina JR, Adjei AA, Jett JR (2006) Advances in Chemotherapy of Non-small Cell Lung Cancer*. Chest 130: 1211-1219.
3. Gu P, Zhao YZ, Jiang LY, Zhang W, Xin Y et al. (2009) Endobronchial ultrasound-guided transbronchial needle aspiration for staging of lung cancer: a systematic review and meta-analysis. Eur J Cancer 45: 1389-1396.
4. Annema JT, Versteegh MI, Veselic M, Welker L, Mauad T et al. (2005) Endoscopic Ultrasound Added to Mediastinoscopy for Preoperative Staging of Patients With Lung Cancer. JAMA 294: 931-936.
5. Horiike A, Kimura H, Nishio K, Ohyanagi F, Satoh Y et al. (2007) Detection of Epidermal Growth Factor Receptor Mutation in Transbronchial Needle Aspirates of Non-Small Cell Lung Cancer*. Chest 131: 1628-1634.
6. Nakajima T, Yasufuku K, Suzuki M, Hiroshima K, Kubo R et al. (2007) Assessment of Epidermal Growth Factor Receptor Mutation by Endobronchial Ultrasound-Guided Transbronchial Needle Aspiration*. Chest 132: 597-602.
7. Tournoy KG, Rintoul RC, van Meerbeeck JP, Carroll NR, Praet M et al. (2009) EBUS-TBNA for the diagnosis of central parenchymal lung lesions not visible at routine bronchoscopy. Lung Cancer 63: 45-49.
8. Micames CG, McCrory DC, Pavey DA, Jowell PS, Gress FG (2007) Endoscopic ultrasound-guided fine-needle aspiration for non-small cell lung cancer staging: A systematic review and metaanalysis. Chest 131: 539-548.
9. Annema JT, Versteegh MI, Veselic M, Voigt P, Rabe KF (2005) Endoscopic ultrasound-guided fine-needle aspiration in the diagnosis and staging of lung cancer and its impact on surgical staging. J Clin Oncol 23: 8357-8361.
10. Detterbeck FC, Jantz MA, Wallace M, Vansteenkiste J, Silvestri GA (2007) Invasive mediastinal staging of lung cancer: ACCP evidence-based clinical practice guidelines (2nd edition). Chest 132: 202S-220S.
11. De Leyn P, Lardinois D, Van Schil PE, Rami-Porta R, Passlick B et al. (2007) ESTS guidelines for preoperative lymph node staging for non-small cell lung cancer. Eur J Cardiothorac Surg 32: 1-8.
12. Rossi G, Pelosi G, Graziano P, Barbareschi M, Papotti M (2009) Review Article: A Reevaluation of the Clinical Significance of Histological Subtyping of Non--Small-Cell Lung Carcinoma: Diagnostic Algorithms in the Era of Personalized Treatments. International Journal of Surgical Pathology 17: 206-218.
13. Gazdar AF (2009) Activating and resistance mutations of EGFR in non-small-cell lung cancer: role in clinical response to EGFR tyrosine kinase inhibitors. Oncogene 28 Suppl 1: S24-S31.
14. Jang TW, Oak CH, Chang HK, Suo SJ, Jung MH (2009) EGFR and KRAS mutations in patients with adenocarcinoma of the lung. Korean J Intern Med 24: 48-54.

15. Ladanyi M, Pao W (2008) Lung adenocarcinoma: guiding EGFR-targeted therapy and beyond. Mod Pathol 21 Suppl 2: S16-S22.
16. Lim EH, Zhang SL, Li JL, Yap WS, Howe TC et al. (2009) Using whole genome amplification (WGA) of low-volume biopsies to assess the prognostic role of EGFR, KRAS, p53, and CMET mutations in advanced-stage non-small cell lung cancer (NSCLC). J Thorac Oncol 4: 12-21.
17. Monaco SE, Nikiforova MN, Cieply K, Teot LA, Khalbuss WE et al. (2010) A comparison of EGFR and KRAS status in primary lung carcinoma and matched metastases. Human Pathology 41: 94-102.
18. Motoi N, Szoke J, Riely GJ, Seshan VE, Kris MG et al. (2008) Lung Adenocarcinoma: Modification of the 2004 WHO Mixed Subtype to Include the Major Histologic Subtype Suggests Correlations Between Papillary and Micropapillary Adenocarcinoma Subtypes, EGFR Mutations and Gene Expression Analysis. The American Journal of Surgical Pathology 32.
19. Sasaki H, Okuda K, Kawano O, Endo K, Yukiue H et al. (2007) Nras and Kras mutation in Japanese lung cancer patients: Genotyping analysis using LightCycler. Oncol Rep 18: 623-628.
20. Kalikaki A, Koutsopoulos A, Trypaki M, Souglakos J, Stathopoulos E et al. (2008) Comparison of EGFR and K-RAS gene status between primary tumours and corresponding metastases in NSCLC. Br J Cancer 99: 923-929.
21. Hirsch FR, Varella-Garcia M, Bunn PA, Jr., Franklin WA, Dziadziuszko R et al. (2006) Molecular Predictors of Outcome With Gefitinib in a Phase III Placebo-Controlled Study in Advanced Non-Small-Cell Lung Cancer. J Clin Oncol 24: 5034-5042.
22. Zou ZQ, Zhang XH, Wang F, Shen QJ, Xu J et al. (2009) A novel dual PI3Kalpha/mTOR inhibitor PI-103 with high antitumor activity in non-small cell lung cancer cells. Int J Mol Med 24: 97-101.
23. Boldrini L, Gisfredi S, Ursino S, Camacci T, Baldini E et al. (2007) Mutational Analysis in Cytological Specimens of Advanced Lung Adenocarcinoma: A Sensitive Method for Molecular Diagnosis. Journal of Thoracic Oncology 2.
24. Endo K, Konishi A, Sasaki H, Takada M, Tanaka H et al. (2005) Epidermal growth factor receptor gene mutation in non-small cell lung cancer using highly sensitive and fast TaqMan PCR assay. Lung Cancer 50: 375-384.
25. Molina-Vila MA, Bertran-Alamillo J, Reguart N, Taron M, CastellÃ E et al. (2008) A Sensitive Method for Detecting EGFR Mutations in Non-small Cell Lung Cancer Samples with Few Tumor Cells. Journal of Thoracic Oncology 3.
26. Kotoula V, Charalambous E, Biesmans B, Malousi A, Vrettou E et al. (2009) Targeted KRAS mutation assessment on patient tumor histologic material in real time diagnostics. PLoS One 4: e7746.
27. van Krieken JH, Jung A, Kirchner T, Carneiro F, Seruca R et al. (2008) KRAS mutation testing for predicting response to anti-EGFR therapy for colorectal carcinoma: proposal for an European quality assurance program. Virchows Arch 453: 417-431.

28. Forbes SA, Bhamra G, Bamford S, Dawson E, Kok C et al. (2008) The Catalogue of Somatic Mutations in Cancer (COSMIC). Curr Protoc Hum Genet Chapter 10: Unit.
29. Jancik S, Drabek J, Radzioch D, Hajduch M (2010) Clinical relevance of KRAS in human cancers. J Biomed Biotechnol 2010: 150960.
30. Brose MS, Volpe P, Feldman M, Kumar M, Rishi I et al. (2002) BRAF and RAS Mutations in Human Lung Cancer and Melanoma. Cancer Research 62: 6997-7000.
31. Okudela K, Suzuki M, Kageyama S, Bunai T, Nagura K et al. (2007) PIK3CA mutation and amplification in human lung cancer. Pathol Int 57: 664-671.
32. Kutyavin IV, Afonina IA, Mills A, Gorn VV, Lukhtanov EA et al. (2000) 3'-minor groove binder-DNA probes increase sequence specificity at PCR extension temperatures. Nucleic Acids Res 28: 655-661.
33. Yung TK, Chan KC, Mok TS, Tong J, To KF et al. (2009) Single-molecule detection of epidermal growth factor receptor mutations in plasma by microfluidics digital PCR in non-small cell lung cancer patients. Clin Cancer Res 15: 2076-2084.
34. van Eijk R., van Puijenbroek M, Chhatta AR, Gupta N, Vossen RH et al. (2010) Sensitive and specific KRAS somatic mutation analysis on whole-genome amplified DNA from archival tissues. J Mol Diagn 12: 27-34.
35. Benlloch S, Paya A, Alenda C, Bessa X, Andreu M et al. (2006) Detection of BRAF V600E mutation in colorectal cancer: comparison of automatic sequencing and real-time chemistry methodology. J Mol Diagn 8: 540-543.
36. Samuels Y, Velculescu VE (2004) Oncogenic mutations of PIK3CA in human cancers. Cell Cycle 3: 1221-1224.

Chapter 7

Concluding remarks and future directions

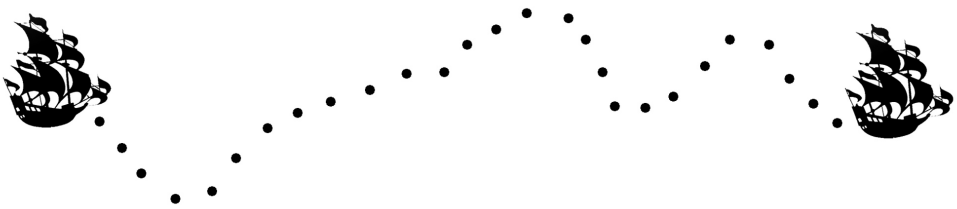

As a result of revolutionary technological advances, the molecular analysis of cancer field is growing rapidly. Mutations in *KRAS*, *BRAF* and *EGFR* have been discovered, and these biomarkers appear to be pivotal in critical cancer pathways. This knowledge led to the discovery of specific inhibitors that have been implemented in personalized medicine, for example in colorectal cancer and non-small-cell lung carcinoma [1]. Cancer genomes from tumor subtypes have been sequenced, revealing a landscape of somatic mutations. Potential critical mutations have been identified which may be favorable prognostic markers [2]. Epigenetic and transcriptional profiling of tumors contributed to the development of validated molecular classification tests such as Oncotype DX and MammaPrint for breast cancer. Therefore, the expectation is high that technological advances and an understanding of the molecular basis of cancer will translate to benefits for cancer patients [3].

What will technological advances in the next 5, 10 or 25 years bring to pathology? In his book *De Toekomst van Gezondheid* (The future of health), futurologist and trendwatcher Adjiedj Bakas predicts that in 2025 90% of oncology patients will be cured. Kurzweil, an American futurist and the current director of engineering at Google, believes that people living in 2050 could be close to immortal as a result of the combination of biotechnology and nanotechnology. In his book *The Singularity is Near: When Humans Transcend Biology* he predicts that cell repair nanobots will flow through the bloodstream in an era when artificial intelligence has become reality. These predictions are tempting and promising although only future will tell if they become reality or remain science fiction. Still, the question can be prompted whether a general direction in pathology can be distinguished by current advances and directions in technology. From a clinical point of view, future decision making strategies in pathology will continue to depend on histopathological features, and tumor typing, grading and staging will remain critical [4].

Major advances will be made with the expected implementation of digital pathology within the next decade. As a successor to standard microscopy digital pathology will imply that ultra-high-resolution (fluorescent) scanners for microscopic imaging will become available, and that pathologists will perform diagnostics using high-resolution monitors with “Google Earth”-like zooming technology [5]. This field is expected to progress based on the development and application of specialized software for image analysis: “Apps” for digital pathology. These include algorithms for computer-assisted recognition of cells in which a plethora of cellular data (DNA, RNA, and protein) will be automatically assimilated in a form beyond the current scope of pathological diagnosis and the compass of the human eye [6]. In digital pathology genomic information can be accessed through the various techniques described in this thesis, while proteomic information may be accessed through new developments in spectral flow cytometry, Matrix-assisted laser desorption ionization (MALDI) imaging mass spectrometry (IMS), or a combination of mass spectrometry and flow cytometry [7–9]

Currently, metastatic cancer remains incurable and resistance or unresponsiveness to targeted therapies often develop. Therefore genetic screening should be

performed to identify new combined targeted agents and further efforts must be made to develop better anti-metastatic cancer drugs [10,11]. To identify patients who will benefit from novel, personalized therapies, more specialized methods must be continuously developed and adapted to routine diagnostic pathology [12]. Developments in research and progress in clinical practice make it essential to intensify collaborations between pathologists and clinicians as well as between molecular biologists, bio-informaticians and intermediaries. Database managers will be needed to organize and facilitate the dissemination of the massive amount of complex data.

Currently, the application of high-throughput sequencing in FFPE material to molecular tumor diagnostics and research is not yet widespread. Methods and approaches have been developed that should be applied and evaluated on DNA isolated from FFPE samples. The routine sequencing of whole-cancer genomes will be the ultimate goal in high-throughput sequencing [13,14]. In the meantime, many labs will study the exons of all protein-coding genes in the genome. Alternatively, whole transcriptomes [15] or the epigenome [16] will be analyzed. High-throughput sequencing in molecular tumor diagnostics will most likely begin with the rapid sequencing of smaller subsets of genes on multiple samples with sufficient sequence depth to identify rare somatic variants in heterogeneous tumors [17–19]. This demand can be fulfilled by making use of smaller, faster, bench-top sequencers, such as the Illumina Miseq™ and Life Technologies Ion PGM™ and Ion Proton™ sequencers, in combination with the targeted sequencing of “DNA barcoded” samples [20].

The currently available high throughput or next generation sequencing (HT-NGS) equipment is based on PCR, which may introduce artifacts that will be detected by this sensitive method. Therefore, methods that are suitable for sequencing DNA from a single molecule will eliminate the need for PCR and will be the next step in implementing “third-generation” sequencing in the laboratory. One of the first applications of single-cell sequencing was the Heliscope™ single molecule sequencer [21], and other approaches for single-cell sequencing, such as Single molecule real-time (SMRT™, Pacific Biosciences®) sequencing and *RNA polymerase* (RNAP) sequencing, have been developed [2,22].

Single-molecule nanopore sequencing does not require fluorescent labeling, which could further simplify sample preparation protocols, increase sequencing speed and reduce costs [23]. This method is patented by Oxford Nanopore Technologies® and is applied in the GridION and MinION sequencing systems. The MinION system is a miniaturized, portable device that is the size of a large USB flash drive and may bring next-generation sequencing to the operating room, bedside, or remote areas with few resources (http://www.nanoporetech.com/ accessed September 2012).

The implementation of this third-generation sequencing technology in molecular tumor diagnostics seems to be a matter of time and investment. It remains to be observed if next- or third-generation whole genome sequencing in clinical diagnostics will be cost effective, particularly if additional costs for analysis and data storage are taken into consideration [19]. Sanger sequencing has become

one of the first commercially exploited molecular technologies, and HT-NGS will likely become daily practice in sequencing efforts. In the near future, the basic steps in sample and library preparation will be performed in research and clinical laboratories, while the actual sequencing will be outsourced to commercial companies.

Other issues in the progression toward implementing whole genome sequencing in clinics concern ethical considerations. How will doctors be educated about these testing methods and the interpretation of results? How will we manage novel variants of uncertain significance? How will we address incidental findings? How will concerns regarding privacy, potential abuse and discrimination be tackled [18,24]? These are serious considerations, particularly during a time period when it is possible and affordable for individual persons to have their “own” genome sequenced by commercial companies without any a priori clinical questions. In summary, a challenging future lies ahead; 70 years after Prof. Lignac’s seminal publication, his question can be repeated: “Quo Vadis?”.

As a consequence of the major technological advances in molecular pathology, SNP arrays and MLPA have been developed for the simultaneous analysis of many genetic loci in a relatively limited number of specimens. Applications of hydrolysis probe assays, PCR with M13-tailed primers, HRM as a mutation prescreening method and Sanger sequencing have contributed to the implementation of a largely automated workflow to detect mutations in extended series of samples. The implementation of next-generation sequence technology in molecular pathology is at hand. However, the application of these technologies using degraded DNA isolated from tiny amounts of formalin-fixed and paraffin-embedded material remains a challenge. Specialized analytical tools have been developed by commercial companies. However, these software packages are not always appropriate for the analysis of tumors in which imbalances between wild-type and mutant alleles are often observed. Databases and laboratory information management systems (LIMSs) must be implemented and maintained in the analysis workflow. Original, “raw” and analyzed data should be archived and accessible at all times for data mining, review and future reference. Therefore, the development of dedicated software, analysis approaches and a reliable and secure data storage facility is critical to continuously keep pace with the newest developments and specific demands. In the near future, electronic pathological archives with microscopic images together with whole genome and whole transcriptome sequence data will become as important as the FFPE tissue archives have proven to be over the previous decades.

Finally, molecular outcomes are not as black and white as the pharmaceutical industry would like. Factors such as minimal input, allelic imbalance, tumor heterogeneity and the role of the stroma must be considered and may present major challenges to mutation detection. Small subpopulations of cells, individual circulating tumor cells or tumor DNA may direct future therapeutic decisions and biomarker development, and the stroma is a key element of the tumor microenvironment [25,26]. Consequently, genomic analyses on individual tumor and stromal cells should be performed with an understanding of the risk of

contamination. DNA contamination must be considered because minimal amounts of patient material are available and the sensitivity of the utilized methods is increasing. Standard hydrolysis probe assays detect a mutation content of 1%, and if the wildtype allele is inhibited, a content of 0.1% or less can be identified. High-throughput sequencers can detect one mismatched DNA copy in 1000 or 10,000 reads, depending on the methodology. Digital PCR, which has become the method of choice for detecting circulating tumor DNA or cells, has a detection limit of 1:100,000 [27]. In addition to the challenging question of how patients with a low copy mutant allele will respond to therapeutics, we must realize that DNA, contaminating or not, is present everywhere, and these are challenges for future molecular testing that will require high standards at the test facilities.

These constantly evolving biological and technological insights make it necessary to concentrate molecular analysis in specialized laboratories. Only technologies that are general and widely used and validated can be applied in non-specialized routine laboratories. For instance, at the end of the 19th century H&E staining was first described and a specialized technique that could only be performed in specialized laboratories, but over time, virtually every hospital implemented this technique. In the same way, for some molecular testing methods, it is only a matter of time before tests become available for use in every hospital. However, keeping pace with new biological insights and technological developments and the implementation and maintenance of laboratories for molecular pathology in each hospital will likely be impossible and a waste of resources. More seriously, striving to keep pace with all technological advancements may even contribute to unnoticed false-positive and false-negative diagnoses. Therefore, a more rational direction for molecular tumor diagnostics must be taken, and initiatives for a few specialized centers that can be utilized by many hospitals must be exploited further. These well-equipped centers should have specialized employees to perform the tests and should continuously implement and develop new methods. These combined efforts will contribute to future advances in molecular pathology and will improve and extend the use of archival material to benefit patients.

Reference List

1. Ong FS, Das K, Wang J, Vakil H, Kuo JZ et al. (2012) Personalized medicine and pharmacogenetic biomarkers: progress in molecular oncology testing. Expert Rev Mol Diagn 12: 593-602.
2. Wong KM, Hudson TJ, McPherson JD (2011) Unraveling the genetics of cancer: genome sequencing and beyond. Annual review of genomics and human genetics 12: 407-430.
3. Tran B, Dancey JE, Kamel-Reid S, McPherson JD, Bedard PL et al. (2012) Cancer Genomics: Technology, Discovery, and Translation. J Clin Oncol 30: 647-660.
4. Grade M, Becker H, Ghadimi BM (2004) The impact of molecular pathology in oncology: The clinician's perspective. Analytical Cellular Pathology 26: 275-278.
5. Al-Janabi S, Huisman A, Van Diest PJ (2012) Digital pathology: current status and future perspectives. Histopathology 61: 1-9.
6. Taylor CR (2011) From microscopy to whole slide digital images: a century and a half of image analysis. Applied immunohistochemistry & molecular morphology : AIMM / official publication of the Society for Applied Immunohistochemistry 19: 491-493.
7. Cazares LH, Troyer DA, Wang B, Drake RR, Semmes OJ (2011) MALDI tissue imaging: from biomarker discovery to clinical applications. Analytical and bioanalytical chemistry 401: 17-27.
8. Nolan JP, Condello D (2001) Spectral Flow Cytometry. In: Current Protocols in Cytometry. John Wiley & Sons, Inc.
9. Bandura DR, Baranov VI, Ornatsky OI, Antonov A, Kinach R et al. (2009) Mass Cytometry: Technique for Real Time Single Cell Multitarget Immunoassay Based on Inductively Coupled Plasma Time-of-Flight Mass Spectrometry. Anal Chem 81: 6813-6822.
10. Watson J (2013) Oxidants, antioxidants and the current incurability of metastatic cancers. Open Biology 3.
11. Prahallad A, Sun C, Huang S, Di Nicolantonio F, Salazar R et al. (2012) Unresponsiveness of colon cancer to BRAF(V600E) inhibition through feedback activation of EGFR. Nature 483: 100-103.
12. Dietel M, Sers C (2006) Personalized medicine and development of targeted therapies: the upcoming challenge for diagnostic molecular pathology. A review. Virchows Archiv 448: 744-755.
13. Yost SE, Smith EN, Schwab RB, Bao L, Jung H et al. (2012) Identification of high-confidence somatic mutations in whole genome sequence of formalin-fixed breast cancer specimens. Nucleic Acids Research 40: e107.
14. Kerick M, Isau M, Timmermann B, Sultmann H, Herwig R et al. (2011) Targeted high throughput sequencing in clinical cancer Settings: formaldehyde fixed-paraffin embedded (FFPE) tumor tissues, input amount and tumor heterogeneity. BMC medical genomics 4: 68.
15. Stratton MR (2011) Exploring the Genomes of Cancer Cells: Progress and Promise. Science 331: 1553-1558.

16. Ku CS, Naidoo N, Wu M, Soong R (2011) Studying the epigenome using next generation sequencing. Journal of medical genetics 48: 721-730.
17. Dahl F, Stenberg J, Fredriksson S, Welch K, Zhang M et al. (2007) Multigene amplification and massively parallel sequencing for cancer mutation discovery. Proceedings of the National Academy of Sciences of the United States of America 104: 9387-9392.
18. ten Bosch JR, Grody WW (2008) Keeping up with the next generation: massively parallel sequencing in clinical diagnostics. The Journal of molecular diagnostics : JMD 10: 484-492.
19. Ku CS, Wu M, Cooper DN, Naidoo N, Pawitan Y et al. (2012) Technological advances in DNA sequence enrichment and sequencing for germline genetic diagnosis. Expert Rev Mol Diagn 12: 159-173.
20. Loman NJ, Misra RV, Dallman TJ, Constantinidou C, Gharbia SE et al. (2012) Performance comparison of benchtop high-throughput sequencing platforms. Nat Biotech 30: 434-439.
21. Harris TD, Buzby PR, Babcock H, Beer E, Bowers J et al. (2008) Single-molecule DNA sequencing of a viral genome. Science (New York, N Y) 320: 106-109.
22. Pareek C, Smoczynski R, Tretyn A (2011) Sequencing technologies and genome sequencing. Journal of Applied Genetics 52: 413-435.
23. Clarke J, Wu HC, Jayasinghe L, Patel A, Reid S et al. (2009) Continuous base identification for single-molecule nanopore DNA sequencing. Nat Nano 4: 265-270.
24. Lantos JD, Artman M, Kingsmore SF (2011) Ethical Considerations Associated with Clinical Use of Next-Generation Sequencing in Children. The Journal of Pediatrics 159: 879-880.
25. Hamilton SR (2012) Molecular pathology. Molecular oncology 6: 177-181.
26. Gerlinger M, Rowan AJ, Horswell S, Larkin J, Endesfelder D et al. (2012) Intratumor Heterogeneity and Branched Evolution Revealed by Multiregion Sequencing. N Engl J Med 366: 883-892.
27. Heyries KA, Tropini C, Vaninsberghe M, Doolin C, Petriv OI et al. (2011) Megapixel digital PCR. Nature methods 8: 649-651.

Chapter 8

Summary and “Nederlandse samenvatting”

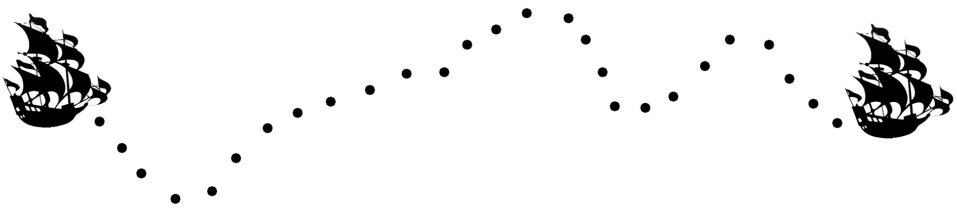

Summary
This thesis describes technical advances in molecular tumor pathology that are related to the improved use of archives of formalin-fixed and paraffin-embedded tissue for molecular tumor diagnostics and research. The importance of isolating sufficient amounts of quality DNA from small fractions of FFPE material was confirmed, and we present examples of laboratory methodologies and analytical tools that have a large impact on cancer diagnosis, prognosis and therapeutics.

In **chapter 1**, important developments in pathology are described in a general and locally applied historical perspective. An overview of different pathological consultations is presented with a short introduction of the most commonly used molecular technologies in research and diagnostics. Analysis strategies, beginning with the arrival of the tissue in the laboratory to the reporting of the test results, are discussed using a DNA analysis workflow.

In **chapter 2**, we show that due to early diagnosis and adjuvant therapies, molecular tumor diagnostics has focused on the use of very limited pre-operative material. This makes high-quality DNA isolation challenging, particularly if the number of patients and the number of consultations per sample are increasing. A molecular analysis can only be performed if DNA of sufficient quality and quantity can be extracted from the archived tissue specimen. Therefore, we tested a fully automated DNA isolation system and compare it to our classical DNA isolation method. We determined that the fully automated method delivers high-quality DNA from small tissue cores and micro-dissected tissue. When the DNA is used in hydrolysis probe assays, we achieve a 24-hour faster turnover time, with 80% less hands-on time.

Multiplex ligation-dependent probe amplification (MLPA) is introduced in **chapter 3**. MLPA can be used to detect multiple chromosomal aberrations in a single experiment. We developed an MLPA-based assay to determine losses in FFPE tissue from oligodendroglial tumors (OG) and validated the MLPA results by comparing them with fluorescence in situ hybridization (FISH). The MLPA results were reproducible in all samples for which repeated experiments were performed, and we conclude that MLPA is a valid and reproducible method for the detection of 1p/19q chromosomal deletions in OGs.

For a reliable workflow in MLPA, tools are needed for administrative support, data management, normalization, visualization, reporting and interpretation. In **chapter 4**, we describe a MLPA data management system that was developed in-house in which a statistical approach is applied for the normalization and analysis of a large series of MLPA traces, making use of multiple control samples and internal controls. This integrated approach aids in the automated handling of a large series of MLPA data and guarantees a quick and streamlined dataflow from the beginning of the experiment to the authorized report.

The accurate detection of *KRAS* mutations is critical for the molecular diagnosis of cancer and may guide proper treatment selection. In **chapter 5**, we introduce a protocol for screening somatic mutations in *KRAS* that combines a whole-genome amplification (WGA) and a high-resolution melting analysis (HRM) as a prescreening method for samples harboring mutations. Direct Sanger sequencing is subsequently applied to define the specific *KRAS* mutations in the samples. We illustrate that this method is feasible for the screening of clinical specimens by analyzing pancreatic cancers and that it can be applied to virtually any potentially mutated region in the genome.

Endobronchial ultrasound-guided transbronchial needle aspiration (EBUS-TBNA) and trans-esophageal ultrasound scanning with fine needle aspiration (EUS-FNA) are important techniques for the diagnosis and staging of NSCLC. In **chapter 6**, we demonstrate that allele-specific quantitative real-time PCR with hydrolysis probes can be accurately applied to EBUS and EUS fine needle cytological aspirates from NSCLC patients and that the mutations detected in the histological material of primary tumors can also be identified in cytological samples from the same patient.

Chapter 7 presents concluding remarks and provides future directions in molecular pathology. Major improvements in molecular technologies have been achieved in recent decades. The clinical value of different tests has been proven. Next-generation sequencing and digital pathology are challenging new technologies that will be implemented in due time in the clinic to achieve better and extended use of the current FFPE tissue archives and to the benefit of the individual patient.

Nederlandse samenvatting

In de weefsel archieven van de afdeling Pathologie bevinden zich grote aantallen “blokjes” met formaline gefixeerd en in paraffine ingebed (FFPE) weefsel. Dit proefschrift beschrijft recente technologische vooruitgang in de moleculaire tumorpathologie waardoor de toegankelijkheid van deze archieven sterk is verbetert en de mogelijkheden voor moleculaire tumor diagnostiek en wetenschappelijk onderzoek sterk zijn toegenomen. Aangetoond wordt hoe belangrijk het is voldoende kwalitatief goed DNA van kleine fracties FFPE materiaal te isoleren. Voorbeelden worden gegeven van laboratorium-methoden en analyse tools die bijdragen aan verbeterde diagnose, prognose en therapie van kanker.

In **hoofdstuk 1** worden belangrijke ontwikkelingen in de pathologie vanuit een algemeen en lokaal toegepast historisch perspectief beschreven. Een overzicht wordt gepresenteerd van verschillende pathologische onderzoeksvragen en er wordt een korte introductie gegeven van de meest gebruikte moleculaire technieken in onderzoek en diagnostiek. Analyse-strategieën, te beginnen met de binnenkomst van het weefsel in het laboratorium, tot aan de rapportage van de testresultaten, worden besproken aan de hand van een schematische DNA-analyse workflow.

In **hoofdstuk 2** laten we zien dat als gevolg van vroege diagnose en adjuvante therapieën, moleculaire tumor diagnostiek zich heeft ontwikkeld in de richting van analyses op uiterst kleine hoeveelheden pre-operatief materiaal. Dit maakt het isoleren van DNA van voldoende kwaliteit een uitdaging, vooral als zowel het aantal patiënten als het aantal consulten dat op het materiaal wordt aangevraagd toeneemt. Een moleculaire analyse kan alleen worden uitgevoerd als DNA van voldoende kwaliteit en kwantiteit wordt geïsoleerd uit het gearchiveerde FFPE weefsel. Daarom is een volledig geautomatiseerd DNA-isolatie systeem uitgetest en vergeleken met de klassieke DNA-isolatie methode. We stellen vast dat de volledig automatische methode DNA van hoge kwaliteit oplevert als het word geïsoleerd uit kleine hoeveelheden materiaal uit FFPE blokjes of gemicrodissecteerd materiaal van weefsel coupes. Als het DNA vervolgens wordt gebruikt in de zogenaamde hydrolyse probe assays wordt de doorloop tijd met 24 uur verkort terwijl de “hands-on” tijd 80% minder wordt.

Multiplex ligatie-afhankelijke probe amplificatie (MLPA) wordt geïntroduceerd in **hoofdstuk 3**. MLPA kan worden gebruikt om een relatief groot aantal chromosomale afwijkingen tegelijkertijd te onderzoeken in een enkel experiment. Een MLPA test is ontwikkeld om verlies van heterozygositeit in FFPE materiaal van oligodendrogliale tumoren (OGT) te bepalen. De MLPA resultaten zijn gevalideerd door ze te vergelijken met “fluorescentie in situ hybridisatie” (FISH) experimenten. De resultaten zijn reproduceerbaar en we concluderen dat MLPA een betrouwbare methode is voor de detectie van 1p/19q chromosomale deleties in OGT.

Voor een goede MLPA-workflow is een geautomatiseerd data-analyse systeem van groot belang. In **hoofdstuk 4** beschrijven we een zelfontwikkeld MLPA data management systeem waarin een statistische benadering wordt toegepast voor de normalisatie en de analyse van MLPA patronen. Deze geïntegreerde aanpak helpt bij de administratieve ondersteuning, normalisatie, visualisatie, rapportage en interpretatie van grote series MLPA gegevens.

De nauwkeurige detectie van mutaties in het *KRAS* gen is van groot belang voor de moleculaire diagnose van verschillende typen kanker en kan helpen bij de keuze van de behandelingstrategie van de patiënt. In **hoofdstuk 5** introduceren we een protocol voor het screenen van somatische mutaties in *KRAS*. Hierin word aansluitend aan een volledige genoom-amplificatie (WGA) een hoge-resolutie smelt analyse (HRM) uitgevoerd, die dient als mutatie pre-screenings methode. Vervolgens wordt op de monsters met een afwijkend smeltpatroon de specifieke *KRAS* mutatie vastgesteld met behulp van sequentiebepaling volgens de Sanger methode. We concluderen dat deze methode geschikt is voor de screening van klinische monsters pancreaskanker en dat de methode potentieel kan worden toegepast op vrijwel elk mogelijk gemuteerd gebied in het genoom.

Endobronchiale echogeleide transbronchiale naald aspiratie (EBUS-TBNA) en trans-oesofageale echografie met fijne naald aspiratie (EUS-FNA) zijn belangrijke technieken voor de diagnose en stadiëring van niet-kleincellig longcarcinoom (NSCLC). In **hoofdstuk 6** tonen we aan dat allel-specifieke kwantitatieve real-time PCR met hydrolyse probes betrouwbaar kan worden toegepast op vaak minimale hoeveelheden via EBUS-TBNA en EUS-FNA verkregen cytologisch materiaal van NSCLC patiënten, en dat de gedetecteerde mutaties overeenkomen met de mutaties in het histologische materiaal van primaire tumoren van dezelfde patiënt.

De toekomstige ontwikkelingen in de moleculaire pathologie en enkele concluderende overwegingen worden beschreven in **Hoofdstuk 7**. In de afgelopen decennia zijn belangrijke verbeteringen in moleculaire technologieën verwezenlijkt. De klinische waarde van verschillende moleculair pathologische testen is bewezen. “Next-generation”-sequentiebepaling en digitale pathologie zijn belangrijke nieuwe methodes die in de nabije toekomst in de kliniek zullen worden toegepast waarbij de huidige archieven met FFPE materiaal op een nog betere manier gebruikt zullen worden in het voordeel van de individuele patiënt.

List of publications

Ronald van Eijk; Lisa Stevens; Hans Morreau; Tom van Wezel
Assessment of a fully automated high-throughput DNA extraction method from formalin-fixed, paraffin-embedded tissue for KRAS, and BRAF somatic mutation analysis.
Exp. Mol. Pathol. 94, 121 (2013)

Remi A Nout; Tjalling Bosse; Carien L Creutzberg; Ina M Jürgenliemk-Schulz; Jan J Jobsen; Ludy C H W Lutgens; Elzbieta M van der Steen-Banasik; Ronald van Eijk; Natalja T Ter Haar; Vincent T H B M Smit
Improved risk assessment of endometrial cancer by combined analysis of MSI, PI3K-AKT, Wnt/β-catenin and P53 pathway activation.
Gynecol. Oncol. 126, 466 (2012)

A Middeldorp; R van Eijk; J Oosting; G I Forte; M van Puijenbroek; M van Nieuwenhuizen; W E Corver; D Ruano; T Caldes; J Wijnen; et al.
Increased frequency of 20q gain and copy-neutral loss of heterozygosity in mismatch repair proficient familial colorectal carcinomas.
Int. J. Cancer 130, 837 (2012)

Willem E Corver; Dina Ruano; Karin Weijers; Wietske C E den Hartog; Merlijn P van Nieuwenhuizen; Noel de Miranda; Ronald van Eijk; Anneke Middeldorp; Ekaterina S Jordanova; Jan Oosting; et al.
Genome haploidisation with chromosome 7 retention in oncocytic follicular thyroid carcinoma.
PLoS ONE 7, (2012)

Twinkal C Pansuriya; Ronald van Eijk; Pio d'Adamo; Maayke A J H van Ruler; Marieke L Kuijjer; Jan Oosting; Anne-Marie Cleton-Jansen; Jolieke G van Oosterwijk; Sofie L J Verbeke; Daniëlle Meijer; et al.
Somatic mosaic IDH1 and IDH2 mutations are associated with enchondroma and spindle cell hemangioma in Ollier disease and Maffucci syndrome.
Nat. Genet. 43, 1256 (2011)

Arantza Fariña Sarasqueta; Eliane C M Zeestraten; Tom van Wezel; Gesina van Lijnschoten; Ronald van Eijk; Jan Willem T Dekker; Peter J K Kuppen; Ines J Goossens-Beumer; Valery E P P Lemmens; Cornelis J H van de Velde; et al.
PIK3CA kinase domain mutation identifies a subgroup of stage III colon cancer patients with poor prognosis.
Cell Oncol (Dordr) 34, 523 (2011)

Ronald van Eijk; Jappe Licht; Melanie Schrumpf; Mehrdad Talebian Yazdi; Dina Ruano; Giusi I Forte; Petra M Nederlof; Maud Veselic; Klaus F Rabe; Jouke T Annema; et al.
Rapid KRAS, EGFR, BRAF and PIK3CA mutation analysis of fine needle aspirates from non-small-cell lung cancer using allele-specific qPCR.
PLoS ONE 6, (2011)

Eddy H J van Roon; Marjo van Puijenbroek; Anneke Middeldorp; Ronald van Eijk; Emile J de Meijer; Dianhdra Erasmus; Kim A D Wouters; Manon van Engeland; Jan Oosting; Frederik J Hes; et al.
Early onset MSI-H colon cancer with MLH1 promoter methylation, is there a genetic predisposition?
BMC Cancer 10, 180 (2010)

Ronald van Eijk; Paul H C Eilers; Remco Natté; Anne-Marie Cleton-Jansen; Hans Morreau; Tom van Wezel; Jan Oosting
MLPAinter for MLPA interpretation: an integrated approach for the analysis, visualisation and data management of Multiplex Ligationdependent Probe Amplification.
BMC Bioinformatics 11, 670 (2010)

Ronald van Eijk; Marjo van Puijenbroek; Amiet R Chhatta; Nisha Gupta; Rolf H A M Vossen; Esther H Lips; Anne-Marie Cleton-Jansen; Hans Morreau; Tom van Wezel
Sensitive and specific KRAS somatic mutation analysis on wholegenome amplified DNA from archival tissues.
J Mol Diagn 12, 270 (2010)

Anneke Middeldorp; Shantie Jagmohan-Changur; Ronald van Eijk; Carli Tops; Peter Devilee; Hans F A Vasen; Frederik J Hes; Richard Houlston; Ian Tomlinson; Jeanine J Houwing-Duistermaat; et al.
Enrichment of low penetrance susceptibility loci in a Dutch familial colorectal cancer cohort.
Cancer Epidemiol. Biomarkers Prev. 18, 3062 (2009)

Salvatore Romeo; Maria Debiec-Rychter; Martine Van Glabbeke; Heidi Van Paassen; Paola Comite; Ronald Van Eijk; Jan Oosting; Jaap Verweij; Philippe Terrier; Ulrike Schneider; et al.
Cell cycle/apoptosis molecule expression correlates with imatinib response in patients with advanced gastrointestinal stromal tumors.
Clin. Cancer Res. 15, 4191 (2009)

Cristiana E T da Costa; Karoly Szuhai; Ronald van Eijk; Manja Hoogeboom; Raphael Sciot; Fredrik Mertens; Helga Björgvinsdóttir; Maria Debiec-Rychter; Ronald R de Krijger; Pancras C W Hogendoorn; et al.
No genomic aberrations in Langerhans cell histiocytosis as assessed by diverse molecular technologies.
Genes Chromosomes Cancer 48, 239 (2009)

Maartje Nielsen; Noel F C C de Miranda; Marjo van Puijenbroek; Ekaterina S Jordanova; Anneke Middeldorp; Tom van Wezel; Ronald van Eijk; Carli M J Tops; Hans F A Vasen; Frederik J Hes; et al.
Colorectal carcinomas in MUTYH-associated polyposis display histopathological similarities to microsatellite unstable carcinomas.
BMC Cancer 9, 184 (2009)

Juul T Wijnen; Richard M Brohet; Ronald van Eijk; Shanty Jagmohan-Changur; Anneke Middeldorp; Carli M Tops; Mario van Puijenbroek; Margreet G E M Ausems; Encarna Gómez García; Frederik J Hes; et al.
Chromosome 8q23.3 and 11q23.1 variants modify colorectal cancer risk in Lynch syndrome.
Gastroenterology 136, 131 (2009)

Willem E Corver; Anneke Middeldorp; Natalja T ter Haar; Ekaterina S Jordanova; Marjo van Puijenbroek; Ronald van Eijk; Cees J Cornelisse; Gert Jan Fleuren; Hans Morreau; Jan Oosting; et al.
Genome-wide allelic state analysis on flow-sorted tumor fractions provides an accurate measure of chromosomal aberrations.
Cancer Res. 68, 10333 (2008)

A Middeldorp; M van Puijenbroek; M Nielsen; W E Corver; E S Jordanova; N ter Haar; C M J Tops; H F A Vasen; E H Lips; R van Eijk; et al.
High frequency of copy-neutral LOH in MUTYH-associated polyposis carcinomas.
J. Pathol. 216, 25 (2008)

Esther H Lips; Ronald van Eijk; Eelco J R de Graaf; Pascal G Doornebosch; Noel F C C de Miranda; Jan Oosting; Tom Karsten; Paul H C Eilers; Rob A E M Tollenaar; Tom van Wezel; et al.
Progression and tumor heterogeneity analysis in early rectal cancer.
Clin. Cancer Res. 14, 772 (2008)

Esther H Lips; Ronald van Eijk; Eelco J R de Graaf; Jan Oosting; Noel F C C de Miranda; Tom Karsten; Cornelis J van de Velde; Paul H C Eilers; Rob A E M Tollenaar; Tom van Wezel; et al.
Integrating chromosomal aberrations and gene expression profiles to dissect rectal tumorigenesis.
BMC Cancer 8, 314 (2008)

Anne-Marie Cleton-Jansen; Ronald van Eijk; Marcel Lombaerts; Marjanka K Schmidt; Laura J Van't Veer; Katja Philippo; Rhyenne M E Zimmerman; Johannes L Peterse; Vincent T B H M Smit; Tom van Wezel; et al.
ATBF1 and NQO1 as candidate targets for allelic loss at chromosome arm 16q in breast cancer: absence of somatic ATBF1 mutations and no role for the C609T NQO1 polymorphism.
BMC Cancer 8, 105 (2008)

Marjo van Puijenbroek; Anneke Middeldorp; Carli M J Tops; Ronald van Eijk; Heleen M van der Klift; Hans F A Vasen; Juul Th Wijnen; Frederik J Hes; Jan Oosting; Tom van Wezel; et al.
Genome-wide copy neutral LOH is infrequent in familial and sporadic microsatellite unstable carcinomas.
Fam. Cancer 7, 319 (2008)

E H Lips; E J de Graaf; R A E M Tollenaar; R van Eijk; J Oosting; K Szuhai; T Karsten; Y Nanya; S Ogawa; C J van de Velde; et al.
Single nucleotide polymorphism array analysis of chromosomal instability patterns discriminates rectal adenomas from carcinomas.
J. Pathol. 212, 269 (2007)

Jan Oosting; Esther H Lips; Ronald van Eijk; Paul H C Eilers; Károly Szuhai; Cisca Wijmenga; Hans Morreau; Tom van Wezel
High-resolution copy number analysis of paraffin-embedded archival tissue using SNP BeadArrays.
Genome Res. 17, 368 (2007)

M Lombaerts; T van Wezel; K Philippo; J W F Dierssen; R M E Zimmerman; J Oosting; R van Eijk; P H Eilers; B van de Water; C J Cornelisse; et al.
E-cadherin transcriptional downregulation by promoter methylation but not mutation is related to epithelial-to-mesenchymal transition in breast cancer cell lines.
Br. J. Cancer 94, 661 (2006)

Esther H Lips; Jan Willem F Dierssen; Ronald van Eijk; Jan Oosting; Paul H C Eilers; Rob A E M Tollenaar; Eelco J de Graaf; Ruben van't Slot; Cisca Wijmenga; Hans Morreau; et al.
Reliable high-throughput genotyping and loss-of-heterozygosity detection in formalin-fixed, paraffin-embedded tumors using single nucleotide polymorphism arrays.
Cancer Res. 65, 10188 (2005)

Marjo van Puijenbroek; Jan Willem F Dierssen; Patrick Stanssens; Ronald van Eijk; Anne Marie Cleton-Jansen; Tom van Wezel; Hans Morreau
Mass spectrometry-based loss of heterozygosity analysis of single nucleotide polymorphism loci in paraffin embedded tumors using the MassEXTEND assay: single-nucleotide polymorphism loss of heterozygosity analysis of the protein tyrosine phosphatase receptor type J in familial colorectal cancer.
J Mol Diagn 7, 623 (2005)

Nathalie L G Sieben; Jan Oosting; Adrienne M Flanagan; Jaime Prat; Guido M J M Roemen; Sandra M Kolkman-Uljee; Ronald van Eijk; Cees J Cornelisse; Gert Jan Fleuren; Manon van Engeland
Differential gene expression in ovarian tumors reveals Dusp 4 and Serpina 5 as key regulators for benign behavior of serous borderline tumors.
J. Clin. Oncol. 23, 7257 (2005)

Remco Natté; Ronald van Eijk; Paul Eilers; Anne-Marie Cleton-Jansen; Jan Oosting; Mathilde Kouwenhove; Johan M Kros; Sjoerd van Duinen
Multiplex ligation-dependent probe amplification for the detection of 1p and 19q chromosomal loss in oligodendroglial tumors.
Brain Pathol. 15, 192 (2005)

Elza C de Bruin; Simone van de Pas; Esther H Lips; Ronald van Eijk; Minke M C van der Zee; Marcel Lombaerts; Tom van Wezel; Corrie A M Marijnen; J Han J M van Krieken; Jan Paul Medema; et al.
Macrodissection versus microdissection of rectal carcinoma: minor influence of stroma cells to tumor cell gene expression profiles.
BMC Genomics 6, 142 (2005)

Ronald van Eijk; Jan Oosting; Nathalie Sieben; Tom van Wezel; Anne-Marie Cleton-Jansen
Visualization of regional gene expression biases by microarray data sorting.
BioTechniques 36, 592 (2004)

G M Terwindt; R A Ophoff; R van Eijk; M N Vergouwe; J Haan; R R Frants; L A Sandkuijl; M D Ferrari;
Involvement of the CACNA1A gene containing region on 19p13 in migraine with and without aura.
Neurology 56, 1028 (2001)

I Stec; M van Vliet; R van Eijk; H Meijers; K H Kroeze; J G Dauwerse; G J van Ommen; C J Cornelisse; J T den Dunnen; P Devilee
A partial BRCA1 sequence homology mapping to 4q28.
Cytogenet. Cell Genet. 94, 26 (2001)

T Peelen; W de Leeuw; K van Lent; H Morreau; R van Eijk; M van Vliet; J Wijnen; M Ligtenberg; H B Ginjaar; R Zweemer; et al.
Genetic analysis of a breast-ovarian cancer family, with 7 cases of colorectal cancer linked to BRCA1, fails to support a role for BRCA1 in colorectal tumorigenesis.
Int. J. Cancer 88, 778 (2000)

H Papelard; G H de Bock; R van Eijk; T P Vliet Vlieland; C J Cornelisse; P Devilee; R A Tollenaar
Prevalence of BRCA1 in a hospital-based population of Dutch breast cancer patients.
Br. J. Cancer 83, 719 (2000)

M van der Looij; A M Cleton-Jansen; R van Eijk; H Morreau; M van Vliet; N Kuipers-Dijkshoorn; E Oláh; C J Cornelisse; P Devilee
A sporadic breast tumor with a somatically acquired complex genomic rearrangement in BRCA1.
Genes Chromosomes Cancer 27, 295 (2000)

G M Terwindt; R A Ophoff; J Haan; M N Vergouwe; R van Eijk; R R Frants; M D Ferrari
Variable clinical expression of mutations in the P/Q-type calcium channel gene in familial hemiplegic migraine. Dutch Migraine Genetics Research Group.
Neurology 50, 1105 (1998)

A Petrij-Bosch; T Peelen; M van Vliet; R van Eijk; R Olmer; M Drüsedau; F B Hogervorst; S Hageman; P J Arts; M J Ligtenberg; et al.
BRCA1 genomic deletions are major founder mutations in Dutch breast cancer patients.
Nat. Genet. 17, 341 (1997)

R A Ophoff; G M Terwindt; M N Vergouwe; R van Eijk; P J Oefner; S M Hoffman; J E Lamerdin; H W Mohrenweiser; D E Bulman; M Ferrari; et al.
Familial hemiplegic migraine and episodic ataxia type-2 are caused by mutations in the Ca2+ channel gene CACNL1A4.
Cell 87, 543 (1996)

R A Ophoff; G M Terwindt; M N Vergouwe; R van Eijk; H Mohrenweiser; M Litt; M H Hofker; J Haan; M D Ferrari; R R Frants
A 3-Mb region for the familial hemiplegic migraine locus on 19p13.1-p13.2: exclusion of PRKCSH as a candidate gene. Dutch Migraine Genetic Research Group.
Eur. J. Hum. Genet. 4, 321 (1996)

J Haan; G M Terwindt; R A Ophoff; P L Bos; R R Frants; M D Ferrari; T Krommenhoek; D L Lindhout; L A Sandkuyl; R Van Eyk
Is familial hemiplegic migraine a hereditary form of basilar migraine?
Cephalalgia 15, 477 (1995)

A May; R A Ophoff; G M Terwindt; C Urban; R van Eijk; J Haan; H C Diener; D Lindhout; R R Frants; L A Sandkuijl
Familial hemiplegic migraine locus on 19p13 is involved in the common forms of migraine with and without aura.
Hum. Genet. 96, 604 (1995)

R H Boerman; R A Ophoff; T P Links; R van Eijk; L A Sandkuijl; A Elbaz; J E Vale-Santos; A R Wintzen; J C van Deutekom; D E Isles
Mutation in DHP receptor alpha 1 subunit (CACLN1A3) gene in a Dutch family with hypokalaemic periodic paralysis.
J. Med. Genet. 32, 44 (1995)

R A Ophoff; R van Eijk; L A Sandkuijl; G M Terwindt; C P Grubben; J Haan; D Lindhout; M D Ferrari; R R Frants
Genetic heterogeneity of familial hemiplegic migraine.
Genomics 22, 21 (1994)

D J Peters; L Spruit; J J Saris; D Ravine; L A Sandkuijl; R Fossdal; J Boersma; R van Eijk; S Nørby; C D Constantinou-Deltas
Chromosome 4 localization of a second gene for autosomal dominant polycystic kidney disease.
Nat. Genet. 5, 359 (1993)

R van Eyk; L Chan; B Top; A F Stalenhoef; L M Havekes; R R Frants
An additional MspI RFLP at the human hepatic lipase (HL) gene locus.
Nucleic Acids Res. 18, 3110 (1990)

M M Van Lookeren Campagne; C Erneux; R Van Eijk; P J Van Haastert
Two dephosphorylation pathways of inositol 1,4,5-trisphosphate in homogenates of the cellular slime mould Dictyostelium discoideum.
Biochem. J. 254, 343 (1988)

W Spek; K van Drunen; R van Eijk; P Schaap
Opposite effects of adenosine on two types of cAMP-induced gene expression in Dictyostelium indicate the involvement of at least two different intracellular pathways for the transduction of cAMP signals.
FEBS Lett. 228, 231 (1988)

Acknowledgements

De totstandkoming van dit proefschrift volgt op een reis van 25 jaar als analist. Velen hebben er aan bijgedragen dat het een voortdurende plezierreis is geworden met natuurlijk, af en toe, een weinig storm en hier en daar wat tegenwind. Het is onmogelijk iedereen die aan deze reis heeft bijgedragen hier persoonlijk te bedanken. Velen kunnen en moeten echter wel bedankt worden. Velen in de definitie van Hans en Tom, jullie hebben mij vaardig door de “promotie jaren” heen geloodst. Daarnaast vele vakgenoten, collega’s en studenten, nationaal en internationaal waarmee ik de afgelopen jaren voor korte of lange tijd, in kleinere of grotere projecten, binnen en buiten het onderzoek heb samengewerkt of nog steeds mee samenwerk. Mijn dank is groot, er zijn mooie havens aangedaan. Dan mijn ouders, jullie hebben aan de basis van mijn reis gestaan. Maar bovenal Marianne voor je geduld, liefde en vriendschap: Oost West, thuis best.

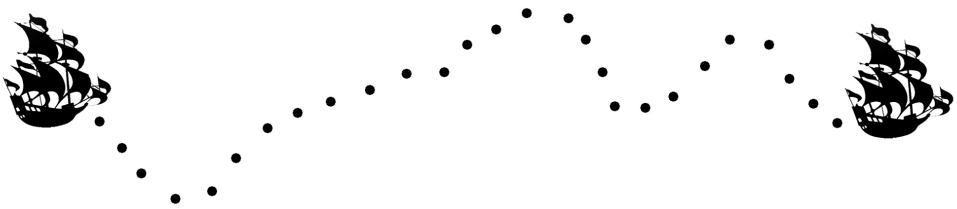

Curriculum Vitae

Ronald van Eijk is in 1964 geboren in Leiden. In 1981 behaalde hij het HAVO diploma aan de Louise de Coligny Scholengemeenschap in Leiden waarna werd begonnen aan de studie Hoger Laboratorium Onderwijs aan de Laboratoriumschool Rijnland te Leiderdorp waarvoor het diploma, in de richting Biochemie, in 1986 werd behaald. Van 1985-1989 werkte hij als analist bij de Rijks Universiteit Leiden bij de vakgroep Celbiologie en genetica in de groep van Theo Konijn aan signaal transductie en genexpressie in Dictyostelium Discoideum. Van 1989-2001 werkte hij in het Sylvius laboratorium bij het Centrum voor Humane en Klinische Genetica van het LUMC. In de groep onder leiding van Rune Frants werd gedurende twee jaar aan overervingpatronen in complexe plasma lipoproteinen gewerkt waarna werd begonnen aan het onderzoek aan Hemiplegisch Migraine. Dit onderzoek leidde in 1996 tot de publicatie van een verantwoordelijk gen, CACNL1A4. Vervolgens werd 4 jaar lang als research analist gewerkt in de groep van Peter Devilee waar grote series patiënten werden gescreend voor mutaties in de aan borstkanker gerelateerde genen *BRCA1* en *BRCA2*. In deze periode werd ook gezocht naar een onbekend borstkanker gen middels een linkage project uitgevoerd aan het Sanger Instituut in de groep van Mike Stratton. In 2001 was hij werkzaam bij het Leiden Genome Technology Center, geleid door Johan den Dunnen. Vanaf 2002 werd onder leiding van Anne-Marie Cleton binnen de afdeling Pathologie van het LUMC als senior research analist gewerkt aan de implementatie van nieuwe moleculaire technieken binnen de research en diagnostiek waarbij een brug werd gevormd tussen laboratorium automatisering en de bioinformatica. Dit werk is vanaf 2007 voortgezet in de werkgroep erfelijke tumoren onder leiding van Hans Morreau als promotor en Tom van Wezel als co-promotor.